Master Thesis
Sustainable Energy Technology
DPM 2138

# Battery Sizing Optimization for Grid-Tied PV Systems

Nafsika Gkioka
Student number: 2966476

Graduation committee:

Chair: Prof. dr. I. Gibson
Supervisor: Dr. ir. E. Shirazi
External: Dr. ir. G. Hoogsteen

September, 2024

Department of Design, Production and Management,
Faculty of Engineering Technology,
University of Twente

UNIVERSITY OF TWENTE.

# Contents

**Abstract**

In the pursuit of climate neutrality and sustainability, the European Union (EU) has established multiple goals to reduce environmental impact and promote sustainability across various sectors, including industry. Manufacturing industries, major contributors to environmental impact, are part of this transformation [1]. By adopting sustainable practices, enhancing energy efficiency and circular economy, the manufacturing sector can contribute to the EU's climate objectives. One pillar of sustainable manufacturing is the integration of renewable energy sources as a source of energy into the production process.

Particularly, on-site solar energy generation stands out as one of the most feasible options. However, due to the intermittent nature of Photovoltaic (PV) energy, batteries can play an important role in effectively addressing the problem of non-dispatchable energy generation and unbalanced supply and demand. Moreover, with the grid experiencing considerable congestion issues due to the increased demand and penetration of renewable energy sources, the amount of energy, that can be exported to or imported from the grid, is restricted. This implies the necessity of storage solutions to store the excess solar energy that would be otherwise curtailed or wasted, allowing it to be used during peak demand hours.

Determining the optimal battery size for a PV system can be a challenge due to multiple factors, including the intermittent nature of the renewable energy sources, the fluctuations of the energy demand profiles and prices, the continuously evolving regulatory framework and the trade-offs between the different objectives of the system, meaning that the different objectives may conflict with each other.

This master thesis develops a framework for battery sizing optimization for grid-tied PV-battery systems. The research is done for the Fraunhofer Innovation Platform for Advanced Manufacturing at the University of Twente. A PV system of 36.9 kWp is installed on the roof of the building and the generated energy is utilized to supply power to a machine on the shop floor. Firstly, the optimization of the battery size is realized using a Mixed Integer Linear Programming (MILP) model, taking into consideration four different objectives, namely cost minimization, $CO_2$ emissions minimization, self-sufficiency and self-consumption maximization. Various scenarios are analyzed to account for different economic contexts and regulatory constraints. Due to the trade-offs among these objectives, a co-optimization analysis is also conducted. Furthermore, the $CO_2$ emissions of the resulting optimal systems are calculated and a financial analysis is performed to assess the financial implications of the optimized systems. Lastly, the system's data are projected over the expected lifetime of the battery, considering changes in the performance of the PV-battery system, consumption profile, costs and regulatory framework, to analyse potential variations in the resulting optimal battery size.

The results of the analysis indicate that the optimal battery size of the system is influenced by a combination of technical, financial, environmental and regulatory factors. In cases where the electricity prices are low or the system operates under specific schemes, such as net metering, a battery is not economically beneficial for the system. Additionally, scenarios that include restrictions on grid interaction generally tend to result in larger battery sizes. However, when the objective of the system excludes cost considerations, such as minimizing $CO_2$ emissions or maximizing self-sufficiency or self-consumption, the

optimal battery capacity becomes unrealistically large. Thus, co-optimizing cost along with these objectives is necessary to obtain a more balanced outcome. Moreover, the results show that larger battery sizes minimize the environmental impact of the resulting PV-battery systems, yet only a few of the analysed scenarios are proven to be financially viable. Lastly, while for certain models, the long-term analysis results in battery sizes of similar magnitude to those determined by the short-term analysis, in other models the optimal size differs significantly.

*Keywords*: PV-battery systems, battery sizing optimization, cost minimization, $CO_2$ emissions, self-sufficiency, self-consumption, financial feasibility, MILP

## Acknowledgement

I would like to express my gratitude to my thesis supervisor, Dr. ir. Elham Shirazi, for the guidance, support and continuous feedback throughout this master's thesis. Her expertise was really useful and valuable for formulating the direction and quality of this research.

Furthermore, I am thankful to Barry te Dorsthorst for providing the necessary data for the completion of this study.

I would also like to thank Prof. dr. Ian Gibson and Dr.ir. Gerwin Hoogsteen for their valuable contribution as members of the examination committee.

Lastly, special thanks to my family and friends for their love, support and understanding throughout this master's journey.

# Chapter 1

# Introduction

In response to the EU's climate neutrality and sustainability goals, the manufacturing sector needs to minimize its environmental impact. An innovative way to achieve this objective is through the adoption of sustainable manufacturing processes that can reduce the environmental footprint of the industry, achieve resource efficiency, enhance the circularity of products and promote economic resilience. A key component of the sustainable manufacturing strategy is the incorporation of renewable energy sources into the production process. Solar energy is one of the most promising on-site solutions due to its scalability, accessibility and affordability. The green energy generated by the PV systems can be utilized in manufacturing process, reducing in this way the environmental footprint of both the production process and the resulting goods.

However, due to the intermittent and variable nature of renewable energy sources, challenges arise. Solar energy production fluctuates over time, meaning that prediction of the power output is challenging. At the same time, it is non-dispatchable, meaning that the generation cannot be ramped up or down to match the demand. These characteristics of sustainable energy sources highlight the importance of effectively balancing energy supply and demand. Energy storage systems, such as batteries, can provide a solution to this challenge by allowing excess energy produced during peak production moments to be stored for later use when energy production is low or zero. Since batteries can be considered energy buffers, after the incorporation of a battery, the autonomy and independence of the system can be enhanced, minimizing in this way the total operational cost [2].

Additionally, the growing adoption of PV systems on residential and commercial buildings has led to a shift from a centralized energy production, where energy is generated centrally and flows in one direction towards the consumers, to a decentralized model, where energy flow is bi-directional (Figure 1.1) [3]. While traditional power systems used to operate with the demand determining the supply, nowadays supply is the factor that shapes the consumer's demand. Nevertheless, since the grid was designed for uni-directional flow and central power generation, local over-voltage issues may occur, resulting in grid congestion problems [3]. To address this issue, regulations may impose restrictions on the amount of energy imported from or exported to the grid. Thus, incorporating a battery into a sustainable energy system could effectively achieve compliance with the regulations and prevent curtailment of energy or unmet demand.

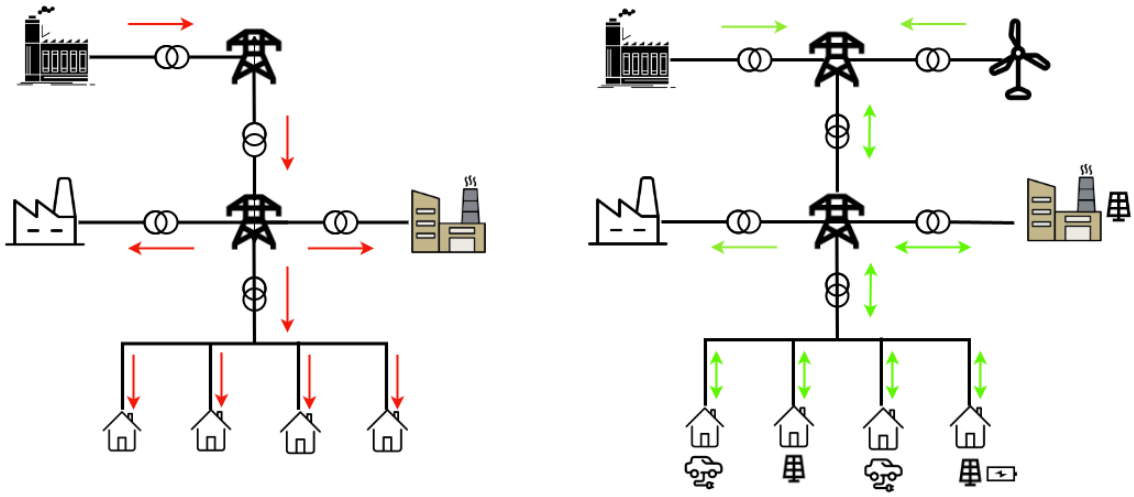

FIGURE 1.1: Traditional centralized electricity grid (left) vs. modern restructured electricity grid (right) (adapted from [4]).

## 1.1 Problem Definition

Photovoltaic generation systems are expected to be one of the main technological drivers in achieving the EU's climate goals [5]. Nevertheless, solar energy is produced intermittently and does not always follow the demand of the manufacturing process. The incorporation of storage solutions into PV systems can mitigate some of the consequent challenges. By effectively balancing supply and demand, enhancing power supply reliability and alleviating grid stress, storage systems facilitate the integration of renewable sources of energy into manufacturing processes [6].

A critical aspect of optimizing the performance of a grid-tied PV-battery system is the effective sizing of its storage. Determining the optimal battery size for a specific system involves considering multiple factors. Firstly, the energy demand profile can reveal patterns of energy consumption throughout the day and secondly, climate conditions can significantly influence energy production, affecting in this way the storage capacity requirements of the system. Moreover, electricity tariffs and battery costs are crucial factors in determining the economic feasibility of the system. Regulatory frameworks can also influence the optimal battery size, by restricting the amount of energy permitted to be imported from or fed into the grid. Additionally, regulations may define subsidies and financial schemes that can have a significant impact on the system's economic viability.

Battery sizing optimization is challenging due to the complexity and variability of the involved factors, such as the intermittency of solar energy production, the dynamic energy demand and the fluctuating electricity prices. Furthermore, with the battery's lifespan varying between 10 and 15 years [7] [8] and taking into account the significant number of sustainability and climate action initiatives established in recent years, regulatory framework changes are expected during the lifetime of the system. Such changes can influence the feasibility of grid-connected PV-battery systems, potentially undermining the chosen size of the energy storage system.

Additionally, during the design phase of a grid-tied PV-battery system, it is essential to determine the system's objective. It is important to note that the optimization of battery

size may involve conflicting goals. While a larger battery size may decrease the system's dependence on the grid, maximizing in this way the self-consumption rate or reducing the total $CO_2$ emissions of the system, it may, on the other hand, increase the initial investment cost, resulting in misalignment with the objective of cost minimization.

## 1.2 Research Layout

In this section, the research questions and desirable outcomes of the thesis are displayed. Additionally, the general structure of the thesis is described.

### 1.2.1 Research Questions

The main research question of the thesis is the following:

- How to define the optimal battery size of a grid-tied PV system considering technical, financial, environmental and regulatory aspects?

Additionally, some sub-questions arise:

- What are the factors that influence the selection of the optimal battery size for a grid-tied PV system? How can the variation of these factors affect the optimal battery size?
- What are the environmental impacts associated with different battery sizes in grid-tied PV systems and how can these be minimized through strategic system design and operation?
- What are the economic implications of the different battery sizes in the context of a grid-tied PV system?
- How do regulatory frameworks and incentives impact the feasibility and economic viability of grid-tied PV systems? In what ways can regulatory and policy frameworks influence the optimal sizing of batteries in grid-tied PV systems?

### 1.2.2 Research Outcomes

The desirable outcomes of this thesis are the following:

- A simulation model for grid-tied PV-battery systems that aims at the optimization of the battery size.
- The optimal battery size for various objectives of the case study, namely cost minimization, $CO_2$ emissions minimization, self-consumption maximization and self-sufficiency maximization.
- The impact of different battery sizes on the performance of the system.
- The environmental impact associated with different battery sizes in grid-tied PV-battery systems.
- The financial feasibility of the resulting optimal PV-battery systems by analysing metrics, such as payback time, return on investment and net present value.
- Changes in optimal battery size when considering the expected lifetime of the battery system using projected data.

### 1.2.3 Thesis Structure

This thesis is structured in various chapters to address the research objectives. The rest of the report is structured as follows: Chapter 2 performs a literature review, establishing the theoretical framework for the study. The methodology section in Chapter 3 describes the followed approach to conduct the research, Chapter 4 provides background information on the case study of this assignment and Chapter 5 presents the results of the analysis. In Chapter 6, a discussion regarding the findings is conducted and finally in Chapter 7, a conclusion that summarizes the key findings is included, the research questions are answered and recommendations for future research are suggested.

# Chapter 2

# Literature Review

In this chapter, a literature review, relevant to this thesis, is presented. The approach of sustainable manufacturing is described, different types of batteries are compared, the regulatory framework in the Netherlands is discussed and various optimization techniques and objectives are presented. Additionally, in this chapter, the economic landscape of PV-battery systems is examined, including trends in battery costs and how specific regulations impact the financial feasibility of the systems.

## 2.1 Sustainable Manufacturing

Sustainable manufacturing represents an innovative way towards reducing environmental impact, achieving resource efficiency and promoting economic resilience. As defined by the U.S. Environmental Protection Agency, sustainable manufacturing is the practice of producing goods using economically viable methods that minimize negative environmental impacts, conserve energy and resources and prioritize employee, community and product safety [9].

Recent regulatory initiatives, such as the "Eco-design for Sustainable Products Regulation" introduced by the European Commission, are crucial for promoting sustainable manufacturing, enhancing energy efficiency and circularity of products [10]. This regulation sets criteria for products to qualify as sustainable, emphasizing waste prevention, material recovery increase, extended product lifespan, support for the circular economy, utilization of recycled materials and reduced environmental footprint throughout the life cycle of the product [10]. Products, meeting these criteria, can be issued with the "Digital Product Passport", a passport that provides information to consumers regarding the product's sustainability characteristics [10]. The provision of the "Digital Product Passport can help consumers make informed decisions when buying products but also offer a competitive advantage to a business. By adopting sustainable manufacturing, companies can gain significant environmental, economic and social benefits while contributing to a more sustainable future. The integration of sustainable manufacturing processes is related to lower production costs, increased operational efficiency, improved sales and brand recognition, greater access to financing and capital, resilience to energy price volatility, new business opportunities, as well as lower regulatory compliance costs [9].

A crucial aspect of sustainable manufacturing is the integration of renewable energy sources into the production process, with solar energy being the most promising on-site solution. Unlike fossil-fuels-based energy production systems, PV panels operate without releasing

hardly any greenhouse gases or harmful emissions. In 2023, the Dutch electricity sector emitted 40.16 million metric tons of $CO_2$ equivalent [11]. The share of solar energy in the Dutch electricity mix was 18.03% for the same year, while it was accountable for only 2.51% of the total emissions [11], primarily associated with the manufacturing process of solar panels. The green energy generated by commercial PV systems can be utilized in manufacturing processes, reducing in this way the environmental footprint of both the production processes and the resulting goods. This also contributes to another pillar of sustainable manufacturing which is resource and material efficiency. This principle aims to get the most out of the value of the resources and materials used in the production process while minimizing waste. This approach can preserve critical resources, such as energy, contributing to the adoption of sustainable manufacturing processes.

## 2.2 Battery Storage System

The importance of energy storage in PV systems is undeniable. Given the intermittent and non-dispatchable nature of energy production, storage is crucial for balancing electricity supply and demand, enhancing power quality and facilitating the integration of renewable sources of energy into the grid [6]. The most suitable storage technology depends on a variety of factors, such as the power capacity of the PV system and the energy output of the latter, the cost, the location, the space availability and the grid restrictions [6]. For small-scale PV systems, batteries are the ideal storage solution because of their high efficiency, reliability, fast response time, easy use and minimal maintenance requirements [12]. Nevertheless, some limitations of the batteries include their comparatively high cost, restricted lifetime compared to other energy storage alternatives and environmental concerns, as critical materials, like lithium and cobalt, need to be used for their manufacture [12]. The most widely used rechargeable batteries for PV applications, that incorporate electrochemical technology, are lithium-ion, lead-acid, nickel-metal hydride and nickel-cadmium batteries [12] [6]. The advantages and disadvantages of each battery type are analysed in the subsequent sections.

### 2.2.1 Lithium-Ion (Li-ion) Batteries

Lithium-ion batteries are the most prominent battery type with a global battery market share of almost 53% [13]. Lithium-ion batteries are ideal for renewable energy applications and micro-scale systems due to their ability to supply steady electrical power [12]. Lithium-ion batteries, as their name suggests, consist of lithium paired with other reactive metals, such as cobalt, manganese and iron [14].

The advantages of lithium-ion batteries are the long lifetime, the high charge and discharge efficiency, the broad temperature range of operation, the high energy density, the rapid charging and the low maintenance cost [12]. On the other hand, lithium-ion batteries entail high initial investment cost. However, this upfront expense is counterbalanced over time by the longer lifetime and the reduced need for replacement compared to alternative battery storage solutions. Some more characteristics of lithium-ion batteries, that restrict their implementation, are poor performance in increased temperatures and the limited raw material availability [6]. Detailed characteristics of the lithium-ion battery technology are outlined in Table 2.1.


FIGURE 2.1: Lithium-ion battery [15].

### 2.2.2 Lead-Acid (Pb-A) Batteries

Lead-acid battery technology stands out as the oldest and most established battery technology that has been used in photovoltaic systems and stationary applications, as well as in the automotive industry [16] [6]. The main components of a lead-acid battery are metallic lead, lead sulfate, lead dioxide and sulfuric acid [17].

Although lead-acid batteries have plenty of advantages, such as low cost, high cell voltage, high performance in the case of varying temperatures and good recycling ability with an efficiency of 95%, they also include important limitations [12] [6] [16]. The regular maintenance needs, the heavy structure, the moderate efficiency, the limited energy density, the susceptibility to acid stratification and acid leaks and the number of life cycles, which is relatively lower compared to other battery technologies, are the main drawbacks of lead-acid batteries, that limit their applicability [12] [6] [16]. Given the toxicity of lead, lead-acid batteries necessitate recycling when they reach the end of their operational lifetime [14]. Detailed characteristics of the lead-acid battery technology are outlined in Table 2.1.


FIGURE 2.2: Lead-acid battery [18].

### 2.2.3 Nickel-Metal Hydride (Ni-MH) Batteries

Nickel-metal hydride batteries are primarily used in hybrid electric vehicles and smart energy storage systems [6]. The battery consists of a cathode incorporating nickel hydroxide, an anode composed of metal hydride and an electrolyte containing potassium hydroxide

[12].

Advantages of the nickel-metal hydride batteries include long shelf life and long lifetime, high energy density, efficient performance even under extremely high and low temperatures, good charge retention capabilities and high tolerance to both overcharging and overdischarging [6] [12]. The main disadvantages of the nickel-metal hydride batteries are poor performance under low working temperatures, low specific energy, as well as low specific power [12]. Besides that, this type of battery is related to higher cost compared to lead-acid batteries, but it is more affordable than lithium-ion batteries [12]. With respect to the environmental impact of nickel-metal hydride batteries, nickel, despite not being rare, is a limited element with difficult extraction processes and toxic properties. For this reason, recycling at the end of the battery's lifetime is crucial. Detailed characteristics of the nickel-metal hydride battery technology are outlined in Table 2.1.

FIGURE 2.3: Nickel-metal hydride battery [19].

### 2.2.4 Nickel-Cadmium (Ni-Cd) Batteries

Batteries with nickel-cadmium technology are mainly used in portable devices and hand tools, but also in PV systems [20]. In the case of nickel-cadmium batteries, the anode is made from metallic cadmium, the cathode is composed of nickel oxide hydroxide and the electrolyte is potassium hydroxide [6]. It should be mentioned that according to Directive 2006/66/EC of the European Parliament, various nickel-cadmium batteries are banned due to the inclusion of toxic substances [2] [21]. However, this regulation excludes stationary nickel-cadmium batteries used in PV systems. Nevertheless, proper recycling of them at the end of their lifetime is required [2].

Nickel-cadmium batteries are characterized by low maintenance needs, high number of lifetime cycles, great long-term storage abilities, notable durability, good charge retention and ability to operate under extreme temperature conditions, ($> 40^oC$) and ($< -10^oC$) [6] [12] [2]. The major drawbacks of nickel-cadmium batteries are the high cost, the low energy density and the toxic and caustic nature of the involved substances, which subsequently requires proper recycling [6] [12]. Additionally, it is important to note that nickel-cadmium batteries suffer from strong memory effects [12]. This phenomenon occurs when the battery undergoes recharging without first being fully discharged. Consequently, the battery "memorizes" the shallow discharge level and in this way, it reduces over time its usable capacity [6]. Detailed characteristics of the nickel-cadmium battery technology are outlined in Table 2.1.


FIGURE 2.4: Nickel-cadmium battery [22].

### 2.2.5 Battery Types Comparison

In Table 2.1, the key characteristics of each battery type are presented.

| | **Li-ion** | **Pb-A** | **Ni-MH** | **Ni-Cd** |
|---|---|---|---|---|
| Specific energy ($Wh/kg$) | 80 – 250 | 25 – 50 | 40 – 110 | 30 – 80 |
| Energy density ($kWh/m^3$) | 95 – 500 | 25 – 90 | 40 – 300 | 15 – 150 |
| Efficiency | 75 – 97 % | 63 – 90 % | 50 – 80 % | 60 – 90 % |
| Working temperature ($^oC$) | 20 – 65 | 18 – 45 | – 30 – 70 | - 40 – 50 |
| Lifetime cycles | 100 – 10,000 | 250 – 2,000 | 300 – 1,800 | 1,000 – 5,000 |
| Lifetime (years) | 5 - 15 | 2 - 15 | 2 - 15 | 10 - 20 |
| Depth of discharge | 100 % | 80 % | 100 % | 80% |
| Self-discharge rate (per day) | 0.1 – 0.3 % | 0.1 – 0.3 % | 5 – 20 % | 0.2 – 0.6 % |
| Energy cost (€/kWh) | 150 – 2,100 | 40 – 170 | 170 – 640 | 680 – 1,300 |
| Toxicity | Low | Very high | Low | Very high |
| Maintenance requirement | Not required | 3-6 months | 60-90 days | 30-60 days |

TABLE 2.1: Comparison table of the battery technologies for small-scale PV systems [6] [12] [23] [24].

Based on the analysis, it is evident that despite being on average the most expensive battery type, lithium-ion batteries outperform all other battery technologies. The large number of lifetime cycles, their high efficiency, their energy density and specific energy, as well as the relatively less significant environmental impact compared to the other battery types during operation, are the main factors that distinguish them in the renewable energy market. It should be noted that, as lithium-ion batteries are relatively new in the energy market, a significant price drop is expected in the near future because of their mass production over the last years [24]. According to findings from studies by Symeonidou et al. (2021) [25] and Nair et al. (2010) [26], lithium-ion batteries have a leading role in the renewable energy market, being the most appropriate battery type for small-scale PV applications.

## 2.3 Regulatory Framework

A supportive policy framework is crucial for the widespread adoption of decentralized PV systems within the conventional electricity grid. Both feed-in tariffs and net metering policies are considered important instruments to enhance the financial viability of PV investments and facilitate the integration of renewable energy sources into the electricity network [27].

### 2.3.1 Net Metering

Net metering is a policy framework that permits the prosumers - people who consume electricity from the grid while also producing electricity - to use the generated energy, at any moment, instead of being limited to consuming it only during production [27]. In other words, this scheme is a utility billing method of recording the excess energy generated by the PVs, which is fed into the grid, and applying it to the customer's bill as credit [28]. In order to achieve this, the grid effectively operates as a storage battery. Even though when the regulatory framework was initially introduced in the Netherlands, the net metered quantity was limited to 3,000 kWh/year per customer, in 2011 the limit increased to 5,000 kWh/year per customer and in 2012, the limit was abolished [27]. To qualify for this scheme, the customer must be connected to the electricity grid via a connection with a throughput value of $\leq 3 * 80A$ [27].

The net metering scheme has undeniably made the installation of PVs more financially attractive in the market. Coupled with the significant price reduction of PV technology, the net metering practice has been considered to be a pivotal factor in reducing the payback period of PV systems and in driving the consequent capacity growth of the corresponding systems in recent years [27]. With this policy in place, the payback time of the investment decreases and the overall cost of operating and maintaining the system experiences a cost reduction.

However, over the past years, the net metering policy has been a subject of continuous debate in the Netherlands. Despite its role in establishing the Netherlands as the country with the highest solar capacity per capita within the European Union [29], the Dutch Climate and Energy Ministry is considering phasing out this measure for various reasons. Firstly, since there is a downward trend in the prices of PV systems, there are growing concerns that the current net metering scheme is providing too much financial incentive for people who want to invest in solar energy. This could potentially result in excessive profitability and an imbalance in the energy system. Secondly, it is evident that net metering policy leads to a reduction of the governmental tax revenue. Since the popularity of PV systems continues to rise steadily, these losses can become significant. Estimations suggest that by 2031, these losses could reach approximately €2.8 billion [30]. In addition, it is important to note that net metering policy does not have negative consequences only for the government but also for the citizens, who do not own a PV system. Since electricity bills typically include a fixed cost for operating and maintaining the electricity network, customers, who exploit the net metering policy, contribute less to these expenses, despite using the grid system. Therefore, customers, who do not exploit the net metering scheme, end up having to compensate for that, meaning that they are burdened with higher costs to maintain the system [30]. Lastly, the net metering policy has practical drawbacks that can affect the local power quality and the grid capacity used [27]. Specifically, the scheme encourages customers to limit the capacity of the PV system to their annual energy con-

sumption rather than to the available rooftop surface, resulting in underutilized rooftop potential [31]. In the same context, net metering policy does not motivate the owners of PV systems to increase their self-consumption rate, increasing in this way the used power grid capacity [27]. As a result, this trend can exacerbate the issue of grid congestion in the Netherlands.

### 2.3.2 Network Tariffs

In the Dutch energy market, customers have the choice of signing an electricity contract with one of the energy suppliers in three forms: fixed contract, variable contract or contract with dynamic energy prices. With a fixed contract, as the name implies, the customer pays a fixed price for electricity throughout the entire term period. When a fixed-term contract expires, it turns automatically into a variable contract. In contrast, with a variable contact, energy suppliers have the flexibility to adjust energy prices periodically, with changes occurring a few times per year or even monthly in recent times [32]. According to the Netherlands Authority for Consumers and Markets (ACM), half of the Dutch energy consumers have currently a variable energy contract [33]. Due to increasing uncertainty in the energy market nowadays, energy suppliers hardly provide fixed electricity contracts, as it is more challenging and expensive for them to keep prices stable over long periods. Regarding contracts with dynamic energy prices, the electricity prices are directly tied to the prices on the spot market, meaning that the rates fluctuate on an hourly basis. Therefore, the electricity prices become known only one day prior. Despite the uncertainty and reliance on the fluctuations of the market, the dynamic energy pricing contract can benefit customers. Through the implementation of smart energy management solutions and the adjustment of electricity consumption during periods of lower prices, customers can achieve a substantial reduction in their electricity expenses.

Figure 2.5 shows the day-ahead electricity prices in €/MWh for March 1, 2024 in the Netherlands. Firstly, significant hourly fluctuations in electricity prices throughout the day are evident. Secondly, at noon, when the PV power generation peaks, electricity prices demonstrate a decline compared to morning and evening times. This is the result of synchronised solar energy production and the consequent increased utilization of the grid capacity. In instances when solar energy production exceeds overall electricity demand, feed-in tariffs become negative. This practice discourages energy injection into the grid by requiring the customer to pay in order to export energy. Such occurrences appear to be increasingly frequent during noon. This phenomenon indicates the importance of implementing a battery storage system to store the surplus energy produced, particularly during noon, and prevent the synchronised injection of solar energy into the grid.

## 2.4 Optimization Techniques

Optimization algorithms are methods used to find the best possible solution from a set of feasible options while simultaneously fulfilling specific conditions. Based on the operational principles, optimization methods for battery sizing problems can be classified according to the literature into five different categories, namely probabilistic, analytical, mathematical optimization, heuristic and hybrid methods [35] [36] (Figure 2.6).

Probabilistic methods are considered one of the simplest methods for battery sizing op-

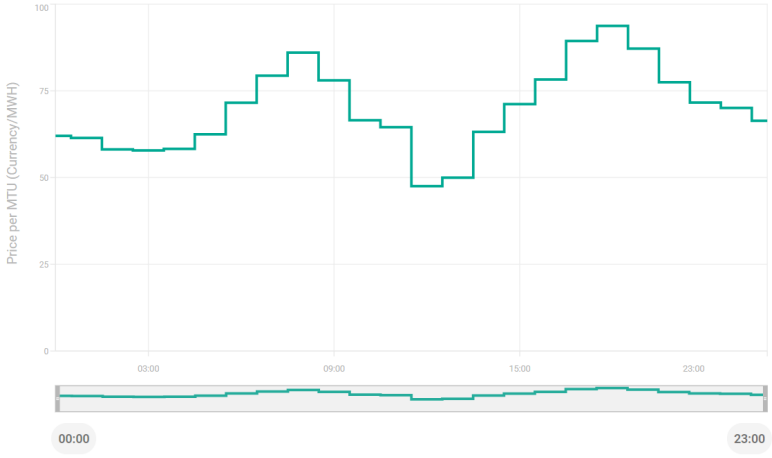


FIGURE 2.5: Day-ahead electricity prices in €/MWh for March 1, 2024 in the Netherlands [34].

timization problems, as the number of parameters, that can be optimized, is restricted [37]. The main advantage of this method is that for the optimization process, only limited data availability is required. However, as the approach can optimize a small number of performance criteria, its applicability in more complex problems is narrow [36]. For the optimization of the battery size, probabilistic methods account for the uncertainty in the parameters of the problem, thus creating a risk model [37] [36].

Analytical methods analyse a series of feasible power system configurations by varying the model elements [36]. These model elements need to be optimized according to specific predetermined rules [37]. The process aims to find the best configuration for the system components by comparing single or multiple performance indexes of the different configurations by repetitive calculations [38] [36].

Mathematical optimization involves various mathematical programming techniques, designed to identify the optimal solution to a problem among a set of potential solutions. A necessary part of mathematical optimization is the construction of an objective function that represents the quantity to be either maximized or minimized. Through an iterative process, the algorithm adjusts decision variables within the constraints of the problem, calculates the value of the objective function and converges towards the optimal solution. This iterative process continues until the best possible result is reached [36].

Heuristic optimization algorithms are suitable for problems, where finding an optimal solution is challenging, thus exploring suboptimal solutions is allowed [39]. Although the algorithms frequently lack a mathematically validated foundation for acquiring optimal solutions, the advantages of the heuristic method are low computational time and high accuracy rate [37].

Each of the optimization methods explained earlier includes different advantages and drawbacks. Therefore, instead of relying solely on a single optimization technique, hybrid methods combine the strengths of different methods to overcome their individual limitations and achieve better solutions [36]. Hybridization of two algorithms can take place either in a decoupled or coupled manner. In decoupled hybridization, two optimization methods op-

erate independently of each other, while coupled hybridization involves the simultaneous collaboration of two methods [36].

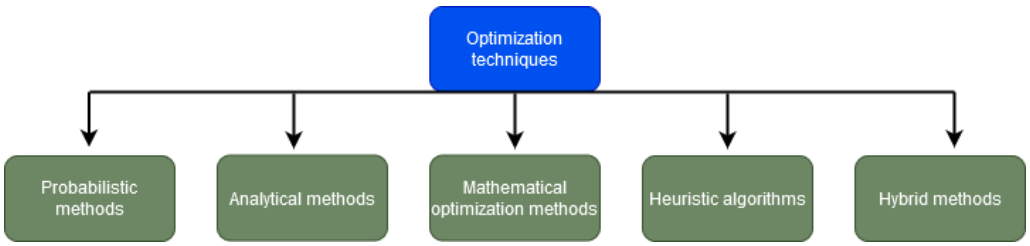


FIGURE 2.6: Classification of optimization techniques for battery sizing [35].

According to the literature, most of the battery sizing optimization problems are represented as mathematical models [40] [41]. The capacity of the battery is treated as a decision variable and the net benefits or losses of the system become the objective function to be maximized or minimized, respectively [41]. These mathematical optimization problems are usually solved using pre-existing, available optimization solvers, such as CPLEX or Gurobi solvers.

Various mathematical optimization techniques can be used for the purpose of optimal energy system design or operational plan optimization. Among the most common algorithms used are Linear Programming (LP), Mixed Integer Linear Programming (MILP) and Mixed Integer Non-Linear Programming (MINLP) [42]. The aforementioned algorithms differ in the type of variables they can handle and the complexity of the optimization problems they can solve. While LP and MILP algorithms can exclusively handle linear objective functions and constraints, dealing with only continuous or both continuous and integer variables respectively, MINLP is a more powerful optimization technique that addresses nonlinear problems that include a combination of continuous and discrete variables [43]. The nonlinearities can be included either within the objective function or within the constraints of the problem.

In the case of battery sizing optimization problems, binary variables are necessary to represent key operational characteristics of the energy system, such as the on/off status of the battery's charging and discharging power or the importing and exporting power from/to the electricity grid [44]. Therefore, this type of problems contains not only continuous variables but also binary variables (0,1) and non-linear terms. To handle these nonlinearities, multiple techniques can be employed to convert the nonlinear terms of the model into their linear equivalents [41]. By using approaches, such as the piecewise linear approximation, the convex relaxation and the Big-M method, a battery sizing optimization problem can be effectively formulated as a MILP problem [41].

## 2.5 Optimization Objectives

In the literature, various optimization objectives with respect to battery sizing optimization can be found. These can be categorised into three different groups, namely economical, technical and environmental objectives [39]. Economical objectives focus on achieving the financial viability of a system. The most common objective refers to cost minimization

which aims to minimize the overall cost of the system, including investment, operational, maintenance and replacement costs and maximize the total profit [45] [46]. Regarding the technical category, optimization focuses on enhancing technical aspects, such as maximizing self-sufficiency and self-consumption or minimizing the system's dependence on the grid [47]. Lastly, environmental objectives aim to minimize the environmental footprint of the system by minimizing $CO_2$, $NO_x$ or $SO_x$ emissions [46].

However, the aforementioned categories of optimization objectives may include contradictory goals. For instance, while a specific battery size may significantly reduce the system's emissions, it may also result in high system costs, raising questions about the economic feasibility of the system and whether the scenario represents a real case option. For this reason, many energy systems adopt a multiple objective optimization approach that considers simultaneously objectives from different categories [39]. These problems are called multi-objective optimization problems and they take into consideration potentially conflicting goals, resulting in a more balanced solution.

Generally, there are two methods for solving multi-objective optimization problems, the weighted sum method and the lexicographic goal programming [39]. While the former transforms the multi-objective optimization problem into a single objective optimization problem by assigning weights to the multiple individual objectives, the latter follows a hierarchical approach by prioritizing objectives based on their importance [39].

## 2.6 Economic Landscape of PV - (Li-ion) Battery Systems

Lithium-ion battery market has experienced rapid growth due to the increasing demand for energy storage solutions across various industries. In 2023, the market was worth 56.8 billion USD, while projections suggest that the market will reach 187.1 billion USD by 2032 [48]. This market growth is the result of the global shift towards renewable energy sources, electrification of transportation, investments in Electric Vehicle (EV) charging infrastructures, technological improvements and supportive government incentives and regulations for sustainable development. These factors have led to increased production, making lithium-ion batteries more affordable and efficient. Figure 2.7 shows the lithium-ion battery prices from 2013 to 2023 on a global scale, clearly illustrating the continuous declining trend of battery costs.

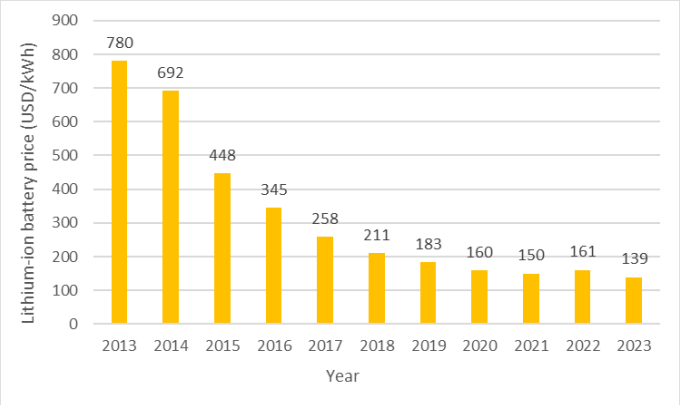


FIGURE 2.7: Lithium-ion battery price worldwide over the years [49].

Despite the reduction in battery costs, the payback time for a PV-battery system remains relatively high, being in this way a barrier to widespread implementation. Research indicates that the average payback time for residential small-scale PV systems with storage in Europe exceeds 25 years, while half of small-scale commercial and residential systems in Europe remain non-competitive [50]. Figure 2.8 provides insight into the range of the payback period for commercial small-scale PV-battery systems in Europe [50].

Furthermore, net metering scheme is a key factor for the determination of the payback period of a PV-battery system and its overall economic viability. According to M. Londo et al. [27], in the Netherlands, the payback time for a residential PV system with net metering amounts on average to 8 years. In contrast, for systems without net metering, the payback time can extend to 15 years, highlighting the importance of supportive policies and incentives in promoting renewable energy systems.

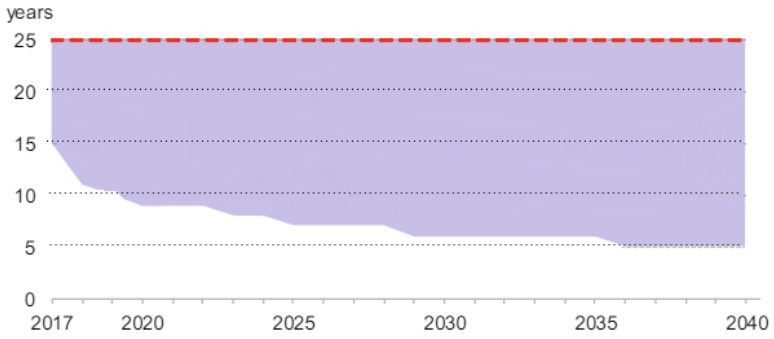


FIGURE 2.8: Payback period for commercial small-scale PV-battery systems in Europe [50].

# Chapter 3

# Methodology

In this section, the schematic layout of the system and the modeling of the battery's behaviour, which is consistent across all the optimization models, are explained. Additionally, for each single objective optimization model, namely cost minimization, $CO_2$ emissions minimization, self-consumption maximization and self-sufficiency maximization, some additional model elements to address the different objectives are introduced. The modeling of the co-optimization algorithms is also analysed. Furthermore, the methodology employed for the $CO_2$ emissions calculation, as well as for the financial analysis of the optimal systems, is explained. Lastly, the required additions in the model for the battery's lifelong analysis are discussed.

For the modeling of the battery's behaviour, a MILP algorithm has been developed. In order to create the mathematical model, the variables, parameters and constraints of the problem are defined. Specifically, variables represent unknown or changing parts of the model, parameters represent the data that must be supplied to perform the optimization process and constraints represent mathematical relationships that define how different parts of a model are connected to each other in a logical and realistic way [51]. Furthermore, in every model, an objective function is determined that needs to be minimized or maximized, depending on the nature of the problem.

## 3.1 System Schematic Layout

The considered system in this assignment currently consists of a PV system, a DC-to-DC converter, which is used to adjust the voltage levels and ensure that the voltage produced by the PVs matches the inverter's operational characteristics, a DC-to-AC inverter, crucial for compatibility with the AC voltage utilized by the machine, the load and the grid. The schematic layout of the current system is depicted in Figure 3.1 with connections shown in blue colour.

This assignment aims to evaluate whether the addition of a lithium-ion battery, the capacity of which needs to be optimized, is beneficial for the system. Along with the battery, a DC-to-DC converter needs to be included in the system in order to ensure that the battery's voltage requirements are met. The potentially new components need to be incorporated into the system as illustrated by the red lines of Figure 3.1.

For this assignment, the PV energy directly consumed by the system or fed into the grid accounts for the efficiency losses of the existing system's DC-to-DC converter and the DC-

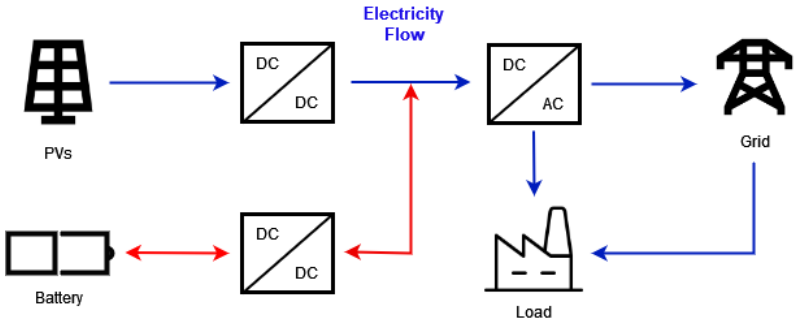


FIGURE 3.1: Schematic layout of the grid-connected PV-battery system.

to-AC inverter, based on the provided data. However, the energy stored in the battery is assumed to not account for losses of the new DC-to-DC converter component. Nevertheless, in real-world applications, there is an efficiency loss, with the converter typically operating at around 95% efficiency [52]. This efficiency loss could reduce the available PV energy for consumption, potentially affecting the result of the battery sizing optimization algorithm.

## 3.2 Battery Modeling

Across all optimization objectives, the modeling of the battery's behaviour and performance presents common characteristics. In order to determine the optimal battery size, the battery system needs to be modeled considering multiple parameters, variables and constraints, each directly affecting the result of the analysis. In this section, the battery model is presented.

With respect to the parameters of the battery model, the average efficiency of the lithium-ion battery, according to Table 2.1 in Section 2.2.5, is 0.86. Furthermore, it is assumed that the C-rate is 0.5, meaning that the battery can be fully discharged within two hours. The Depth of Discharge (DoD), representing the percentage at which the battery can be discharged relative to its total capacity, is set at 0.2. A relatively shallow depth is chosen to prevent a reduction in the number of full charge/discharge cycles over the useful lifetime of the battery [53]. Besides this, the battery's behaviour can be modeled linearly when the State of Charge (SoC) ranges between 20%-80%. Beyond this certain range, batteries exhibit non-linear characteristics, meaning that the battery's behaviour can not be modeled as a MILP algorithm. Lastly, the lifetime of the battery ranges between 10 and 15 years [7] [8], with the average value of 12.5 years being selected for the modeling of the battery system. The aforementioned operational parameters are necessary for the accurate simulation of the behavior and performance of the battery system.

Table 3.1 presents an overview of the defined parameters, that are consistent across all models, regardless of the optimization objective, and their corresponding values.

In addition to the parameters, the model incorporates variables representing unknown or dynamic components of the algorithm. Table 3.2 provides a comprehensive list of these variables. Notably, $C_B$ is the decision variable, representing the battery capacity that needs to be optimized. Moreover, the defined boolean variables are auxiliary model elements to replicate real-world scenarios, ensuring the avoidance of simultaneous charging and discharging, as well as simultaneous energy import from and export to the grid.

| Parameters | Value |
|---|---|
| Depth of Discharge ($DoD$) | 0.2 |
| Efficiency ($\eta_{char/dis}$) | 0.86% |
| $C_{rate}$ | 0.5 |
| Lifetime ($n$) | 12.5 years |

TABLE 3.1: Defined battery operational parameters in the MILP model.

| Variables | |
|---|---|
| Battery capacity (kWh) | $C_B$ |
| Power imported from the grid (kW) | $P_{import_t}$ |
| Power exported to the grid (kW) | $P_{export_t}$ |
| Total power imported/exported from the grid (kW) | $P_{grid_t}$ |
| Battery charge power (kW) | $P_{charge_t}$ |
| Battery discharge power (kW) | $P_{discharge_t}$ |
| Battery Energy (kWh) | $E_t$ |
| Excess energy (kWh) | $E_{excess_t}$ |
| Missing energy (kWh) | $E_{missing_t}$ |
| Boolean variable for importing power from the grid | $Bool_{import_t}$ |
| Boolean variable for exporting power to the grid | $Bool_{export_t}$ |
| Boolean variable for charging | $Bool_{char_t}$ |
| Boolean variable for discharging | $Bool_{dis_t}$ |

TABLE 3.2: Defined variables in the MILP model.

Besides the parameters and variables, the battery sizing optimization model is subject to multiple constraints to ensure its feasibility and alignment with real-world conditions. Firstly, constraints associated with power transactions with the electricity network need to be defined. These transactions are represented by two variables: the amount of power imported from the grid in kW at moment $t$, noted as $P_{import_t}$ and the power exported to the grid in kW at moment $t$, noted as $P_{export_t}$. The variables are constrained to be non-negative and non-positive float variables, respectively.

$$P_{import_t} \geq 0 \ \forall t \tag{3.1}$$

$$P_{export_t} \leq 0 \ \forall t \tag{3.2}$$

The sum of $P_{import_t}$ and $P_{export_t}$ represents the net power exchange with the grid in kW at moment $t$. Specifically, when $P_{grid_t}$ is positive, the system imports energy from the grid. In contrast, when the variable is negative, the system feeds in the excess PV energy to the electricity network.

$$P_{grid_t} = P_{import_t} + P_{export_t} \ \forall t \tag{3.3}$$

In addition, constraints that regulate the power flow within the battery are essential. The variable $P_{charge_t}$ denotes the charging power of the battery in kW at moment $t$ and $P_{discharge_t}$ represents the discharging power of the battery in kW at moment $t$. $P_{charge_t}$ is constrained to non-negative values, whereas $P_{discharge_t}$ is restricted to non-positive values.

$$P_{charge_t} \geq 0 \ \forall t \tag{3.4}$$

$$P_{discharge_t} \leq 0 \ \forall t \tag{3.5}$$

Furthermore, it is necessary to include some constraints ensuring that the battery is not charged or discharged at a rate exceeding its maximum capacity in order to prevent potential damage. Equations 3.6 and 3.7 represent this physical constraint, ensuring that $P_{charge_t}$ and $P_{discharge_t}$ are always less than or equal to the maximum battery power, $P_{max}$.

$$P_{charge_t} \leq P_{max} \ \forall t \tag{3.6}$$

$$P_{discharge_t} \geq -P_{max} \ \forall t \tag{3.7}$$

The maximum battery power is calculated based on Equation 3.8.

$$P_{max} = C_{rate} \times C_B \tag{3.8}$$

where $C_B$ is the battery capacity and $C_{rate}$ is the parameter that represents the charging or discharging rate relative to the battery size and equals 0.5, as defined in Table 3.1.

Moreover, a constraint that limits the amount of energy, that can be stored in the battery at every moment $t$, needs to be set. This quantity, measured in kWh, is represented by the non-negative variable $E_t$.

$$E_t \geq 0 \ \forall t \tag{3.9}$$

The depth of discharge factor ($DoD$) is also introduced in the model to preserve the battery's health over time and ensure that the battery's behaviour remains linear. Therefore, the lower and upper limits of $E_t$ can be described by Equations 3.10 and 3.11, respectively.

$$E_t \geq C_B \times DoD \ \forall t \tag{3.10}$$

$$E_t \leq C_B \times (1 - DoD) \ \forall t \tag{3.11}$$

The amount of energy stored in the battery ($E_t$) can be explicitly described at every moment $t$ by Equation 3.12.

$$E_t = E_{t-1} + \eta_{char/dis} \times (P_{charge_t} + P_{discharge_t}) \times t_{step} \ \forall \ t \geq 1 \tag{3.12}$$

where $E_{t-1}$ is the battery's energy in the previous time step, $\eta_{char/dis}$ denotes the charging and discharging efficiency and $t_{step}$ is the duration of each time interval, which is set to one hour for the purpose of this assignment.

The battery energy ($E_t$) is initialized at $t = 0$ to be equal to half of the battery capacity. Similarly, at the end of the time horizon $T$, which represents the length of the time steps, the battery energy is also equal to half of the battery capacity. For consistency reasons, the battery should start and finish half-charged.

$$E_0 = 0.5 \times C_B \tag{3.13}$$

$$E_T = 0.5 \times C_B \tag{3.14}$$

Furthermore, a constraint ensuring energy balance within the system is added. Equation 3.15 describes that the amount of energy bought from the grid at moment $t$, in case of deficit of energy, equals the demand of the system ($E_{demand_t}$) that is not covered by the PV power production ($PV_t$) or the discharge of the battery. Conversely, in case of excess PV energy production, the amount of energy sold to the grid at moment $t$, equals the excess PV power production that is neither consumed by the system nor used to charge the battery.

$$P_{grid_t} \times t_{step} = E_{demand_t} - PV_t + (P_{charge_t} + P_{discharge_t}) \times t_{step} \quad \forall t \tag{3.15}$$

In order to ensure that the system does not import and export power simultaneously, it needs to be defined that at every moment $t$, at least one of the variables, $P_{import_t}$ and $P_{export_t}$, equals zero. For this reason, the Boolean variables $Bool_{import_t}$ and $Bool_{export_t}$ are introduced and the Big-M method is implemented. Specifically, when $Bool_{import_t}$ is zero, $P_{import_t}$ must be also zero, meaning that no import of power occurs at moment $t$. Similarly, when $Bool_{export_t}$ equals zero, $P_{export_t}$ is consequently zero, indicating the absence of export activity at moment $t$.

The Big-M method is used in optimization problems with binary variables in order to exclude some constraints under specific conditions. This is achieved by using a variable M, which is chosen to be larger than any reasonable value that a continuous variable may take [54]. As aforementioned in Section 2.4, the Big-M method is considered a linearization technique, which converts the nature of the problem from non-linear to linear.

Equations 3.16 - 3.20 ensure that the export and import of power do not occur simultaneously with the implementation of the Big-M method.

$$P_{import_t} \leq M \times (1 - Bool_{export_t}) \ \forall t \tag{3.16}$$

$$P_{import_t} \geq -M \times Bool_{import_t} \ \forall t \tag{3.17}$$

$$P_{export_t} \leq M \times (1 - Bool_{import_t}) \ \forall t \tag{3.18}$$

$$P_{export_t} \geq -M \times Bool_{export_t} \ \forall t \tag{3.19}$$

$$Bool_{import_t} + Bool_{export_t} \leq 1 \ \forall t \tag{3.20}$$

In the same context, it is necessary to prevent the simultaneous charging and discharging of the battery. For this purpose, the Big-M method is used again and two Boolean variables for charging ($Bool_{char_t}$) and discharging ($Bool_{dis_t}$) are specified. The following constraints are incorporated into the model:

$$P_{charge_t} \leq M \times (1 - Bool_{dis_t}) \ \forall t \tag{3.21}$$

$$P_{charge_t} \geq -M \times Bool_{char_t} \ \forall t \tag{3.22}$$

$$P_{discharge_t} \leq M \times (1 - Bool_{char_t}) \ \forall t \tag{3.23}$$

$$P_{discharge_t} \geq -M \times Bool_{dis_t} \ \forall t \tag{3.24}$$

$$Bool_{char_t} + Bool_{dis_t} \leq 1 \ \forall t \tag{3.25}$$

Additionally, auxiliary variables are required to quantify the excess and missing energy, measured in kWh, of the system at every time step. These variables are denoted as $E_{excess_t}$ $E_{missing_t}$ and are both constrained to be non-negative.

$$E_{excess_t} \geq 0 \ \forall t \tag{3.26}$$

$$E_{missing_t} \geq 0 \ \forall t \tag{3.27}$$

Conditional constraints, that identify at every moment $t$, if there is excess or deficit of energy, need to be included in the model. Equations 3.28 and 3.29 represent these constraints. When the PV production exceeds the load demand, the system has excess energy, while a deficit of energy occurs when the PV production is insufficient to meet the demand.

$$E_{excess_t} = \begin{cases} PV_t - E_{demand_t}, & \text{if } PV_t > E_{demand_t} \\ 0, & \text{otherwise} \end{cases} \quad \forall t \tag{3.28}$$

$$E_{missing_t} = \begin{cases} E_{demand_t} - PV_t, & \text{if } PV_t < E_{demand_t} \\ 0, & \text{otherwise} \end{cases} \quad \forall t \tag{3.29}$$

Lastly, it is essential to incorporate in the model some constraints that define how surplus and deficit of energy are managed within the system. Specifically, when there is an excess of energy, it can be either used to charge the battery or fed into the grid. In contrast, in the case of an energy deficit, the additional energy required can be obtained by discharging the battery or importing energy from the grid. Under these conditions, discharging the battery to export energy to the grid or importing energy to charge the battery is not possible. This assumption is made to ensure that the battery's usage does not impact negatively its lifetime. Equations 3.30 and 3.31 describe these constraints.

$$(P_{charge_t} + |P_{export_t}|) \times t_{step} = E_{excess_t} \ \forall t \tag{3.30}$$

$$(P_{import_t} + |P_{discharge_t}|) \times t_{step} = E_{missing_t} \ \forall t \tag{3.31}$$

## 3.3 Battery Sizing Optimization: Single-Objective Approach

In this section, the methodology for the single objective optimization model is presented. The considered objectives are cost minimization, $CO_2$ emissions minimization, self-sufficiency maximization and self-consumption maximization.

### 3.3.1 Cost Minimization Objective

The objective of cost minimization aims at determining the optimal capacity of the battery system while minimizing the total investment, operational and maintenance costs over a specified analysis period. This approach attempts to find the most cost-effective size of the battery system.

For the purpose of this assignment, various scenarios with respect to cost minimization are examined. These scenarios can provide insight into how market prices and regulatory policies influence the feasibility of PV-battery systems. The six considered scenarios are the following:

- S1: Baseline scenario with fixed electricity prices
- S2: Fixed electricity prices scenario under net metering scheme
- S3: Dynamic prices scenario
- S4: Fixed electricity prices without any economic benefit from exporting surplus energy to the grid
- S5: Scenario with constraints on exported energy
- S6: Peak shaving scenario

**S1: Baseline Scenario with Fixed Electricity Prices**
In order to determine the optimal battery size, multiple economic parameters need to be defined. Firstly, the investment cost of the battery is a factor that can significantly affect the final result. With the price of lithium-ion batteries continually decreasing, the investment cost for small-scale battery storage is determined at 200€/kWh [55] [56] [57] [58]. Additionally, maintenance costs for lithium-ion batteries typically range between 6 and 13€/kW per year, with an average value of 10€/kW per year being used in the model [59]. Additionally, fixed costs associated with electricity imports and exports need to be specified. For non-household consumers, the purchase cost of electricity is 0.24€/kWh [60], while the feed-in tariff is set at 0.07€/kWh [61].

Table 3.3 shows the defined parameters for the baseline scenario of the cost minimization objective and their corresponding values.

| Parameters | Value |
|---|---|
| Investment ($I_{init}$) | 200€/kWh |
| Maintenance cost ($Cost_m$) | 10€/kW/year |
| Cost of buying electricity ($Cost_{im}$) | 0.24€/kWh |
| Feed-in tariff ($Cost_{ex}$) | 0.07€/kWh |

TABLE 3.3: Defined parameters for the baseline scenario of the cost minimization objective model.

Regarding the objective function and considering that the time resolution of the model is hourly, the investment and maintenance costs need to be adjusted accordingly. Therefore, if $I_{init}$ and $Cost_m$ represent the initial investment cost and the yearly maintenance costs, respectively, accounting for the battery's expected lifetime of 12.5 years as discussed in

Section 3.2, these costs need to be converted into hourly values. With $I_{init_h}$ and $Cost_{m_h}$ being the hourly investment and maintenance costs, respectively, the objective function for the scenario of fixed electricity prices can be described by Equation 3.32.

$$\text{Total cost} = \sum_{t=0}^{T}(P_{import_t} \times t_{step}) \times Cost_{im} + \sum_{t=0}^{T}(P_{export_t} \times t_{step}) \times Cost_{ex} + (I_{init_h} + Cost_{m_h}) \times C_B \times T \tag{3.32}$$

**S2: Fixed Electricity Prices Scenario under Net Metering Scheme**

The parameters for the scenario with fixed electricity prices along with net metering scheme are identical to the baseline scenario, shown in Table 3.3. Nevertheless, some additional constraints need to be defined and the objective function requires some adjustments.

Under the net metering scheme, consumers with renewable energy systems are billed based on their net electricity usage. If they consume more electricity than they generate over a time period, they are charged for the additional imported energy. In contrast, if the energy generated exceeds their total consumption, they receive a credit on their bill. However, whether a system imports more electricity than it exports over the analysis period or vice versa is unknown in advance, meaning that both cases need to be considered. Equation 3.33 describes that when the total exported power over the period T exceeds the total imported power over the same period T, then the net electricity usage will be compensated at the rate of $Cost_{ex}$ per kWh. Conversely, if the energy imports exceed the exports, the system owner will be charged at the rate of $Cost_{im}$ per kWh.

$$cost = \begin{cases} Cost_{ex}, & \text{if } \sum_{t=0}^{T}(P_{import_t}) < \sum_{t=0}^{T}(|P_{export_t}|) \\ Cost_{im}, & \text{if } \sum_{t=0}^{T}(P_{import_t}) > \sum_{t=0}^{T}(|P_{export_t}|) \end{cases} \tag{3.33}$$

Regarding the objective function of the model, Equation 3.34 represents the total cost incurred over the analysis period T. For the scenario of fixed electricity prices with net metering, the first part of Equation 3.34, representing the operational cost, indicates how the system owner is charged or compensated based exclusively on the net electricity usage of the system. The second part of the objective function refers to the investment and maintenance cost of the battery system over the analysis period.

$$\text{Total cost} = (\sum_{t=0}^{T} |P_{import_t} + P_{export_t}| \times t_{step}) \times cost + (I_{init_h} + Cost_{m_h}) \times C_B \times T \tag{3.34}$$

**S3: Dynamic Prices Scenario**

For the scenario of dynamic electricity prices, the hourly electricity costs in the Netherlands are obtained from the ENTSO-E platform [34]. The electricity prices during the analysis period are illustrated in Figure 3.2. The average cost of electricity during the analysis period is calculated to be 0.083€/kWh. It can be seen in the graph that the cost of buying electricity from the grid occasionally reaches negative values, particularly during the summer period. This trend is a result of the significant surplus of solar energy being

fed into the electricity grid during periods of high PV production.

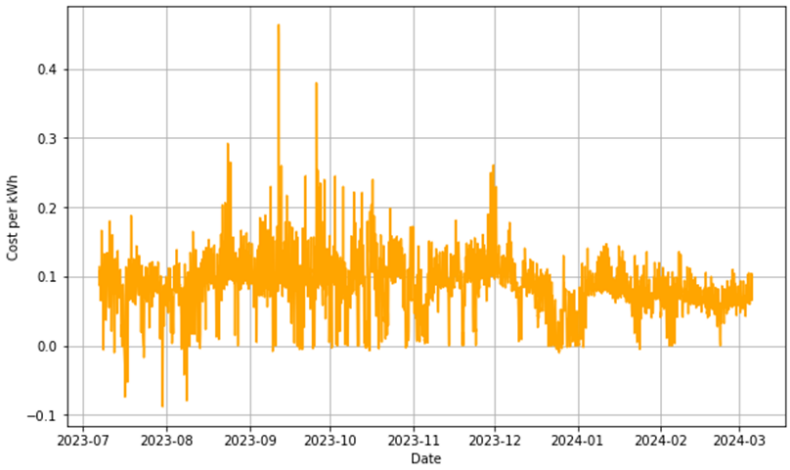


FIGURE 3.2: Dynamic electricity prices from July 2023 to March 2024.

For the scenario of dynamic prices, the investment cost, maintenance cost, as well as the feed-in tariff, are identical to the baseline scenario. However, as the cost of importing energy varies dynamically, the objective function needs to be slightly adjusted (Equation 3.35).

$$\text{Total cost} = \sum_{t=0}^{T}(P_{import_t} \times t_{step} \times Cost_{im_t}) + \sum_{t=0}^{T}(P_{export_t} \times t_{step}) \times Cost_{ex} + (I_{init_h} + Cost_{m_h}) \times C_B \times T \tag{3.35}$$

**S4: Fixed electricity prices without any economic benefit from exporting surplus energy to the grid**

A potential solution to mitigate the grid congestion problem could be the implementation of zero feed-in tariffs. In this case, the renewable energy producers are not compensated for energy exported to the grid. They are encouraged to consume the generated energy locally or store it for later use rather than exporting it into the grid, reducing in this way the grid load. In a future scenario, where exported energy to the grid is no longer compensated, the role of the battery storage system becomes crucial.

For this scenario, the parameter $Cost_{ex}$, which represents the compensation rate for exported energy, obtains a value of zero. Aside from this, the inputs of the model remain the same with respect to the baseline scenario. Taking into consideration that there is no financial benefit for exporting energy to the grid, the objective function can be described by Equation 3.36.

$$\text{Total cost} = \sum_{t=0}^{T}(P_{import_t} \times t_{step}) \times Cost_{im} + (I_{init_h} + Cost_{m_h}) \times C_B \times T \tag{3.36}$$

**S5: Scenario with Constraints on Exported Energy**

As a result of the restricted grid capacity nowadays, grid operators implement constraints on the amount of energy that can be fed into the electrical grid in order to assure stability and reliability in the network [62]. Such limitations can significantly affect the operational strategy of PV-battery systems, leading to a very rigid operational plan. To provide flexibility to the model, it is decided to permit curtailment of solar energy in this scenario. By allowing curtailment, an excess amount of PV energy, that can not be directly consumed or stored in the battery for later use, is curtailed, ensuring that the system remains technically and economically efficient.

For this scenario, all the parameters defined in the baseline scenario are applied. However, a constraint that limits the amount of exported energy needs to be introduced in the model. The constraint will limit the exported energy at every time step to the baseline scenario's corresponding average value $X$ in order to avoid the excessive export of energy to the grid, particularly during peak solar generation hours. The constraint can be described as:

$$P_{export_t} \leq X \ \forall t \tag{3.37}$$

Additionally, with the introduction of curtailment in the model, the energy balance of the system, described by Equation 3.15, needs to be adjusted. Equation 3.38 describes the adjusted energy balance for this scenario.

$$P_{grid_t} \times t_{step} = E_{demand_t} - PV_t + (P_{charge_t} + P_{discharge_t}) \times t_{step} + E_{curt_t} \quad \forall t \tag{3.38}$$

where $E_{curt_t}$ is the amount of solar energy that is curtailed at moment $t$.

Nevertheless, energy curtailment needs to be penalized. For this study, it is assumed that curtailment occurs at the meter level, specifically in the coupling point with the grid, meaning that curtailment does not necessarily lead to the PV system being turned off. Thus, solar energy may be produced and wasted. The cost of curtailment ($Cost_{curt}$) is defined as the potential revenue lost from not selling the curtailed energy to the grid, along with the production cost, which is equivalent to the LCOE for PVs. With respect to the average LCOE of a small rooftop PV system, it equals 0.08€/kWh [63].

Regarding the objective function for this scenario, the penalty cost of curtailed energy must be included in addition to the baseline scenario components. The objective function is represented by Equation 3.39.

$$\begin{aligned} \text{Total cost} = &\sum_{t=0}^{T}(P_{import_t} \times t_{step}) \times Cost_{im} + \sum_{t=0}^{T}(P_{export_t} \times t_{step}) \times Cost_{ex} \\ &+ (I_{init_h} + Cost_{m_h}) \times C_B \times T \\ &+ \sum_{t=0}^{T} E_{curt_t} \times Cost_{curt} \end{aligned} \tag{3.39}$$

**S6: Peak Shaving Scenario**

Peak shaving is an energy management technique used to reduce peak electricity imports and exports, thus preventing spikes in grid interaction [64]. This approach, when combined

with a storage method, can be used to achieve grid stability [64].

In order to incorporate the peak shaving strategy into the battery sizing optimization algorithm, restrictions on energy imports and exports need to be set. Similarly to the scenario with constraints on exported energy, the exported and imported energy at every moment $t$ need to be limited in the average corresponding values of the baseline scenario.

$$P_{export_t} \leq X \ \forall t \tag{3.40}$$

$$P_{import_t} \leq Y \ \forall t \tag{3.41}$$

Without the option of energy curtailment, the model may result in a rigid operational plan. To introduce operational flexibility, the curtailment of PV energy is permitted and Equation 3.38 is also incorporated in this scenario.

For this scenario, all the parameters defined in the baseline scenario are applied. Furthermore, the objective function of the model is described by Equation 3.42. In addition to the baseline objective function components, the curtailment cost of PV energy and a quadratic function of the total grid energy per interval is included. The last term assures that the import and export peaks are penalized, resulting in this way into a smoother energy profile [65]. It should be mentioned that the quadratic term in the objective function transforms the problem into a Mixed Integer Quadratic Programming (MIQP) problem. Nevertheless, the used solver is capable of handling this problem type, thus no additional modifications are required in the model [66].

$$\begin{aligned} \text{Total cost} = & \sum_{t=0}^{T} (P_{import_t} \times t_{step}) \times Cost_{im} + \sum_{t=0}^{T} (P_{export_t} \times t_{step}) \times Cost_{ex} \\ & + (I_{init_h} + Cost_{m_h}) \times C_B \times T \\ & + \sum_{t=0}^{T} E_{curt_t} \times Cost_{curt} \\ & + \sum_{t=0}^{T} ({P_{grid_t}}^2 \times t_{step}) \end{aligned} \tag{3.42}$$

As the peak shaving penalty does not represent a real cost, to ensure that each term of the objective function contributes appropriately to the overall objective, scaling factors are essential. For this reason, each component is divided by its maximum value derived from the model prior to optimization.

Figure 3.3 graphically illustrates the inputs and outputs of the cost minimization model across all the scenarios, providing a summary of the section.

### 3.3.2 $CO_2$ Emissions Minimization Objective

The objective of $CO_2$ emissions minimization aims to find the optimal battery capacity that minimizes the total $CO_2$ emissions of the system. Taking into consideration the carbon intensity of the imported grid energy and the $CO_2$ emissions associated with the battery

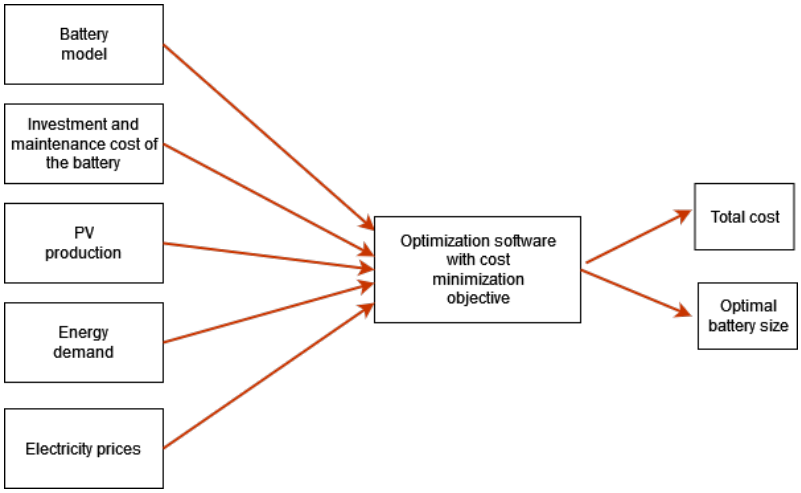


FIGURE 3.3: Inputs and outputs for the cost minimization objective model.

system and the generated PV energy, the model with this objective aims to minimize the overall carbon footprint of the system by optimizing the usage of both grid electricity and battery storage.

With 48% of the Dutch grid electricity being produced by renewable sources of energy in 2023 [67], the average carbon intensity of the Dutch grid electricity in the same year was determined at 301 gr $CO_2$eq./kWh [11]. This number refers to the amount of $CO_2$ emissions produced per unit of electricity generated. However, as shown in Figure 3.4, the hourly carbon intensity of the Dutch electricity mix fluctuates significantly. At moments of high renewable energy production, the carbon intensity drops to 50 gr $CO_2$eq./kWh. For more accurate results, the model incorporates, as parameter, the dynamic carbon intensity of the Dutch grid electricity.

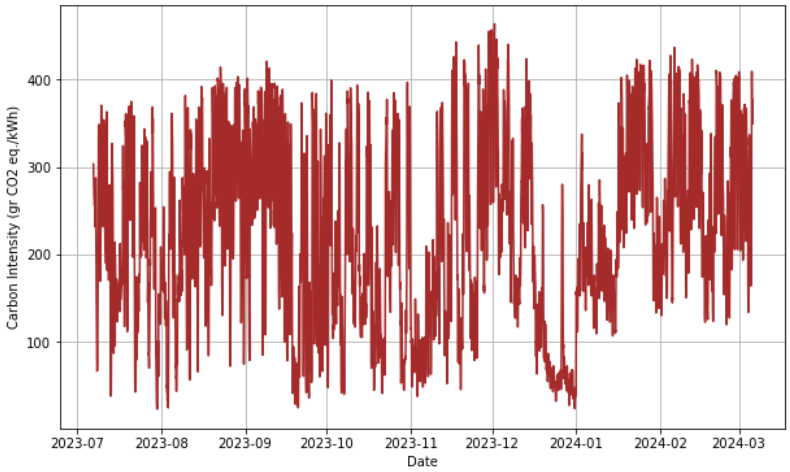


FIGURE 3.4: Dynamic carbon intensity in gr $CO_2$eq./kWh of the Dutch grid electricity from July 2023 to March 2024. [11].

On the other hand, during the production, operational and recycling phase of a lithium-ion battery, the $CO_2$ emissions are estimated to be 62 kg $CO_2$eq./kWh [68] [69]. It should be

noted that this number refers to the emissions associated with storing renewable energy in lithium-ion batteries, thus the operational emissions are negligible. Out of the total battery $CO_2$ emissions, 56 kg $CO_2$eq./kWh are allocated to the production phase, while the remaining emissions are related to the end-of-life phase of the battery [69]. However, since the carbon intensity of grid electricity refers to emissions per generated energy, in order to ensure a fair comparison, only the emissions associated with the production phase of the battery are taken into account in the model.

In addition to the emissions from the production phase of lithium-ion batteries, the emissions associated with the generation of energy by the PV system should be also incorporated in the model. A typical rooftop PV system emits approximately 41 g $CO_2$eq./kWh of energy generated [70]. Similarly to the battery, emissions related to PV energy arise from the manufacturing of PV panels rather than their operational phase.

While emissions from grid electricity and PV energy generation are related to electricity usage, the battery's emissions (56 kg $CO_2$eq./kWh) refer to the emissions associated with the battery capacity of the system. This means that 56 kg $CO_2$eq./kWh are the total emissions over the lifetime of the battery. Therefore, the distributed $CO_2$ emissions during the operation of the system need to be defined. For this reason, the $CO_2$ emissions per kWh of battery capacity are converted to $CO_2$ emissions per kWh of stored energy, as shown in Equation 3.43.

$$CO_{2_{bat}} = \frac{C_B \times CO_{2_{prod}}}{C_B \times N_{cycles}} \tag{3.43}$$

where $CO_{2_{bat}}$ and $CO_{2_{prod}}$ are the variables representing the $CO_2$ emissions per kWh of stored energy and the total emissions during the production phase of the battery, equal to 56 kg $CO_2$eq./kWh, respectively and $C_B$ is the battery capacity in kWh. The denominator of Equation 3.43 refers to the total energy stored in the battery over its lifetime in kWh. This value is equivalent to the maximum possible total energy stored in each cycle, assuming it equals the battery capacity, multiplied by the number of cycles over the battery's lifetime, $N_{cycles}$. Given the assumption that the battery is fully charged to its maximum possible capacity once daily over its lifetime and the expected lifetime of the battery is set at 12.5 years, the number of cycles during its lifespan is equal to 4,562.5. Thus, Equation 3.43 can be written, as shown:

$$CO_{2_{bat}} = \frac{CO_{2_{prod}}}{N_{cycles}} = \frac{56\ kg\ CO_2eq./kWh}{4,562.5} = 12.27 \text{ gr } CO_2\text{eq./kWh} \tag{3.44}$$

The emissions associated with the grid electricity, lithium-ion battery and PV system are the additional parameters that need to be set as inputs in the $CO_2$ minimization objective model (Table 3.4).

| **Parameters** | **Value** |
|---|---|
| Electricity grid carbon intensity ($CO_{2_{grid,t}}$) | Dynamic prices (Figure 3.4) |
| Battery $CO_2$ emissions ($CO_{2_{bat}}$) | 12.27 gr $CO_2$eq./kWh |
| PV system $CO_2$ emissions ($CO_{2_{PV}}$) | 41 gr $CO_2$eq./kWh |

TABLE 3.4: Defined parameters in the $CO_2$ emissions minimization objective model.

The objective function of this optimization problem is described in Equation 3.45. When energy is imported from the grid, the system emits the $CO_2$ equivalent emissions of the grid electricity generation. In contrast, when battery is discharged, meaning that energy becomes available to the system, it emits $CO_2$ equivalent emissions reflective of the production phase of the battery. Similarly, emissions from PV energy generation are associated with the manufacture of solar panels.

$$\text{Total } CO_2 \text{ emissions} = \sum_{t=0}^{T}(P_{import_t} \times CO_{2_{grid,t}}) \times t_{step} + \sum_{t=0}^{T}(P_{discharge_t} \times CO_{2_{bat}}) \times t_{step} + \sum_{t=0}^{T}(PV_t \times CO_{2_{PV}}) \tag{3.45}$$

In Figure 3.5, the inputs and output of the $CO_2$ emissions minimization model can be seen.

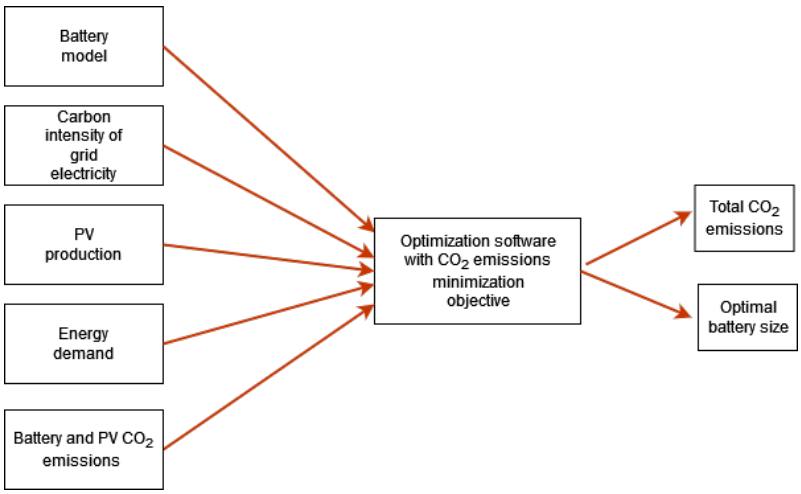


FIGURE 3.5: Inputs and outputs for the $CO_2$ emissions minimization objective model.

### 3.3.3 Self-Sufficiency Maximization Objective

Self-sufficiency is a metric indicating the degree of a system's independence from the grid by measuring the percentage of energy demand met by locally generated resources in relation to the total demand [62]. The optimization model with a self-sufficiency maximization objective aims to maximize the system's autonomy and reduce reliance on external energy sources, such as the electricity grid.

Since self-sufficiency is a metric that does not depend on external factors, such as electricity prices, investment costs or $CO_2$ emissions, the model with a self-sufficiency maximization objective aims to internally shift the operational pattern of the system in order to achieve its goal. Therefore, no additional parameters need to be defined in the model. Figure 3.6 shows the inputs and outputs of the algorithm.

The objective function can be described by Equation 3.46. Self-sufficiency can be quantified as the percentage of the total demand that is not covered by energy imported from the grid [71]. A higher percentage signifies a higher degree of self-sufficiency, indicating that a larger portion of the system's energy demand is met by the generated PV energy. In

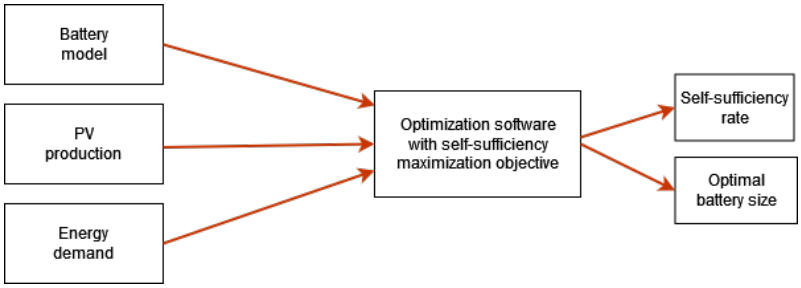


FIGURE 3.6: Inputs and outputs for the self-sufficiency maximization objective model.

contrast, a lower percentage indicates increased dependence on energy imports from the grid.

$$SS = 1 - \frac{\sum_{t=0}^{T}(P_{import_t} \times t_{step})}{\sum_{t=0}^{T}(E_{demand_t})} \times 100\% \tag{3.46}$$

### 3.3.4 Self-Consumption Maximization Objective

Self-consumption is the percentage of electricity locally generated and consumed, either immediately or stored in a battery for later use, with respect to the total energy generation [62]. The objective of maximizing self-consumption involves minimizing the surplus energy exported to the grid, maximizing in this way the direct utilization of the on-site generated energy. As a result, the system's autonomy and independence from the grid can be enhanced, reducing the reliance of the system on the fluctuating market conditions.

Similarly to the objective of self-sufficiency maximization of Section 3.3.3, the self-consumption ratio does not rely on external factors but only on the operational strategy of the system. Figure 3.7 shows the inputs and outputs of the algorithm for this optimization objective.

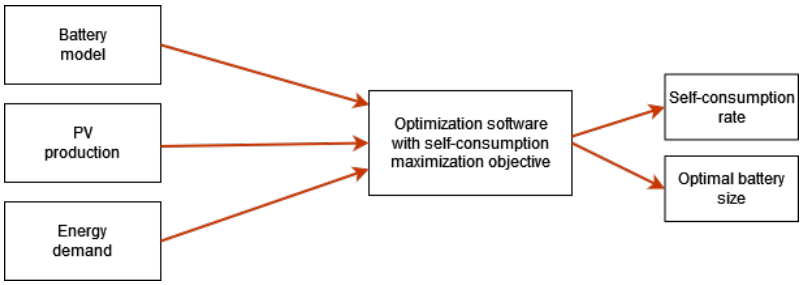


FIGURE 3.7: Inputs and outputs for the self-consumption maximization objective model.

A higher self-consumption rate can be achieved by minimizing the amount of PV energy exported to the electricity grid and consequently, maximizing the on-site utilization of the produced energy. Equation 3.47 shows this relationship and serves as the objective function of the model.

$$SC = 1 - \frac{\sum_{t=0}^{T}(|P_{export_t}| \times t_{step})}{\sum_{t=0}^{T}(PV_t)} \times 100\% \tag{3.47}$$

Figures 3.8 and 3.9 show an example of a daily operational plan of a PV-battery system, clarifying the difference between self-consumption and self-sufficiency [62]. Self-sufficiency is the percentage of the total energy demand that was met by locally generated sources, as indicated by the shaded grey area divided by the sum of the grey and blue areas. On the other hand, self-consumption is the ratio of the total PV energy produced that was used within the system and not exported to the electricity grid, calculated as the ratio of the subtraction of the green and yellow area to the green area. The shadowed areas in the graphs serve as the input values for calculating the respective percentages of self-sufficiency and self-consumption. In the example provided, self-sufficiency and self-consumption are calculated to be 0.23% and 0.97%, respectively. The result indicates that a system can be characterized by high self-consumption and simultaneously by low self-sufficiency, or vice versa, meaning that the two metrics are not inherently interdependent.

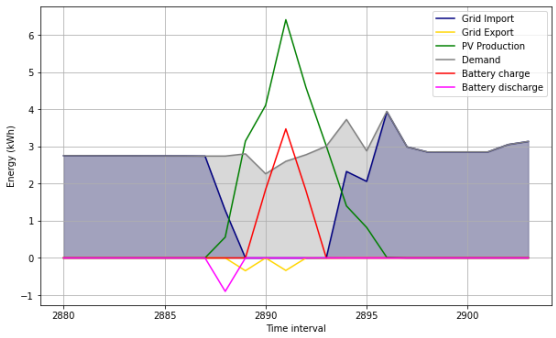


FIGURE 3.8: Generic example of self-sufficiency rate calculation.

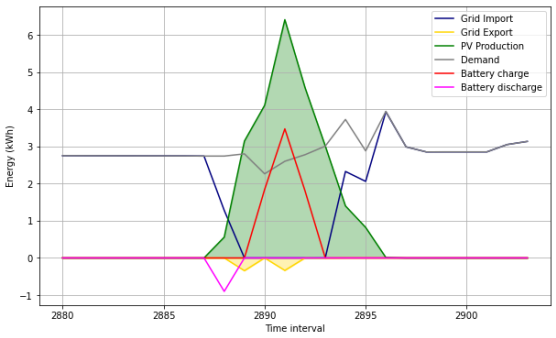


FIGURE 3.9: Generic example of self-consumption rate calculation.

## 3.4 Battery Sizing Optimization: Multi-Objective Approach

The methodology for the multi-objective optimization, also known as co-optimization, is outlined in this section. Co-optimization is performed in pairs, coupling cost minimization with one of the following objectives: $CO_2$ emissions minimization, self-sufficiency maximization or self-consumption maximization. The cost minimization objective is incorporated into all the models, as cost is a crucial decision-making factor in manufacturing industry.

For the co-optimization process, the weighted sum method is followed. This method combines all the single objective functions into one scalar, by assigning weights, namely weighting coefficients, to each objective [72]. These weights indicate the importance of each objective relative to the others.

### 3.4.1 Co-Optimization of Cost and $CO_2$ Emissions

The combined objective function for the objectives of cost minimization and $CO_2$ emissions minimization can be described by Equation 3.48:

$$MOF_{CO_2} = w_1 \times \text{Total cost} + w_2 \times \text{Total } CO_2 \text{ emissions} \tag{3.48}$$

where *Total cost* and *Total* $CO_2$ *emissions* are the individual objective functions and $w_1$ and $w_2$ are the weighting coefficients which need to be positive and satisfy the following constraint [72]:

$$\sum_{i=1}^{N} w_i = 1, \; w_i \in (0, 1) \tag{3.49}$$

However, given the substantial difference in magnitudes between the *Total cost* function and the *Total* $CO_2$ *emissions* function, normalization of both individual objective functions becomes necessary. The normalisation can be achieved by dividing each objective function by its optimum value in the single objective optimization, thus resulting in a dimensionless objective function. Therefore, Equation 3.48 can be reformulated as:

$$MOF_{CO_2} = w_1 \times \frac{\text{Total cost}}{cost_{opt}} + w_2 \times \frac{\text{Total } CO_2 \text{ emissions}}{CO_{2_{opt}}} \tag{3.50}$$

with $cost_{opt}$ and $CO_{2_{opt}}$ being the resulting optimal values of the cost minimization and $CO_2$ emissions minimization individual models, respectively.

### 3.4.2 Co-Optimization of Cost and Self-Sufficiency

Similarly to Section 3.4.1, the objective function for the co-optimization of cost and self-sufficiency can be represented by Equation 3.51. However, unlike the previous case, where both objective functions required minimization, in this case, the cost needs to be minimized, whereas the self-sufficiency rate needs to be maximized. For this reason, self-sufficiency is represented by its negative value, indicating the aim for minimization.

$$MOF_{SS} = w_1 \times \text{Total cost} - w_2 \times \text{SS} \tag{3.51}$$

The normalised objective function for co-optimization of the total cost of the system and its self-sufficiency rate is described by Equation 3.52.

$$MOF_{SS} = w_1 \times \frac{\text{Total cost}}{cost_{opt}} - w_2 \times \frac{\text{SS}}{SS_{opt}} \tag{3.52}$$

where $SS_{opt}$ is the resulting optimal value of the self-sufficiency maximization model.

### 3.4.3 Co-Optimization of Cost and Self-Consumption

The objective function for co-optimization of the total cost and the self-consumption rate of the PV-battery system can be seen below:

$$MOF_{SC} = w_1 \times \text{Total cost} - w_2 \times \text{SC} \tag{3.53}$$

Similarly to the previous sections, the normalised objective function for the co-optimization of the total cost of the system and the self-consumption rate is shown in Equation 3.54.

$$MOF_{SC} = w_1 \times \frac{\text{Total cost}}{cost_{opt}} - w_2 \times \frac{\text{SC}}{SC_{opt}} \tag{3.54}$$

where $SC_{opt}$ is the resulting optimal value of the self-consumption maximization model.

## 3.5 $CO_2$ Emissions Calculation

To determine the environmental impact of the resulting optimal systems, it is necessary to define their $CO_2$ emissions. This process involves applying the principles described in Section 3.3.2.

The total emissions can be allocated between the emissions from the import of grid energy, the PV power production and the energy stored in the battery. While Equations 3.55 , 3.56 and 3.57 describe the emissions of the three subsystems, Equation 3.58 outlines the total $CO_2$ emissions of the system.

$$\text{Grid emissions} = \sum_{t=0}^{T} (P_{import_t} \times CO_{2_{grid,t}}) \tag{3.55}$$

$$\text{PV emissions} = \sum_{t=0}^{T} (PV_t \times CO_{2_{PV}}) \tag{3.56}$$

$$\text{Battery emissions} = \sum_{t=0}^{T} (P_{discharge_t} \times CO_{2_{bat}}) \tag{3.57}$$

$$\text{Total emissions} = \text{Grid emissions} + \text{PV emissions} + \text{Battery emissions} \tag{3.58}$$

The parameters $CO_{2_{grid,t}}$, $CO_{2_{PV}}$, and $CO_{2_{bat}}$, defined in Section 3.3.2, represent carbon intensity of grid energy, PV energy and energy storage, respectively.

## 3.6 Financial Analysis

In order to evaluate the financial feasibility of the optimal battery systems, it is essential to analyse metrics, such as the payback time, return on investment and net present value of the investment. In this section, the methodology for the calculation of these metrics is described.

### 3.6.1 Payback Time

Payback time refers to the length of time required for the cost of an investment to be recovered [73]. It represents the point where the accumulated benefits of an investment offset its initial cost. The metric can be calculated using the following formula:

$$\text{Payback time} = \frac{\text{Cost of Investment}}{\text{Annual Cash Flow}} \tag{3.59}$$

where *Cost of Investment* is the upfront expenditure of the battery system and *Annual Cash Flow* refers to the yearly savings after the incorporation of the battery system which are influenced by multiple factors, such as electricity prices, regulatory constraints and maintenance costs.

### 3.6.2 Return on Investment

Return on Investment (ROI) is a performance measure of an investment's efficiency and profitability [74]. ROI is expressed as a percentage that measures the return of a particular investment relative to the investment's cost [74]. In general, investments with positive ROI

are considered profitable, as in this case, the returns generated exceed the initial investment cost. The metric can be described by Equation 3.60.

$$\text{ROI} = \frac{\text{Net Profit}}{\text{Cost of Investment}} \tag{3.60}$$

where *Net Profit* refers to the accumulated savings generated by the investment over the analysis period and *Cost of Investment* is the upfront expenditure of the battery system.

### 3.6.3 Net Present Value

Net Present Value (NPV) is a financial metric that is used to evaluate the profitability of an investment [75]. The metric is the result of computations that determine the present worth of a future series of payments using an appropriate discount rate [75]. A positive NPV signifies that the expected earnings exceed the expected costs, meaning that the investment is profitable over its lifetime, while a negative NPV indicates the opposite [75]. In contrast to simpler metrics, such as payback time and ROI, NPV can result in more accurate results, as it accounts for the time value of money [75]. NPV can be calculated based on the following equation:

$$\text{NPV} = \sum_{t=0}^{n} \frac{\text{Cash Flow at period } t}{(1+i)^t} \tag{3.61}$$

where *Cash Flow at period t* refers to the annual cash flows resulting from the incorporation of the battery system and $i$ is the long-term interest rate, which is determined at 2.62% for the Netherlands, as of March 31, 2024 [76].

## 3.7 Lifelong Analysis

Since the aim of the battery sizing optimization algorithm is the design of a system with an optimal battery capacity that will be used for approximately 12.5 years, it is insightful to perform the analysis for the entire lifespan of the battery, including in the model factors, such as PV and battery degradation, demand growth, cost variations and regulatory changes.

For this purpose, the PV and demand data, used for the analysis, need to be projected over the expected lifetime of the battery, thus 12.5 years. The model assumes a PV degradation rate of 2.5% during the first year and an additional annual decrease in the PV performance of 1% [77]. Regarding the electricity demand, it is expected to increase annually by 1.4% within the following years in the European Union [78]. For the analysis, it is assumed that this annual demand growth remains constant over the lifetime of the battery. Additionally, the degradation of the battery needs to be incorporated into the model, as it can decrease the available battery capacity over time. Each cycle of the battery is assumed to have Coulombic efficiency of 0.999954, meaning that the degradation rate per cycle is 0.000046 [79]. Under the assumption that the system undergoes one full cycle per day, the amount of the occurring degradation per time step (hourly) can be calculated as:

$$d_{rate} = \frac{0.000046 \times 365}{365 \times 24} = 1.916 \times 10^{-6} \tag{3.62}$$

In order for the model to account for the battery degradation, some additional constraints need to be added. Equation 3.63 counts for the available battery capacity ($C_{av_t}$) at every time step, as follows:

$$C_{av_t} = C_{av_{t-1}} \times (1 - d_{rate}) \; \forall \; t > 1 \tag{3.63}$$

where $C_{av_{t-1}}$ is the available battery capacity in the previous time step and $d_{rate}$ is the constant hourly degradation rate. For $t = 0$, the available battery capacity equals the initial battery size.

$$C_{av_0} = C_B \tag{3.64}$$

Besides the constraints addition, the upper limit of the energy that can be stored in the battery ($E_t$) needs to be adjusted to count for the available battery capacity, rather than the initial capacity (Equation 3.65).

$$E_t \leq C_{av_t} \times (1 - DoD) \; \forall t \tag{3.65}$$

Similarly, for the calculation of the maximum battery power ($P_{max}$), the initial battery size should be replaced by the available battery capacity at every moment $t$ (Equation 3.66).

$$P_{max} = C_{rate} \times C_{av_t} \; \forall t \tag{3.66}$$

For the cost minimization scenarios, the cost of importing and exporting electricity, as well as the dynamic electricity prices need to be projected into the future. Due to the increasing renewable energy production and the subsequent high amount of energy, that is fed into the grid, electricity prices are expected to decrease over the following years [80]. Figure 3.10 shows the future trend of electricity prices in Europe, which is used in the model for the projection of import and dynamic prices [80].

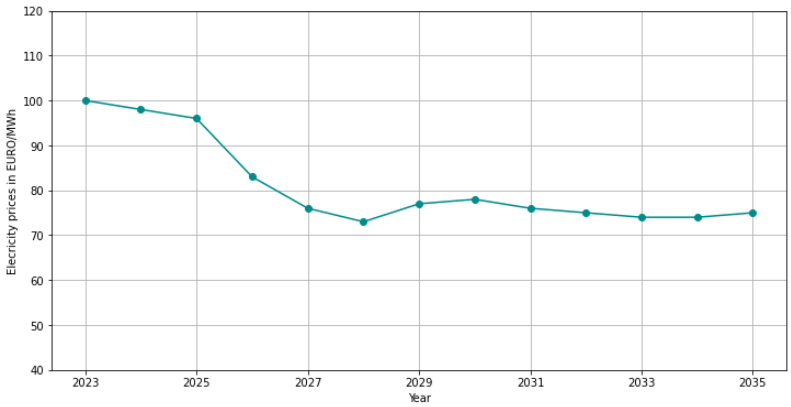


FIGURE 3.10: Development of average electricity prices in Europe over the lifetime of the battery system [80].

Regarding the feed-in tariff, many discussions have been held within the Dutch government concerning the effectiveness of the scheme. Although no clear decision has been made, the value of the feed-in tariff is constantly decreasing and the scheme is gradually being phased out [81]. For this assignment, it is assumed that the annual decrease rate of the feed-in tariff is 9% [82]. As of 2031, the system will no longer receive any tariff for exporting energy to the grid [82].

Similarly, there is high uncertainty regarding the net metering scheme in the Netherlands. Even though it was initially decided that the scheme would phase out in 2023, the latest

information mentions that this will only happen in 2027 [83]. For the corresponding scenario, it is assumed that the application of the net metering scheme will end on January 1, 2027. Until then, the rate of energy subjected to net metering will be 100%.

Since the penetration of electricity from renewable energy sources constantly increases in the grid mix, the $CO_2$ intensity of the grid electricity is anticipated to drop significantly [84]. Therefore, the $CO_2$ emissions of the grid electricity need to be projected accordingly. Specifically, a 77% emissions decrease is expected from 2020 to 2035 in Europe, meaning that the annual emissions reduction is 5.51% [84]. By the end of the battery's lifetime, the $CO_2$ intensity of grid electricity is projected to be as low as 47 g $CO$2eq./kWh [84].

# Chapter 4

# Case Study

In this chapter, the case study for this assignment is described, namely Fraunhofer Innovation Platform for Advanced Manufacturing at the University of Twente. On the rooftop of the building, a PV system is installed, while currently, there is no battery system integrated. The description of the system, as well as the data regarding the PV performance and the consumption profile, are provided in this chapter.

## 4.1 PV System

A PV system with power capacity of 36.9 kWp is installed on the rooftop of the Fraunhofer Innovation Platform for Advanced Manufacturing building at the University of Twente. Positioned at the geographical coordinates with latitude and longitude of 52.2376° N and 6.8479° E, respectively, the PV system aims at a shift towards sustainable energy consumption within the infrastructure of the university.

The system consists of 90 PV modules, each having a maximum power output of 410Wp. The modules are of the "Canadian Solar - TND CS6R-410Wp Black Frame" model, utilizing mono-crystalline technology. Mono-crystalline solar panels offer higher efficiency rates compared to alternative PV technologies, such as thin-film or poly-crystalline panels, allowing for a higher energy production per $m^2$ [85]. Furthermore, mono-crystalline technology performs efficiently under low light conditions, meaning that this type of PV shows enhanced performance in diffuse solar irradiance scenarios [85]. Possible downsides of mono-crystalline panels are the increased cost, the higher shading losses and the waste of silicon during production [85]. The orientation of the PVs is east, implying that their peak production occurs early in the morning.

In Figures 4.1 and 4.2, the configuration of the PV system is illustrated. As can be seen, the rooftop is flat and consists of a tilted Building Applied Photovoltaic (BAPV) system. An important attribute of the system is that the PV array may experience increased shading losses due to the solid structure situated on the southern part of the system and the building walls on the northern part, resulting in possible diminished PV production.

Additionally, Figures 4.3 and 4.4 depict the inverter used in the PV system. The system is equipped with a SolarEdge "SE30K-RW00IBNM4" three-phase inverter with an efficiency of 98.3% [86]. The inverter is installed at the Fraunhofer Innovation Platform for Advanced Manufacturing to convert the DC power generated by the PV system into AC power.

FIGURE 4.1: PV system on the rooftop of Fraunhofer Innovation Platform for Advanced Manufacturing.

FIGURE 4.2: PV system on the rooftop of Fraunhofer Innovation Platform for Advanced Manufacturing.

FIGURE 4.3: Inverter of the PV system of Fraunhofer Innovation Platform for Advanced Manufacturing.


FIGURE 4.4: Inverter of the PV system of Fraunhofer Innovation Platform for Advanced Manufacturing.

In Figures 4.5 and 4.6, the logical and physical layout of the PV-inverter system are illustrated, with data as of July 25, 2024. In these graphs, blue squares represent the PV panels and their corresponding DC energy generation, green squares indicate the DC-to-AC inverter and the purple box represents the AC energy delivered to the building.

The PV production data were sourced from the Application Programming Interface (API) of SolarEdge Cloud-Based Monitoring Platform [87]. The operation of the system was initiated on March 31, 2023. However, the system experienced a breakdown from May 5, 2023, until July 6, 2023, resulting in a lack of data for approximately two months. For this reason, the analysis is decided to be done from July 7, 2023 until March 5, 2024, thus eight months. The data gathered by the API of SolarEdge Cloud-Based Monitoring Platform were provided with an hourly resolution and they are illustrated in Figure 4.7.

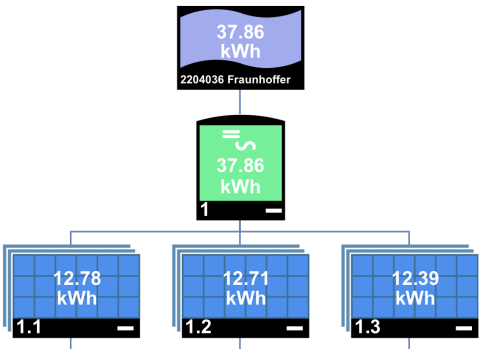


FIGURE 4.5: Logical layout of the PV system of Fraunhofer Innovation Platform for Advanced Manufacturing.

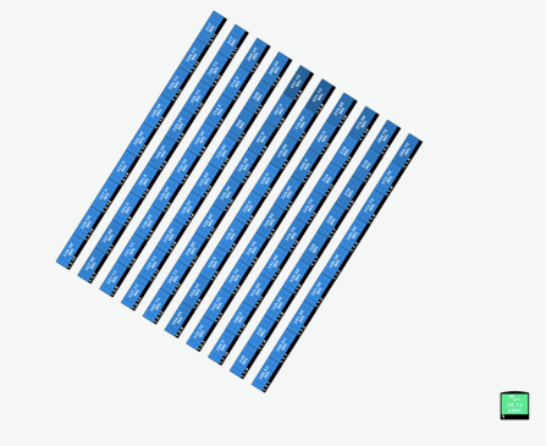

FIGURE 4.6: Physical layout of the PV system of Fraunhofer Innovation Platform for Advanced Manufacturing.

The total PV energy production of the system during the eight-month period amounts to 15.29 MWh.

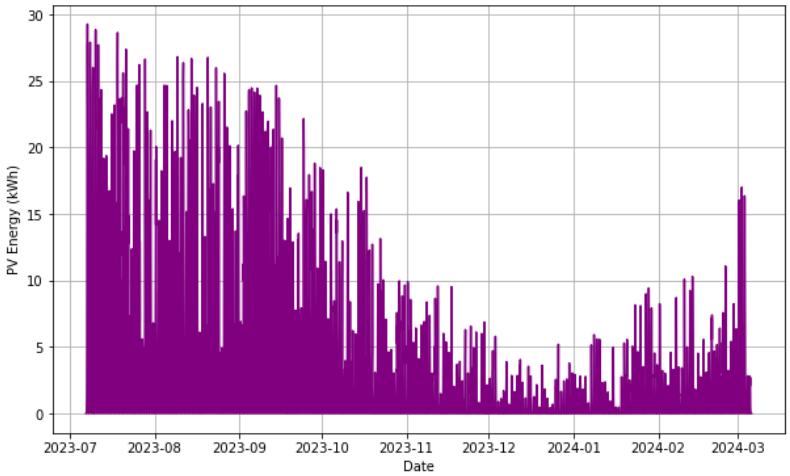


FIGURE 4.7: PV energy production from July 7, 2023 until March 5, 2024.

### 4.1.1 Lifelong Analysis

For the lifelong analysis, the annual PV production data are needed in order to be projected over the expected 12.5 years of the battery lifetime. By the time of the analysis, data are available up to June 25, 2024. To complete a full year, data from PVGIS for the exact location of Fraunhofer Innovation Platform for Advanced Manufacturing have been retrieved for the period from June 26, 2024 until July 6, 2024. In order to count for discrepancies between the actual and PVGIS data, the average difference between the two datasets is calculated and the PVGIS values are adjusted. The annual PV generation profile can be seen in Figure 4.8.

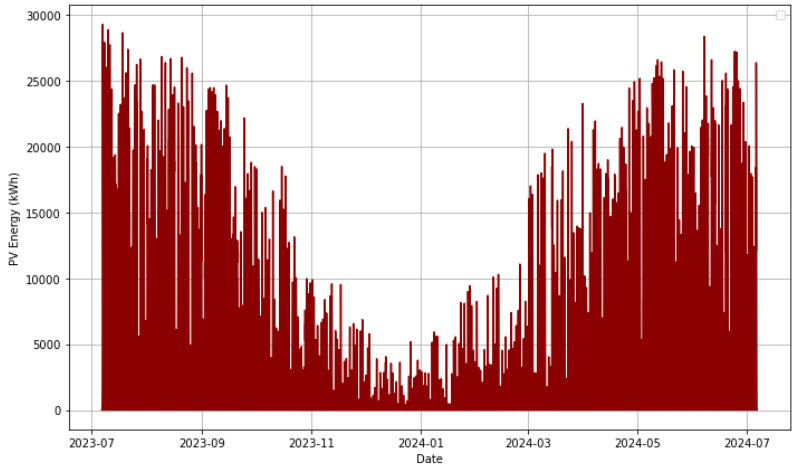


FIGURE 4.8: PV energy production from July 7, 2023 until July 6, 2024.

## 4.2 Consumption Profile

At Fraunhofer Innovation Platform for Advanced Manufacturing, there is currently no smart meter installed, resulting in the absence of recorded information regarding the consumption of electricity within the building. However, a recent addition includes a meter installed specifically for measuring the energy consumption of one of the machines, a 3D printer used for manufacturing titanium objects (Figure 4.9). For this assignment, it is decided that the energy produced by the PV system will be directed towards powering this specific machine. Thus, the resulting manufactured products will be produced using green energy.

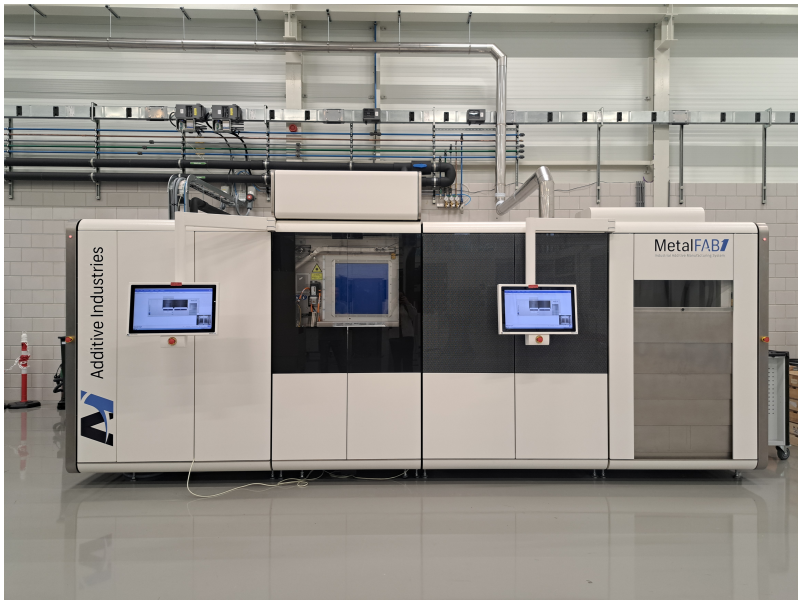


FIGURE 4.9: 3D printer at Fraunhofer Innovation Platform for Advanced Manufacturing.

Nevertheless, the energy consumption data for this machine start from January 11, 2024. Therefore, it is necessary to forecast the energy consumption for the previous months of

the year. Given that the machine is not subjected to seasonal demand variations, it is assumed that the energy demand profile observed from January 11, 2024 to February 10, 2024 is repeated monthly from July 7, 2023 until January 10, 2024. Starting from January 11, 2024, the actual demand profile of the machine is used. Figure 4.10 illustrates the consumption data of the aforementioned machine over the analysis period.

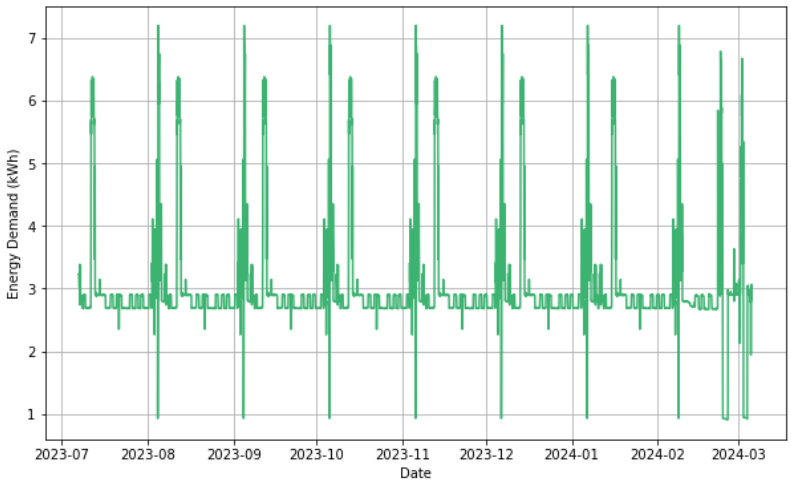


FIGURE 4.10: Consumption data of the 3D printer from July 7, 2023 until March 5, 2024.

### 4.2.1 Lifelong Analysis

By the time of the analysis, five months of consumption data are available. As explained, the demand profile of the machine is independent of seasonal fluctuations, thus it is assumed that the available data repeat every five months. The annual consumption profile for the lifelong analysis is illustrated in Figure 4.11.

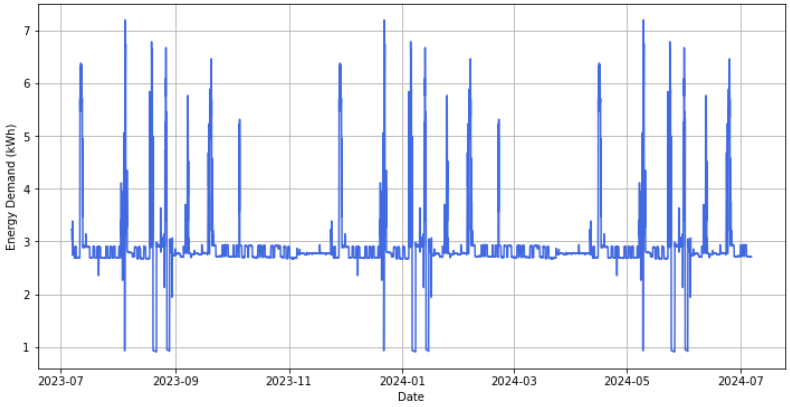


FIGURE 4.11: Consumption data of the 3D printer from July 7, 2023 until July 6, 2024.

# Chapter 5

# Results

In this chapter, the results of the single and multi-objective optimization analysis are displayed. Additionally, the $CO_2$ emissions of the resulting optimal systems are calculated and a financial analysis is conducted. Lastly, the results of the 8-month analysis are compared with the corresponding results of the lifelong analysis.

For this assignment, Gurobi software version 10.0.3 along with the Pyomo library is used to solve the optimization problem within the Python environment. Gurobi optimizer is a useful tool for the formulation and analysis of mathematical models for complex optimization applications. While various packages and libraries, such as Pyomo, are necessary for building the optimization model, Gurobi software is responsible for solving the mathematical optimization and returning the optimized value of the objective function, as well as the final result of the problem's variables to the user [88].

## 5.1 Battery Sizing Optimization: Single-Objective Approach

In this section, the results of the battery sizing optimization model with a single-objective approach are presented. The considered objectives include cost minimization, $CO_2$ emissions minimization, as well as self-sufficiency and self-consumption maximization.

### 5.1.1 Cost Minimization Objective

This section presents the findings of the cost minimization model across six different scenarios: baseline scenario with fixed electricity prices (S1), fixed electricity prices under net metering scheme (S2), dynamic prices scenario (S3), a scenario with fixed electricity prices but without any economic benefit from exporting surplus of energy to the grid (S4), a scenario where constraints on the exported energy are included (S5) and finally a scenario where peak shaving strategy is incorporated (S6).

**S1: Baseline Scenario with Fixed Electricity Prices**
The optimal battery capacity for this scenario is calculated to be 10.2 kWh. Figure 5.1 shows the relation between the battery capacity and the total cost of the system. It can be seen that for a battery capacity of 10.2 kWh, the cost of the system is minimized and it is equal to €2,197. This cost refers to both operational expenses and the distributed investment cost over the eight-month analysis period. Additionally, the graph shows that incorporating a battery leads to a reduction in the total cost of the system. However, beyond a certain battery capacity, the overall cost begins to rise again due to the increase

in the battery's investment cost.

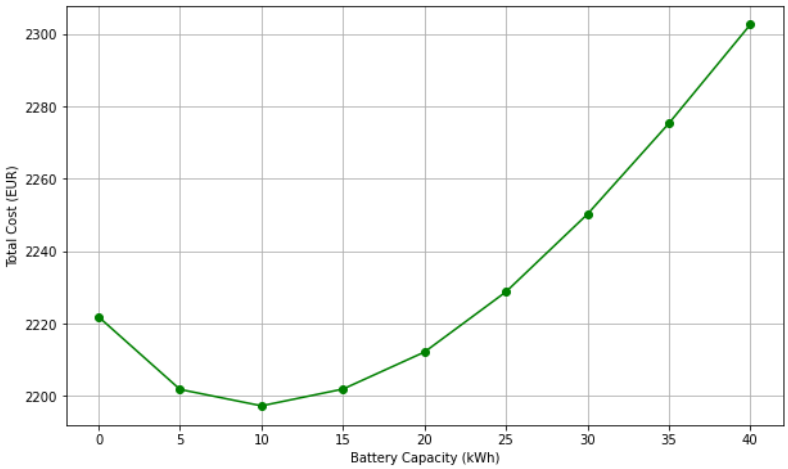


FIGURE 5.1: Relation between the battery capacity and the total cost of the system for scenario S1.

Figures 5.2, 5.3 and 5.4 reveal the operational patterns of the storage system over the eight-month analysis period. It can be seen that during the winter months, the frequency of battery usage decreases compared to the summer months, mainly due to lower PV production. This leads to reduced frequency of charge and discharge cycles, as well as absence of exported energy during the winter period.

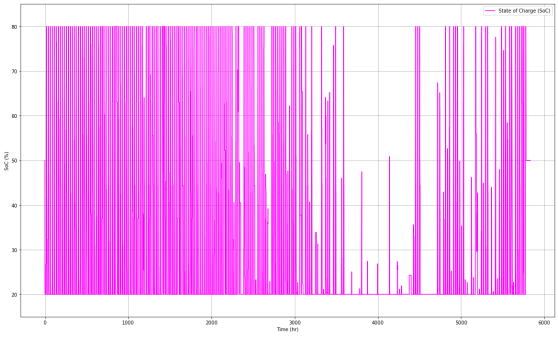

FIGURE 5.2: State of Charge (SoC) pattern during the analysis period for scenario S1.

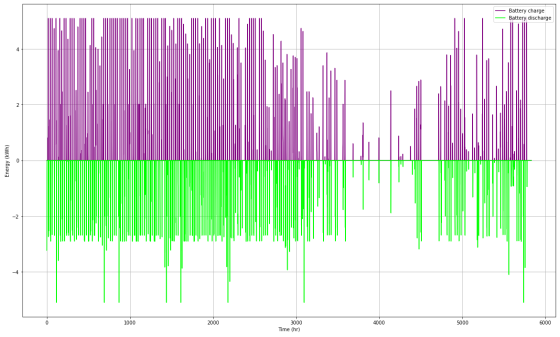

FIGURE 5.3: Charge and discharge pattern during the analysis period for scenario S1.

In order to examine the variations in the operational behaviour of the battery across seasons, a summer and a winter week are analysed. Figures 5.5 and 5.6 depict the battery's State of Charge (SoC) and the import and export patterns during a week in July, while Figures 5.7 and 5.8 illustrate the corresponding metrics for a week in January.

During the summer period, as shown in Figures 5.5 and 5.6, the battery operates at its maximum potential, reaching 80% of its total capacity, as constrained by the $(1 - DoD)$ factor. Additionally, it can be seen that the battery undergoes approximately one complete charge-discharge cycle per day, meaning that the operational life of the battery may be

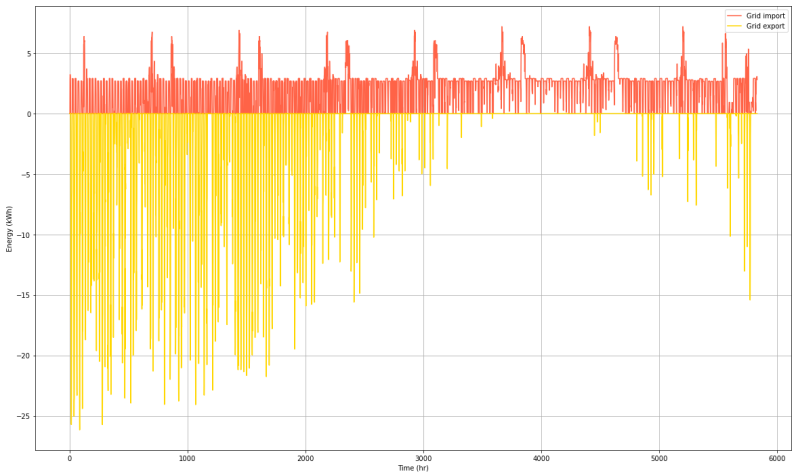


FIGURE 5.4: Import and export pattern during the analysis period for scenario S1.

extended compared to scenarios with a higher number of cycles per day. Regarding energy transactions with the grid, the system exports a significant amount of energy around noon, coinciding with peak PV generation. Additionally, it imports a relatively small amount of energy during the rest of the day in order to supplement the battery and meet the energy demand.

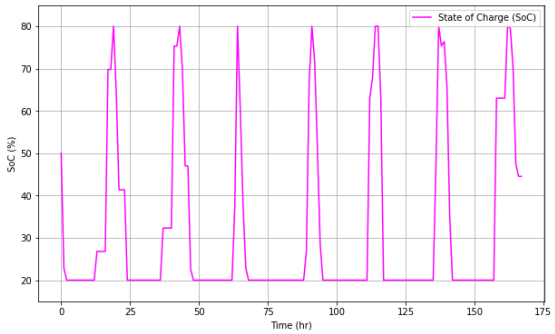


FIGURE 5.5: SoC pattern during the summer week for scenario S1.

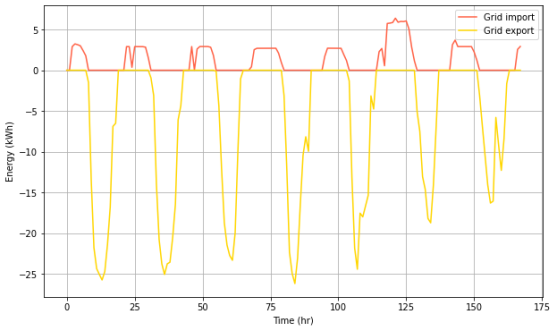


FIGURE 5.6: Import and export pattern during the summer week for scenario S1.

In contrast, during the winter week, the battery does not operate at its maximum potential, undergoing only about three full charge-discharge cycles, as shown in Figure 5.7. On these days, a low amount of energy is fed into the grid, indicating that the PV production around noon along with the battery's discharge is often sufficient to cover the energy demand, as depicted in Figure 5.8. However, for the rest of the week, the battery's SoC is constant at 20%, suggesting that the PV production is insufficient to cover the demand and simultaneously charge the battery.

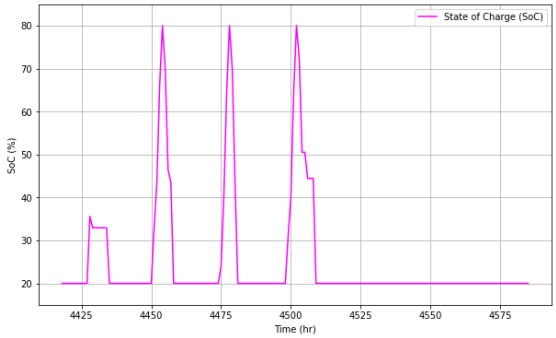


FIGURE 5.7: SoC pattern during the winter week for scenario S1.

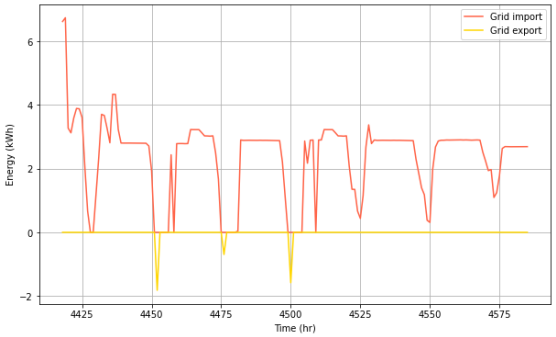


FIGURE 5.8: Import and export pattern during the winter week for scenario S1.

**S2: Fixed Electricity Prices Scenario under Net Metering Scheme**
For the scenario of fixed electricity prices with net metering, the optimal battery size is 0 kWh, resulting in a total cost of €525.4. Figure 5.9 shows the relation between the battery capacity and the total cost of the system. From the analysis, it becomes clear that net metering significantly reduces the operational cost of the system, making the addition of a battery unnecessary. Specifically, in the PV-battery system without a battery, the total imported energy is equal to 12.1 MWh, while 9.9 MWh of energy is exported, meaning that the owner pays only for the net energy consumption of 2.2 MWh.

**S3: Dynamic Prices Scenario**
For the scenario of fluctuating electricity prices, the average electricity cost, as mentioned in Section 3.3.1, is 0.083€/kWh, meaning that the electricity prices are significantly low. Thus, the results of the analysis indicate that the system cost is minimized when no battery is included. In this case, the total operational cost over the eight-month analysis amounts to €369. Figure 5.10 illustrates how the total cost of the system rises with the incorporation of a battery.

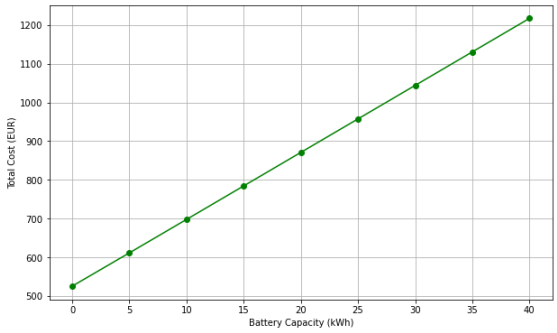


FIGURE 5.9: Relation between the battery capacity and the total cost of the system for scenario S2.

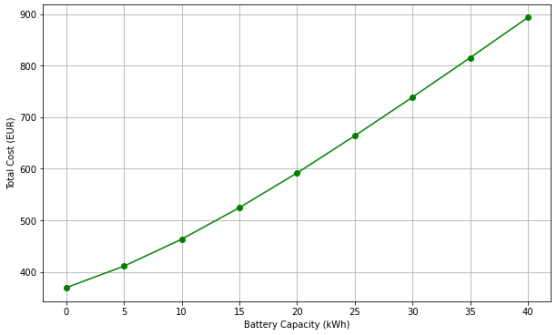


FIGURE 5.10: Relation between the battery capacity and the total cost of the system for scenario S3.

**S4: Fixed Electricity Prices without any Economic Benefit from Exporting Surplus Energy to the Grid**
For this scenario, where no economic benefits are gained from exporting energy to the grid, the optimal battery capacity is 32.4 kWh. The resulting battery capacity is more than three times larger than the size of the resulting battery in the baseline scenario where

feed-in energy is compensated. Despite this considerable increase in battery capacity, the total cost of the system, referring to the operational and distributed investment cost over the eight-month analysis, has only increased by 25% to €2,746. A larger battery size also contributes to a higher self-sufficiency rate compared to the baseline scenario, increasing it by 10% to reach 47%. Figure 5.11 illustrates the considerable cost reduction potential that a battery can bring to the system.

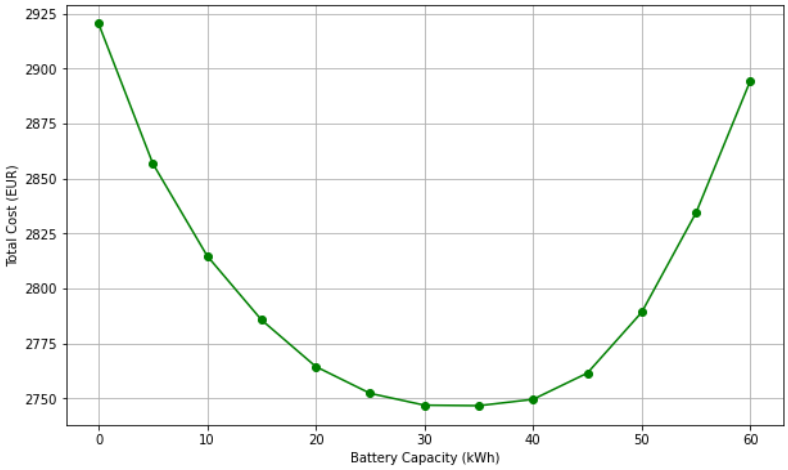


FIGURE 5.11: Relation between the battery capacity and the total cost of the system for scenario S4.

Figures 5.12 and 5.13 illustrate the operational behaviour of the 32.4 kWh battery. Similarly to the baseline scenario, the battery is utilized more frequently during summer compared to winter. Furthermore, there is a reduction in the amount of exported energy compared to the baseline scenario, as the battery capacity is larger and the storage potential is increased.

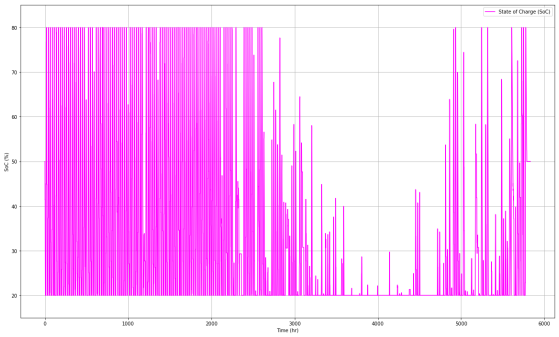

FIGURE 5.12: SoC pattern during the analysis period for scenario S4.

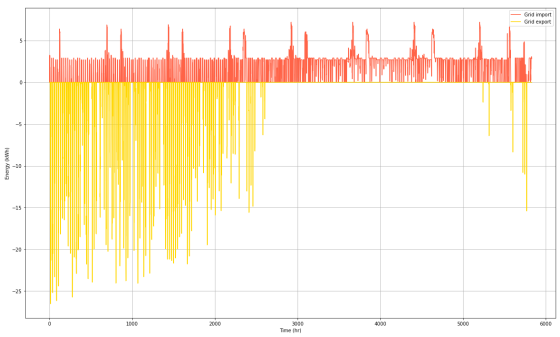

FIGURE 5.13: Import and export pattern during the analysis period for scenario S4.

In the summer week analysis, the battery system operates similarly to the baseline scenario, following a daily cycle of full charge and discharge. Additionally, a significant amount of energy is exported to the grid around noon. However, there is a slight decrease in both imported and exported energy due to the increased size of the battery system which can efficiently store larger quantities of electricity for later use. To avoid repetition, the graphs of the summer week analysis are not included.

With respect to the corresponding winter week, the battery is not utilized to its maximum potential, indicating that the battery's maximum capacity is mostly used during summer. Nevertheless, Figures 5.14 and 5.15 present similar patterns to the baseline scenario. Initially, during the first days of the analysis period, the PV production is sufficient to both meet the demand around noon and charge the battery approximately up to 40%. However, for the rest of the week, the battery's energy state remains constant at 20%. One notable difference compared to the baseline scenario is the absence of exported energy, as a result of the larger battery size.

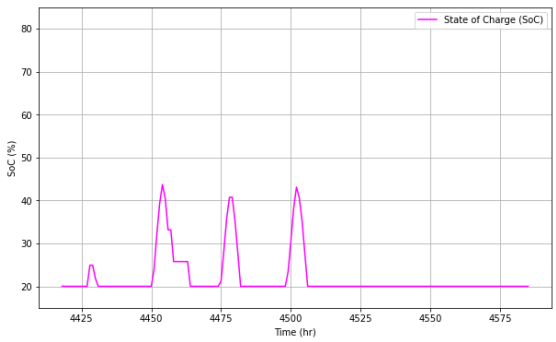


FIGURE 5.14: SoC pattern during the winter week for scenario S4.

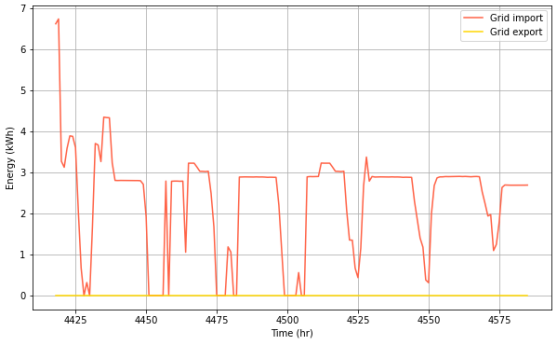


FIGURE 5.15: Import and export pattern during the winter week for scenario S4.

**S5: Scenario with Constraints on Exported Energy**
Introducing constraints on the amount of exported energy to the grid leads to an increased optimal battery size compared to the previously analysed models. Specifically, the optimal battery capacity amounts to 41.37 kWh, while the total cost of the system reaches €2,561 and the amount of curtailed energy is 1.14 MWh. The relation between the total cost of the system throughout the analysis period and the battery size is depicted in Figure 5.16. In this case, the total cost refers to the operational expenses, the distributed investment cost over the eight-month analysis period, as well as the curtailment cost. It should be mentioned that in case curtailment of solar energy was not permitted, the optimal battery size would be 1.1 MWh with a total cost of €20,524, indicating significantly higher expenses over the eight-month period of analysis. For battery sizes smaller than 1.1 MWh under these conditions, the problem becomes infeasible, meaning that curtailment of PV energy is necessary.

The operational strategy of this model is similar to the previously analysed cost minimization models which resulted in a battery capacity greater than zero, with the exception that exported energy is constrained to 8.8 kWh. The system imports energy throughout the year but exports energy only during summer. Additionally, while the battery completes approximately one full charge/discharge cycle daily in summer, its usage is significantly decreased in winter. Figures 5.17 and 5.18 illustrate the battery's operational pattern over the analysis period. For a more detailed perspective, daily graphs of the SoC and import/-export patterns are provided, illustrating both a summer day (August $1^{st}$) and a winter day (January $1^{st}$).

Comparing the summer and winter SoC (Figures 5.19 and 5.20), it can be seen that on the summer day, the battery reaches its maximum capacity around noon and it retains

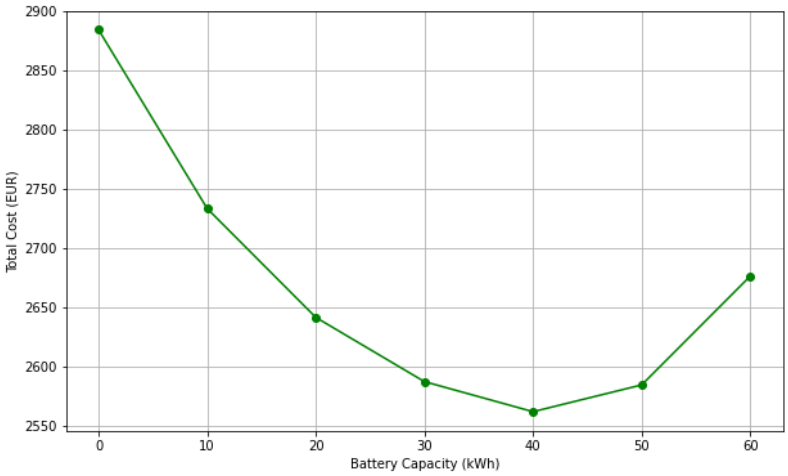


FIGURE 5.16: Relation between the battery capacity and the total cost of the system for scenario S5.

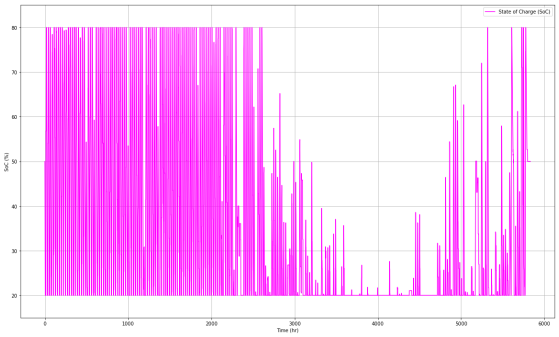

FIGURE 5.17: SoC pattern during the analysis period for scenario S5.

FIGURE 5.18: Import and export pattern during the analysis period for scenario S5.

almost 50% of its charge by the end of the day, whereas in winter, the SoC increases only by 1% throughout the day. Therefore, the generated PV energy is insufficient to charge the battery. However, Figure 5.22 shows that PV energy production is sufficient to cover the demand of the 3D printer around noon on the same day, as imported energy drops to zero. Additionally, energy exports are negligible on January $1^{st}$. In contrast, on the summer day, the system imports energy exclusively early in the morning, while the rest of the day exports the excess PV energy, that can be neither consumed directly nor stored in the battery. On the night of August $1^{st}$, both imported and exported energy drop to zero, meaning that the demand of the system is exclusively covered by the battery.

Figure 5.23 presents the cumulative curtailed energy over the analysis period. It can be seen that curtailment of energy occurs exclusively during summer, as the excess PV energy can neither be fed into the grid nor stored in the battery. By October, the PV production decreases significantly, thus the amount of curtailed energy drops to zero, meaning that the cumulative curtailed energy stabilizes until the end of the studied period.

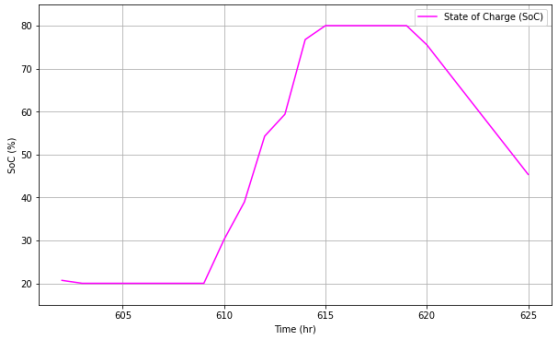


FIGURE 5.19: SoE pattern on August $1^{st}$ for scenario S5.

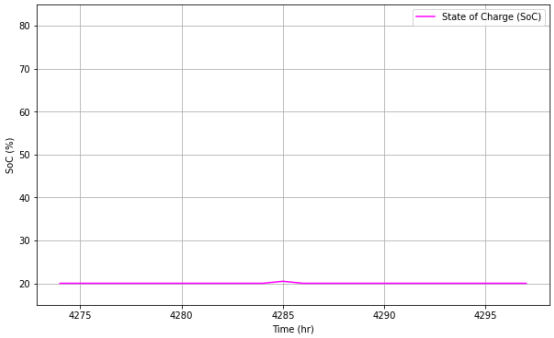


FIGURE 5.20: SoE pattern on January $1^{st}$ for scenario S5.

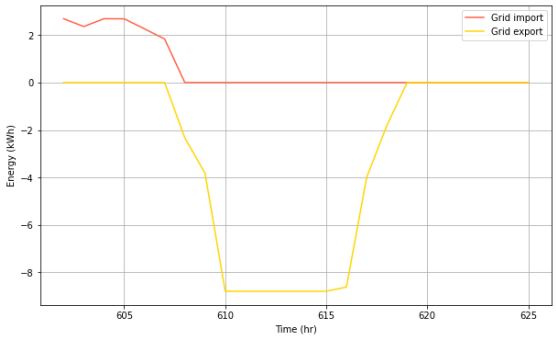


FIGURE 5.21: Import/export pattern on August $1^{st}$ for scenario S5.

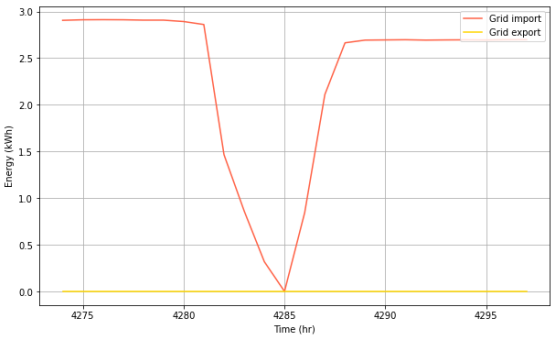


FIGURE 5.22: Import/export pattern on January $1^{st}$ for scenario S5.

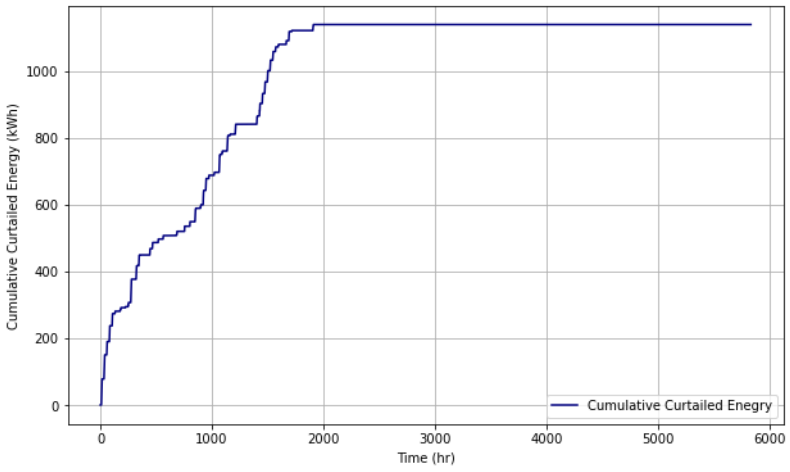


FIGURE 5.23: Cumulative curtailed energy over the analysis period for scenario S5.

**S6: Peak Shaving Scenario**

The model, which incorporates the peak shaving strategy, results in an optimal battery size of 594 kWh, with a total cost of €11,685 over the analysis period. This cost refers to the operational expenses, the distributed investment cost over the eight-month analysis period, as well as the curtailment cost. In this case, the curtailed energy amounts to 179.50

kWh. The model results in a larger battery size compared to the previous models primarily due to the constraint on imported energy. Since the constraint on imported energy can not be satisfied by increasing the curtailed energy, the increase of the battery size is inevitable. In this way, surplus energy produced during periods of high PV production is stored for later use, ensuring the system's ability to cover its energy needs at every moment $t$. Additionally, since the battery size is higher, the need for curtailment of PV energy is minimized.

Figures 5.24 and 5.25 illustrate the SoC and import/export patterns of this optimization model. Both figures present different patterns compared to the previous cost minimization scenarios. Specifically, the battery does not undergo one full charge/discharge cycle per day. In contrast, during summer, the SoC fluctuates significantly but remains above 50%, while in winter the battery experiences increased discharge. The large battery size is necessary during the winter period to ensure that the system can meet the daily energy demand by supplementing energy imports and currently generated PV energy. Furthermore, Figure 5.25 shows that the system exports energy exclusively during summer and imports energy only in winter. This occurs mainly because the battery size is sufficiently large to store enough excess energy and cover the demand of the system without importing energy during summer. In contrast, during winter, there is no excess PV energy available to be exported to the grid.

Additionally, Figure 5.25 shows the effectiveness of the peak shaving strategy. Through the introduction of the objective function penalty in combination with the constraints limiting the energy import and export at 2.7 kWh and 8.8 kWh, respectively, the overall pattern is smooth without any significant peaks.

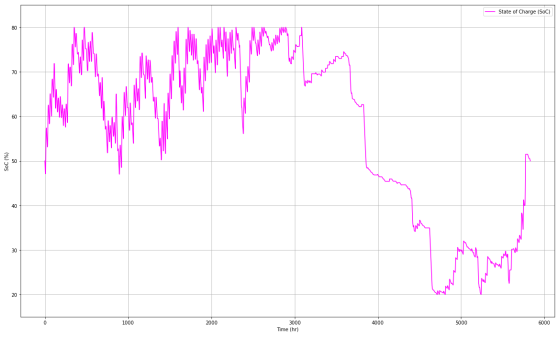


FIGURE 5.24: SoC pattern over the analysis period for scenario S6.

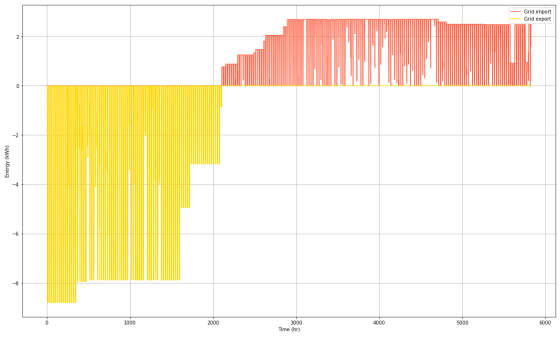


FIGURE 5.25: Import and export pattern over the analysis period for scenario S6.

### 5.1.2 $CO_2$ Emissions Minimization Objective

Regarding the findings of the $CO_2$ emissions minimization model, given that the corresponding emissions from grid electricity are often higher than those emitted by the PV-battery system, the optimization model prioritizes maximizing the size of the battery. As a result, the optimal battery capacity amounts to 15.6 MWh, enabling the storage of all the produced PV energy, minimizing in this way the imported electricity to 2,186 kWh, equivalent to the total demand of the system subtracted by the PV energy generated. In this case, the total $CO_2$ equivalent emissions of the system are equal to 686.2 kg. Figure 5.26 displays the relationship between the total $CO_2$ emissions of the system and varying

battery sizes. It can be seen that the emissions decrease until the battery capacity reaches 15.6 MWh. After this point, the emissions remain constant, as there is no additional PV energy available to be stored, meaning that any unmet demand must be covered by importing energy from the grid.

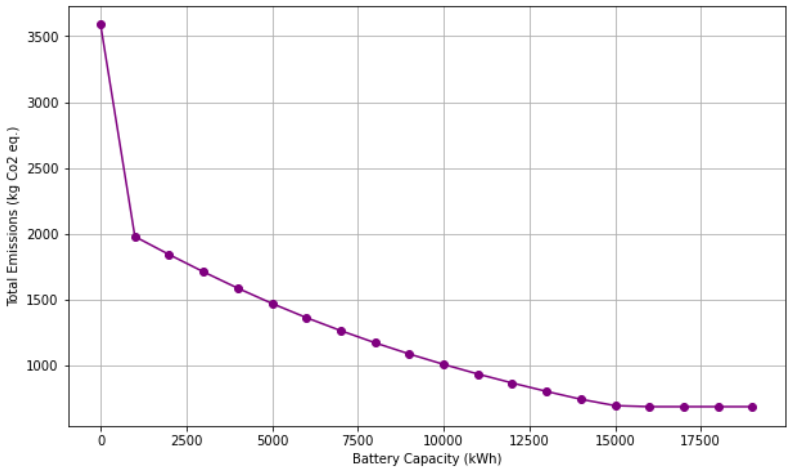


FIGURE 5.26: Relation between the battery capacity and the total $CO_2$ emissions of the system.

Since the optimization strategy aims to store all the surplus PV energy, the model results in storing high amounts of energy during the summer period in order to utilize it in winter, as depicted in Figure 5.27. As a result of this strategy, the system operates without exporting electricity. Additionally, the system imports occasionally energy from the grid during the eight-month period, mainly when $CO_2$ emissions of grid energy are lower than those of the PV-battery system (Figure 5.28).

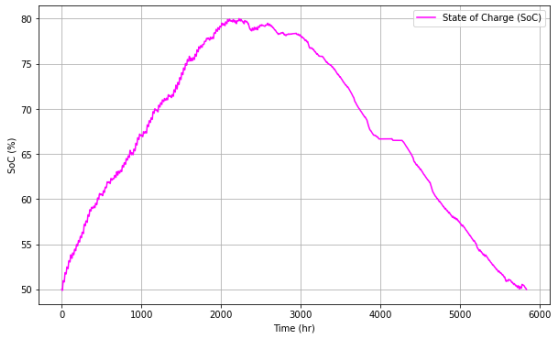


FIGURE 5.27: SoC pattern over the analysis period for the $CO_2$ minimization model.

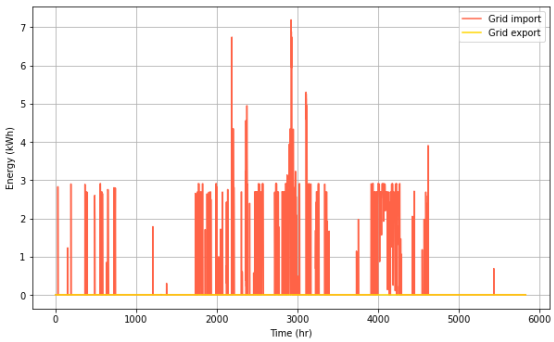


FIGURE 5.28: Import and export pattern over the analysis period for the $CO_2$ minimization model.

Considering that the total $CO_2$ equivalent emissions of the 3D printer without the incorporation of a battery system would amount to 3,588 kg, the reduction of the emissions is significant. However, the total cost of the system, referring to the operational and distributed investment cost over the analysis period, amounts to €270,846, thus a battery size of 15.6 MWh may not be practical in real-case scenarios. Furthermore, the current model underutilizes the battery's capabilities, with the lowest SoC being only 50%.

For this reason, the implementation of a constraint that limits the SoC of the battery on a monthly, weekly or daily basis is examined. Specifically, the SoC constraint ensures that the SoC is the same at the start of each specified period. The purpose of this constraint is firstly to prevent the battery from storing all available energy in the summer for use in the winter and secondly, to potentially maximize the battery's utilization. This approach can lead to a more efficient and realistic battery operation, reducing the optimal battery size and lowering the overall system's cost. The results for each constraint type are shown in Table 5.1. In the table, the total cost of the system refers to the total operational and investment cost distributed during the analysis period. The findings indicate that the optimal battery size decreases as the period of the SoC constraint shortens. This occurs because shorter periods require the battery to balance its SoC more frequently, thus reducing the need for a larger storage capacity to manage long-term energy storage. Consequently, the overall cost of the system during the eight-month analysis period also decreases. However, this leads to an increase in $CO_2$ emissions due to a higher dependency on imported energy from the grid.

| **Constraint type** | **Battery size (kWh)** | **$CO_2$ emissions (kg)** | **Total cost (€)** |
|---|---|---|---|
| Monthly SoC constraint | 489.65 | 2,096 | 9,865 |
| Weekly SoC constraint | 300.21 | 2,123 | 6,578 |
| Daily SoC constraint | 120.20 | 2,308 | 3,537 |

TABLE 5.1: Impact of SoC constraints on the system performance over the analysis period.

Comparing the three different scenarios (Figure 5.29), as the period of the SoC constraint decreases (from monthly to daily), the frequency of charging and discharging cycles increases. For all the cases, the winter period shows relatively stable SoC, while most of the variations occur during summer. This pattern is a result of higher PV production during summer, leading to excess energy available for storage.

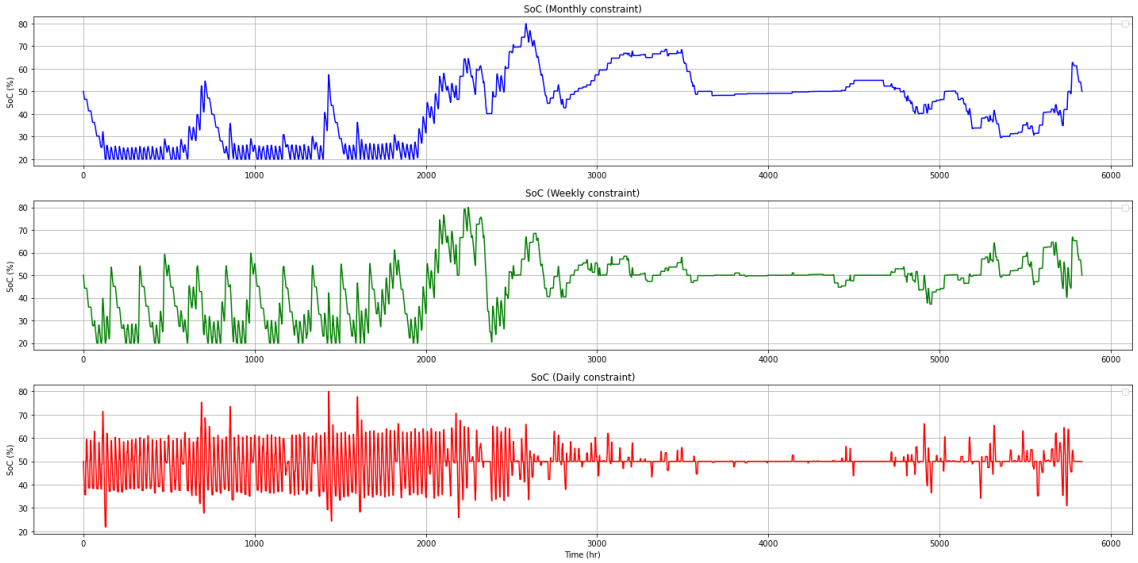


FIGURE 5.29: Comparison of SoC throughout the analysis period for different SoC constraints: monthly, weekly and daily constraints.

Considering all constraint types, the models with monthly and weekly SoC constraints yield

emissions of similar magnitudes. However, the cost associated with the weekly SoC limit is significantly lower, making the weekly constraint more cost-effective. When comparing the weekly with the daily constraint, the battery size required in the daily constraint scenario is only 40% of that needed for the weekly constraint. Despite this reduction in battery size, the emissions in the daily constraint scenario are less than 10% higher. Given these factors, the daily SoC constraint is the optimal choice, as it offers a better balance between cost efficiency and environmental impact.

Figure 5.30 illustrates the pattern of importing and exporting energy from the grid for the $CO_2$ emissions minimization model after the implementation of the daily SoC constraint. Compared to the corresponding graph without the implemented constraint (Figure 5.28), the pattern shows notable differences. After implementing the daily SoC constraint, energy imports are more frequent but of lower magnitude. The system avoids importing energy only when $CO_2$ emissions are low and instead imports energy more consistently over the analysis period. Additionally, the system frequently exports large amounts of energy during summer because the reduced battery size cannot store all the excess PV energy.

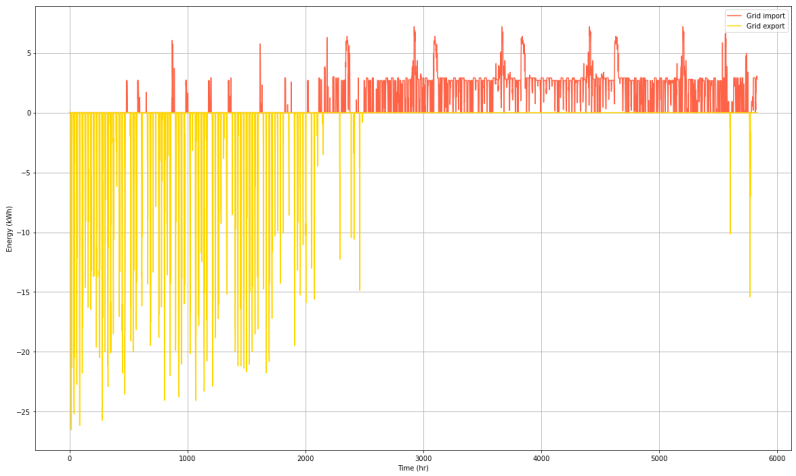


FIGURE 5.30: Import and export pattern during the analysis period for the $CO_2$ minimization model with daily SoC constraint.

### 5.1.3 Self-Sufficiency Maximization Objective

To maximize self-sufficiency, the system needs to minimize the total imported energy and decrease dependence on the grid. In order to achieve this, the optimization algorithm aims to maximize the total stored PV energy, resulting in this way in an optimal battery capacity of 14.7 MWh and a self-sufficiency rate of 87.4%. In this case, the total operational and investment cost of the system over the analysis period amounts to €254,888, indicating that the resulting system's design would be limited in real-world applications.

Figure 5.31 shows the potential increase of the self-sufficiency rate after the incorporation of a battery into the system. Without a storage solution, the self-sufficiency rate of the system is 30%, while a battery with a capacity of 14.7 MWh can increase the metric to 87.4%. Beyond this threshold, the self-sufficiency of the system can not be further optimized, as there is no additional PV energy to be stored.

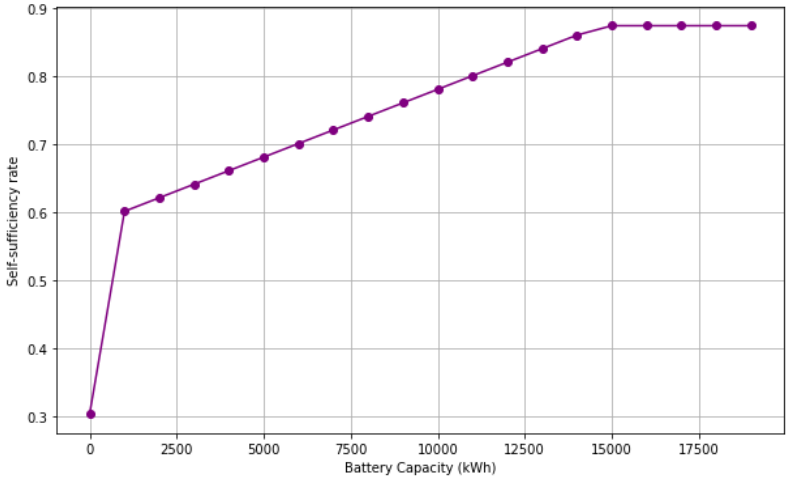


FIGURE 5.31: Relation between the battery capacity and the self-sufficiency rate of the system.

Regarding the battery's SoC pattern, the resulting operational strategy aligns with the corresponding strategy of the $CO_2$ emissions minimization model before the implementation of the SoC constraint, as shown in Figure 5.32. Both models aim to store all excess energy during summer to be utilized during the winter period. However, the import and export patterns differ. While the system does not export any energy throughout the analysis period, it imports energy from the grid only when the stored energy from the summer period is depleted (Figure 5.33).

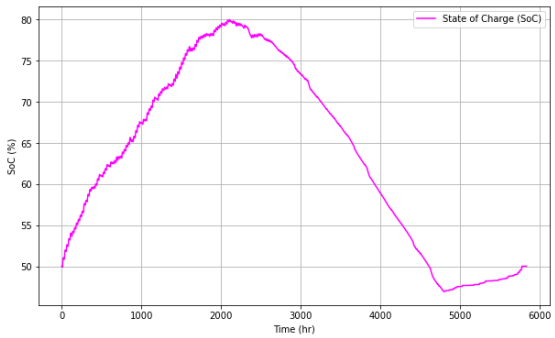


FIGURE 5.32: SoC pattern over the analysis period for self-sufficiency maximization.

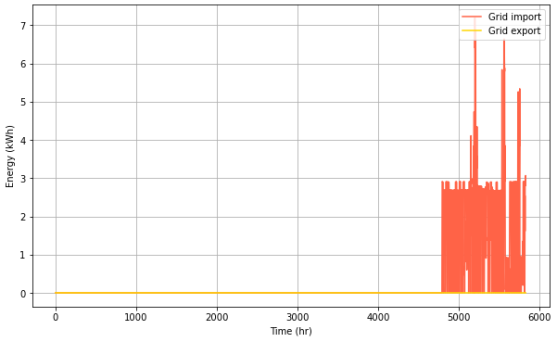


FIGURE 5.33: Import and export pattern over the analysis period for self-sufficiency maximization.

However, due to the high total cost and the large optimal battery size, the resulting system does not represent a realistic model. Therefore, a SoC constraint that limits the battery's SoC on a monthly, weekly and daily basis is examined. Table 5.2 presents the resulting variables of the system for the different constraint types.

In contrast to the $CO_2$ minimization model, the optimal battery size does not necessarily decrease as the period of the SoC constraint shortens. Specifically, the weekly SoC constraint results in a larger battery size compared to the monthly constraint. This can be attributed to the circumstances and specific conditions under which the weekly SoC con-

| Constraint type | Battery size (kWh) | Self-sufficiency rate | Total cost (€) |
|---|---|---|---|
| Monthly SoC constraint | 209.09 | 0.584 | 5,008 |
| Weekly SoC constraint | 262.02 | 0.587 | 5,916 |
| Daily SoC constraint | 120.20 | 0.561 | 3,538 |

TABLE 5.2: Impact of SoC constraints on the system performance over the analysis period.

straint is implemented. If one of the weeks coincides with a period of low PV production or high demand, the system may result in a larger battery capacity to avoid importing large quantities of energy from the grid. However, the self-sufficiency rate remains relatively stable across the different SoC constraints, showing only slight improvements. Despite its slightly lower self-sufficiency rate, the daily SoC constraint proves to be the most cost-effective scenario, due to the significantly reduced battery size and consequently lower overall cost.

The SoC patterns for the three different SoC constraints are illustrated in Figure 5.34. As the period of the SoC constraint shortens, the charging and discharging cycles become more frequent. Additionally, the patterns regarding the monthly and weekly constraints align closely. In all cases, the SoC remains relatively stable during the winter, with most of the variations occurring in the summer.

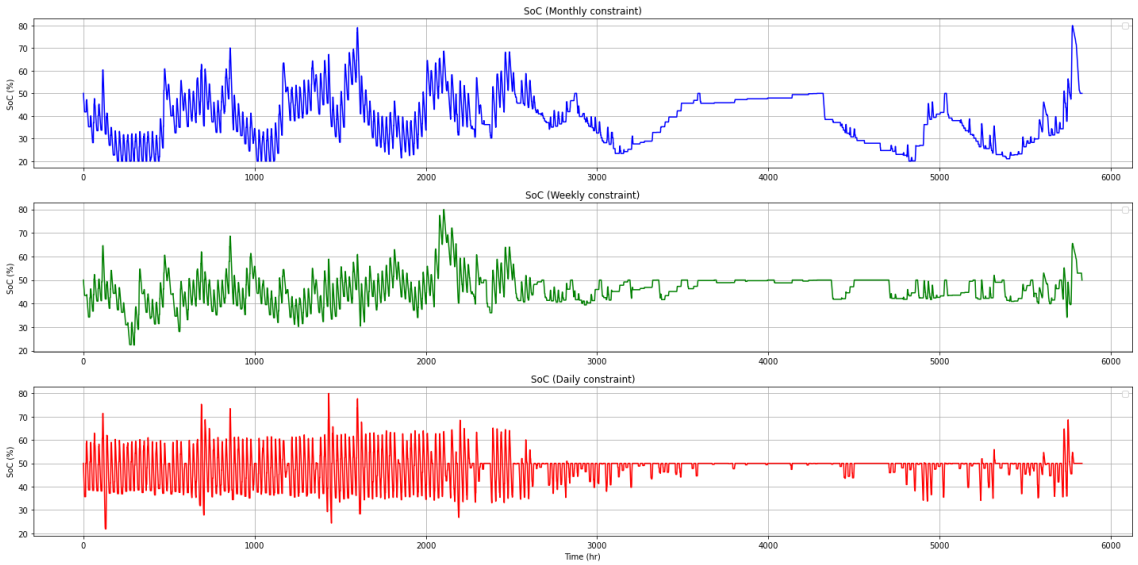


FIGURE 5.34: Comparison of SoC throughout the analysis period for different SoC constraints: monthly, weekly and daily constraints.

Given that the scenario with the daily SoC constraint is the most cost-effective, it has been chosen for integration into the self-sufficiency maximization model. The import and export patterns of this scenario closely align with the corresponding graph of the $CO_2$ emissions minimization model (Figure 5.30). This alignment occurs because firstly, the resulting optimal battery size is the same in both models, and secondly, both models are optimized by storing as much PV energy as possible.

### 5.1.4 Self-Consumption Maximization Objective

The self-consumption rate of a system can be maximized by minimizing the total exported energy. The operational strategy of this model aligns with the self-sufficiency maximization model before implementing the SoC constraint, as the aim of maximizing the percentage of the stored PV energy is common across the models. This indicates that different objectives are not necessarily contradictory. Therefore, the optimal battery size for the optimization model with this objective is also 14.7 MWh with a resulting self-consumption rate of 1.00. It should be mentioned that the self-consumption rate of the system without a storage solution is 35%, as shown in Figure 5.35, and it progressively increases to 1 with the increase of the battery size. Beyond this point, it remains constant, as no more PV energy is available to be stored. The total cost of the system, referring to the operational and distributed investment expenses over the analysis period, is equal to €254,888.

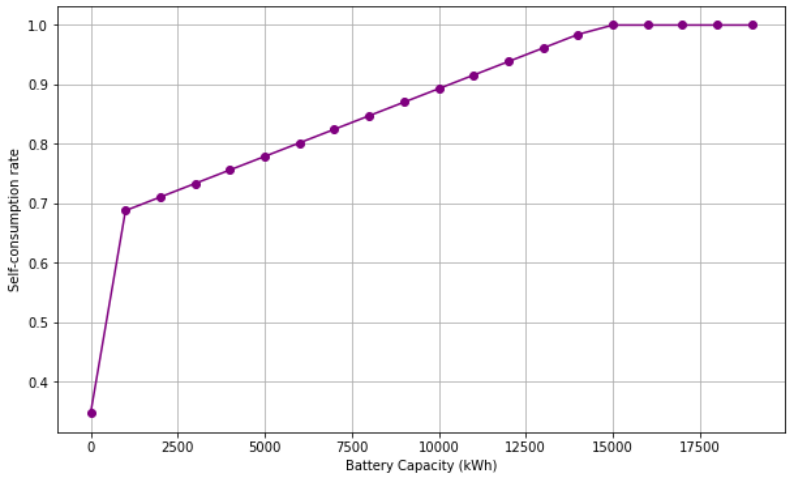


FIGURE 5.35: Relation between the battery capacity and the self-consumption rate of the system.

Since the operational patterns remain consistent across the self-sufficiency and self-consum ption optimization models, it becomes redundant to mention the same resulting metrics. Furthermore, the resulting large battery size and the consequent high overall cost indicate the necessity of implementing a SoC constraint in this model as well. Table 5.3 shows how different SoC constraints impact the optimal battery size, self-consumption rate and total cost of the system.

| Constraint type | Battery size (kWh) | Self-consumption rate | Total cost (€) |
|---|---|---|---|
| Monthly SoC constraint | 209.09 | 0.668 | 5,009 |
| Weekly SoC constraint | 262.02 | 0.670 | 5,917 |
| Daily SoC constraint | 120.20 | 0.642 | 3,538 |

TABLE 5.3: Impact of SoC constraints on the system performance over the analysis period.

The findings of Table 5.3 align with the results of the self-sufficiency model, showing that the self-consumption rates vary only slightly between different SoC constraints. Therefore, the model with the daily SoC constraint, which results in a smaller battery size and con-

sequently lower total cost, is the most suitable.

Figure 5.36 presents the SoC pattern over the analysis period for the self-consumption model after the implementation of the daily SoC constraint. The graph is similar to the corresponding SoC graph of the self-sufficiency model. During summer, the battery undergoes approximately one incomplete charge/ discharge cycle per day, while in winter, the battery is mainly discharged. The battery appears to be underutilized, reaching its maximum SoC (80%) only once during the analysis period. This is because the daily SoC constraint causes the SoC of the battery to return to 50% at the beginning of each day and most of the days, the PV production is not enough to fully charge the battery.

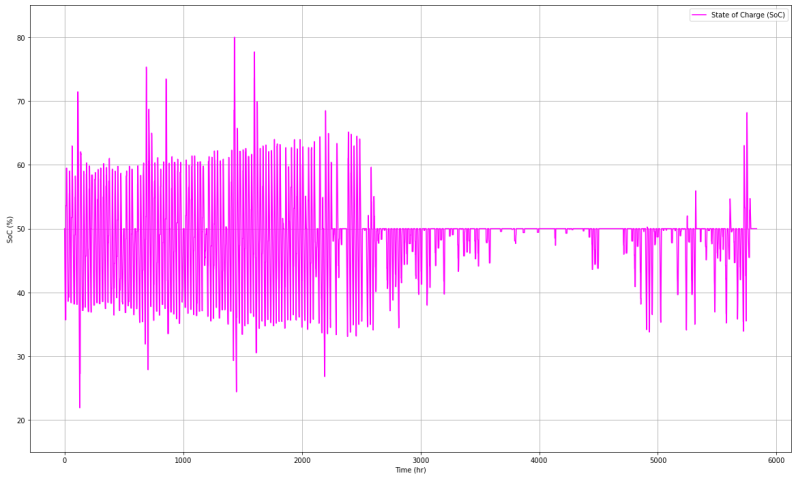


FIGURE 5.36: SoC pattern over the analysis period for the self-consumption model with the daily SoC constraint.

## 5.2 Battery Sizing Optimization: Multi-Objective Approach

In this section, the results of the multi-objective optimization analysis are presented. The co-optimization is performed in pairs, minimizing cost and simultaneously, minimizing $CO_2$ emissions, maximizing self-sufficiency or maximizing self-consumption.

For the cost minimization objective, the first five scenarios, described in Section 3.3.1, are included in the analysis. The peak shaving scenario can not be implemented in any of the co-optimization models with $CO_2$ emissions, self-sufficiency and self-consumption due to convergence issues. Specifically, when the daily SoC constraint of the latter models is implemented in the co-optimization with the peak shaving scenario, the problem leads to infeasibility. This is because the flexibility of the peak shaving scenario is limited, meaning that the battery size can not be lower than 594 kWh. After the incorporation of the daily SoC constraint, the SoC is required to be equal at the beginning of every day, leading to the incapability of the system to meet its demand. Likewise, the weekly and monthly SoC constraints would lead to the same finding.

### 5.2.1 Cost and $CO_2$ Emissions Minimization

Figure 5.37 illustrates the relationship between cost and $CO_2$ emissions resulting from the co-optimization model. Each line represents a distinct scenario of the cost minimization

objective along with the $CO_2$ emissions minimization objective. The data points along each line indicate different weight combinations for each one of the objective functions of the co-optimization model. The graph reveals that cost and $CO_2$ emissions objectives, which both aim for minimization, are conflicting, as reducing cost leads to an increase in $CO_2$ emissions and vice versa.

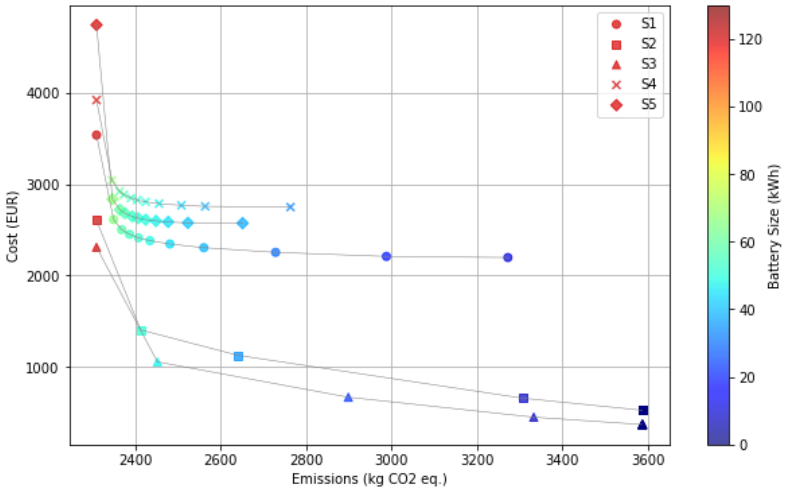


FIGURE 5.37: Co-optimization results of cost and $CO_2$ emissions.

The findings indicate significant variation in the results depending on the scenario selected for the cost minimization objective, as depicted in Figure 5.37. In the scenarios where electricity prices are fixed (S1), there is no financial incentive for feed-in energy (S4) and there is a constraint on exported energy (S5), the generally higher resulting battery sizes, lead to increased costs but reduced $CO_2$ emissions compared to the scenarios with dynamic prices (S3) and net metering scheme (S2). In contrast, the single objective optimization models for scenarios S2 and S3, in Section 5.1.1, concluded that the system is optimized when no battery is integrated. This finding affects also the results of the co-optimization model, as when the cost weight increases, the optimal battery size tends towards zero. For these scenarios, the data points on the graph are fewer due to the algorithm converging to an optimal battery capacity of zero, when the cost weight is only 0.4. Therefore, these scenarios result in lower cost but higher $CO_2$ emissions.

Table 5.4 shows explicitly the resulting optimal battery size corresponding to varying weights assigned to the two objectives of the model. In the table, $w_1$ and $w_2$ are the weights for the cost and the $CO_2$ emissions objective, respectively. The results suggest that when $w_1$ increases, the battery size decreases, while an increase in $w_2$ corresponds to an increase in battery size. This trend mirrors the results of the single-objective analysis where the cost minimization objective results in smaller battery sizes, while the $CO_2$ emissions objective leads to larger capacities. From Table 5.4, it is clear that the multi-objective approach achieves a more balanced result, optimizing both cost and $CO_2$ emissions.

It should be mentioned that there are constraints in some of the single-objective models of cost and $CO_2$ emissions minimization that are not present in both models. However, in the co-optimization algorithm, all these constraints are considered together. For instance, the $CO_2$ minimization model includes the daily SoC constraint, as explained in Section 5.1.2, that is not included in any of the cost models. Nevertheless, the result of the cost models

| | | Battery Capacity (kWh) | | | | |
|---|---|---|---|---|---|---|
| $w_1$ | $w_2$ | **Baseline scenario (S1)** | **Net metering scenario (S2)** | **Dynamic prices scenario (S3)** | **Scenario without feed in tariff (S4)** | **Scenario with constraints on exported energy (S5)** |
| 0.0 | 1.0 | 120.20 | 120.20 | 120.20 | 120.20 | 120.20 |
| 0.1 | 0.9 | 65.47 | 50.88 | 47.31 | 67.78 | 67.03 |
| 0.2 | 0.8 | 58.33 | 34.80 | 23.16 | 59.79 | 59.46 |
| 0.3 | 0.7 | 54.58 | 7.68 | 7.37 | 57.12 | 56.62 |
| 0.4 | 0.6 | 51.49 | 0.00 | 0.00 | 54.02 | 53.54 |
| 0.5 | 0.5 | 48.58 | 0.00 | 0.00 | 51.84 | 51.59 |
| 0.6 | 0.4 | 44.61 | 0.00 | 0.00 | 49.55 | 49.55 |
| 0.7 | 0.3 | 39.26 | 0.00 | 0.00 | 46.65 | 47.28 |
| 0.8 | 0.2 | 30.34 | 0.00 | 0.00 | 42.63 | 44.92 |
| 0.9 | 0.1 | 18.95 | 0.00 | 0.00 | 39.09 | 41.64 |
| 1.0 | 0.0 | 10.20 | 0.00 | 0.00 | 32.23 | 38.02 |

TABLE 5.4: Battery size results for cost and $CO_2$ emissions co-optimization.

remains relatively unchanged when this specific constraint is applied. In scenarios S4 and S5, the optimal battery size when $w_1 = 1$ is slightly lower than the single optimization model, yet the differences are not significant. This is because the battery is already used on daily cycles and does not aim at storing as much energy as possible for long-term energy storage.

### 5.2.2 Cost Minimization and Self-Sufficiency Maximization

Regarding the co-optimization of cost and self-sufficiency, Figure 5.38 presents graphically the findings. While an increase in one objective leads also to an increase in the other, their conflicting nature arises from the need to minimize cost while simultaneously maximizing self-sufficiency. For the scenarios where electricity prices are fixed (S1), there is no financial incentive for feed-in energy (S4) and there is a constraint on exported energy (S5), the resulting battery sizes are larger, leading to increased costs but also enhanced self-sufficiency rates compared to the scenarios with dynamic prices (S3) and net metering (S2). For the latter scenarios, the graph displays fewer data points because the algorithm converges to an optimal battery capacity of zero. This occurs early in the process, even before the two objectives are equally balanced ($w_1 = w_2$). This can be also seen in Table 5.5 where the battery size results of this multi-objective model are presented.

In Table 5.5, $w_1$ and $w_2$ are the weights for the cost and the self-sufficiency objective, respectively. While for scenarios S1, S4 and S5, the model results that a battery is beneficial for the system regardless of the weights assigned in the cost and self-sufficiency objective, for the S2 and S3 scenarios, the outcome differs. Even when the importance of self-sufficiency outweighs that of cost (for instance $w_1$ equals 0.4), the model suggests that incorporating a battery is not advantageous for the system. This can be attributed to the exceptionally low cost of the system when no battery system is integrated, as resulted from the single cost minimization model of scenarios S2 and S3.

Comparing the co-optimization results of the cost-$CO_2$ emissions and cost-self-sufficiency models, it is clear that the resulting optimal battery sizes are of similar magnitude. This similarity arises from the identical battery size resulting from the single objective models

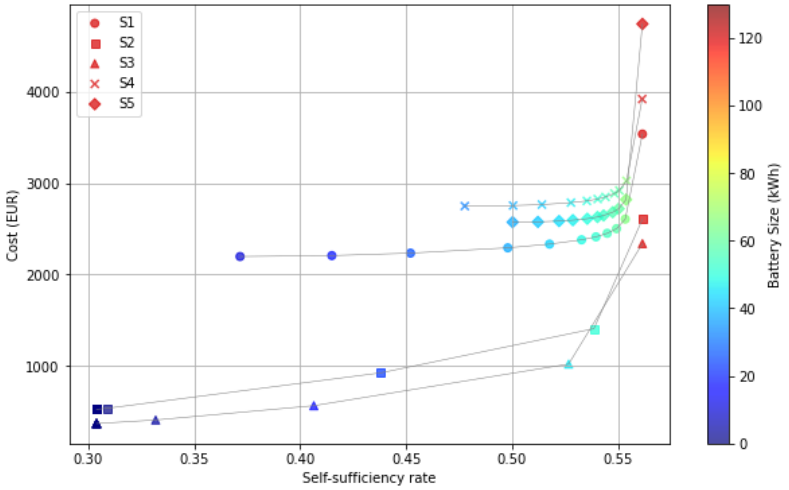


FIGURE 5.38: Co-optimization results of cost and self-sufficiency.

| | | Battery Capacity (kWh) | | | | |
|---|---|---|---|---|---|---|
| $w_1$ | $w_2$ | **Baseline scenario (S1)** | **Net-metering scenario (S2)** | **Dynamic prices scenario (S3)** | **Scenario without feed in tariff (S4)** | **Scenario with constraints on exported energy (S5)** |
| 0.0 | 1.0 | 120.20 | 120.20 | 120.20 | 120.20 | 120.20 |
| 0.1 | 0.9 | 65.07 | 50.97 | 46.16 | 66.67 | 66.07 |
| 0.2 | 0.8 | 58.33 | 23.10 | 16.61 | 59.79 | 59.46 |
| 0.3 | 0.7 | 54.63 | 0.63 | 3.81 | 57.28 | 56.62 |
| 0.4 | 0.6 | 51.49 | 0.00 | 0.00 | 54.13 | 53.54 |
| 0.5 | 0.5 | 48.44 | 0.00 | 0.00 | 51.87 | 51.84 |
| 0.6 | 0.4 | 43.15 | 0.00 | 0.00 | 49.47 | 49.54 |
| 0.7 | 0.3 | 37.40 | 0.00 | 0.00 | 46.54 | 46.90 |
| 0.8 | 0.2 | 26.17 | 0.00 | 0.00 | 41.99 | 44.61 |
| 0.9 | 0.1 | 18.25 | 0.00 | 0.00 | 38.08 | 41.43 |
| 1.0 | 0.0 | 10.20 | 0.00 | 0.00 | 32.23 | 38.02 |

TABLE 5.5: Battery size results for cost and self-sufficiency co-optimization.

for $CO_2$ and self-sufficiency and the similar operational strategy of storing as much excess PV energy as possible.

### 5.2.3 Cost Minimization and Self-Consumption Maximization

The results of cost and self-consumption co-optimization are shown in Figure 5.39. The outcome of the analysis shows similar trends to the co-optimization model of cost and self-sufficiency, since the optimal battery size of the two single-objective algorithms and their operational strategy are identical.

However, for the co-optimization of self-consumption and the cost scenario, that includes a constraint on exported energy (S5), the objective function for self-consumption needs to be revised. As the self-consumption rate is maximized by minimizing the amount of exported energy, the current model assumes that self-consumption can be maximized by curtailing as much energy as possible to avoid exporting it. Thus, the objective function of this co-optimization model should be adjusted to not only minimize exported energy but

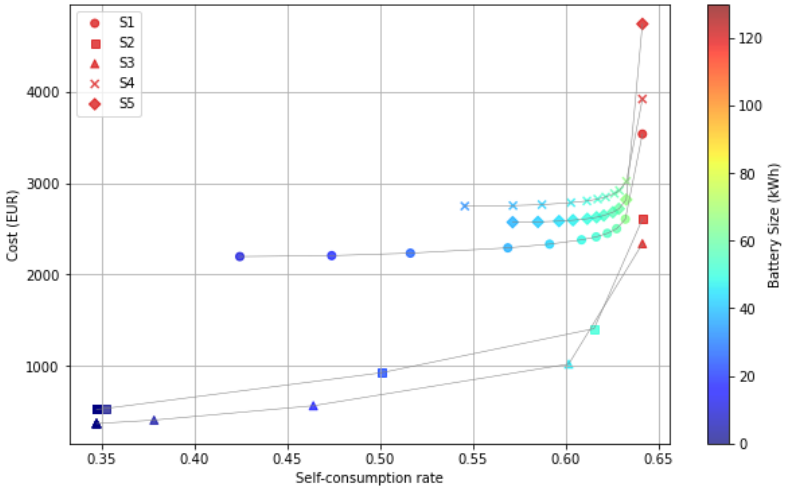


FIGURE 5.39: Co-optimization results of cost and self-consumption.

also minimize energy curtailment.

Table 5.6 presents the resulting optimal battery size for the different scenarios, which closely aligns with the findings of Table 5.5. Again, $w_1$ and $w_2$ are the weights assigned to the cost and the self-consumption objective, respectively.

| | | **Battery Capacity (kWh)** | | | | |
|---|---|---|---|---|---|---|
| $w_1$ | $w_2$ | **Baseline scenario (S1)** | **Net-metering scenario (S2)** | **Dynamic prices scenario (S3)** | **Scenario without feed in tariff (S4)** | **Scenario with constraints on exported energy (S5)** |
| 0.0 | 1.0 | 120.20 | 120.20 | 120.20 | 120.20 | 120.20 |
| 0.1 | 0.9 | 65.07 | 50.97 | 46.16 | 66.38 | 66.07 |
| 0.2 | 0.8 | 58.33 | 23.10 | 16.58 | 59.79 | 59.46 |
| 0.3 | 0.7 | 54.63 | 0.53 | 3.70 | 57.28 | 56.62 |
| 0.4 | 0.6 | 51.49 | 0.00 | 0.00 | 54.13 | 53.54 |
| 0.5 | 0.5 | 48.44 | 0.00 | 0.00 | 51.87 | 51.59 |
| 0.6 | 0.4 | 43.15 | 0.00 | 0.00 | 49.47 | 49.54 |
| 0.7 | 0.3 | 37.40 | 0.00 | 0.00 | 46.54 | 46.90 |
| 0.8 | 0.2 | 26.17 | 0.00 | 0.00 | 41.99 | 44.61 |
| 0.9 | 0.1 | 18.25 | 0.00 | 0.00 | 38.08 | 41.43 |
| 1.0 | 0.0 | 10.20 | 0.00 | 0.00 | 32.23 | 38.02 |

TABLE 5.6: Battery size results for cost and self-consumption co-optimization.

## 5.3 $CO_2$ Emissions of the System

Given that the primary purpose of the designed PV-battery system is the sustainable manufacturing of titanium objects using a 3D printer, the quantity of $CO_2$ emitted from the system for each model and scenario needs to be calculated.

Figure 5.40 presents the total $CO_2$ emissions for each of the single-objective optimization models. The peak shaving scenario (S6) of the cost minimization objective emits the lowest

amount of $CO_2$, since the resulting battery size is the largest among the different models. The system designed based on the $CO_2$ emissions minimization model has the second least environmental impact. Additionally, since the operational strategy of self-sufficiency and self-consumption maximization align closely with that of the $CO_2$ emissions minimization model, the two models result in similarly low emissions for the system. On the other hand, the models with cost minimization objectives with the exception of the peak shaving scenario (S6) result in emissions up to half times higher than those of the $CO_2$ emissions minimization model. It should be noted that the highest emissions correspond to the scenarios that refer to dynamic prices (S3) and net metering (S2), as the resulting system does not include a battery. From the data presented in Figure 5.40, it can be concluded that the total $CO_2$ emissions decrease as battery size increases. This is primarily due to the fact that emissions associated with grid energy tend to be on average higher than those of the PV-battery system.

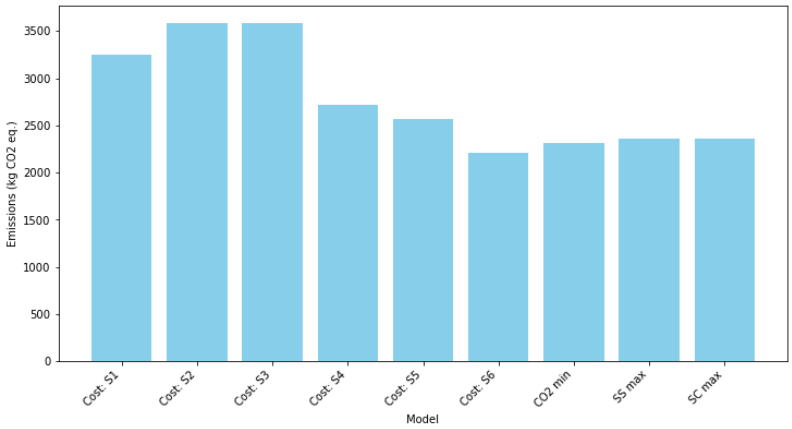


FIGURE 5.40: $CO_2$ emissions for the single-objective optimization models.

Figure 5.41 shows the difference in the resulting $CO_2$ emissions of the $CO_2$ emissions minimization, self-sufficiency and self-consumption maximization models before and after the implementation of the daily SoC constraint. The graph shows that the emissions are considerably higher when the constraint is applied in the model. Regarding the $CO_2$ minimization model, the emissions after the constraint implementation are more than three times higher, whereas, for the other models, they are approximately twice as high. Furthermore, in case the daily SoC constraint was not included, the $CO_2$ minimization, as well as the self-sufficiency and self-consumption maximization models, would result in lower emissions than all the cost minimization models. These findings demonstrate how different operational constraints can significantly impact the system's performance.

For the co-optimization models, the resulting $CO_2$ emissions vary based on the optimal battery size, with $CO_2$ and battery size having an inverse relation. Additionally, the optimal battery size decreases as the cost weight increases. Figure 5.42 displays the total emissions for the co-optimization model of cost and $CO_2$ emissions in relation to the cost weight, while Figure 5.43 illustrates the same metric for the co-optimization model of cost and self-sufficiency. As the battery size results of Tables 5.5 and 5.6 are nearly identical, the resulting emissions of the cost and self-consumption model can also be represented by Figure 5.43.

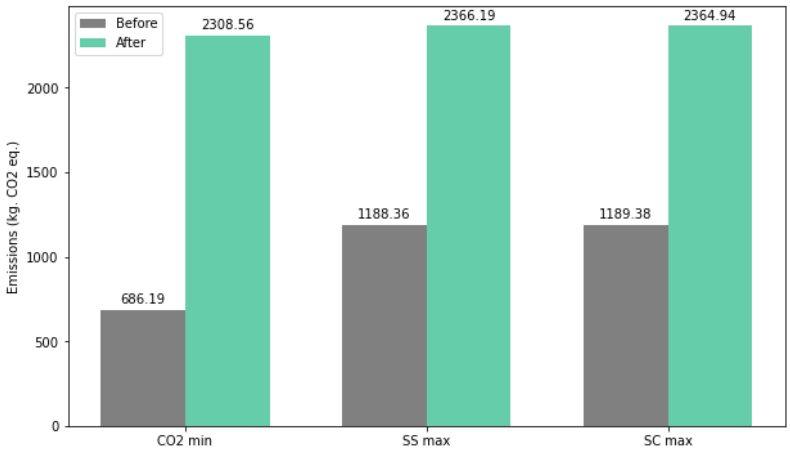


FIGURE 5.41: Comparison of $CO_2$ emissions of the single-objective optimization models before and after the implementation of the daily SoC constraint.

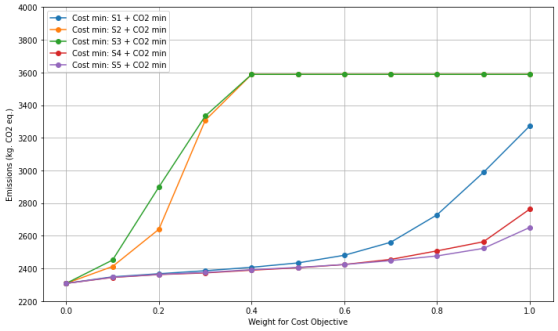


FIGURE 5.42: $CO_2$ emissions for the different weight combinations of cost and $CO_2$ emissions co-optimization model.

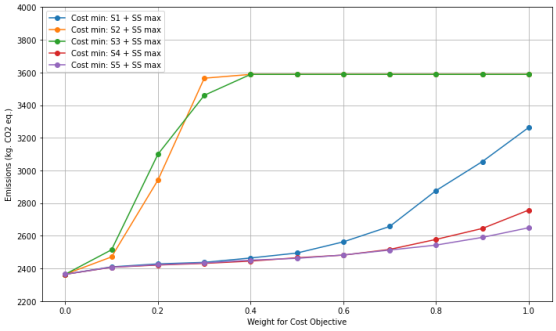


FIGURE 5.43: $CO_2$ emissions for the different weight combinations of cost and self-sufficiency, as well as cost and self-consumption co-optimization models.

Based on the displayed results, implementing a storage system can significantly decrease the total emissions of the system but with a consequent higher cost. The integration of a battery into the system can make the manufacturing process of titanium objects more sustainable and minimize negative environmental impacts. These improvements can be reflected in the "Digital Product Passport" of the products, providing in this way a competitive advantage to the manufacturer.

## 5.4 Financial Analysis

In this section, the results of the financial analysis are displayed. The financial feasibility of the resulting optimal systems is assessed based on the following metrics: payback time, ROI and NPV.

Table 5.7 presents the operational cost of the optimal PV-battery system for every different model and scenario. Since the optimization model showed that a battery is not beneficial for scenarios S2 and S3, the operational cost of the system with a battery is not

applicable in these cases. Regarding the peak shaving scenario (S6) of the cost minimization objective, Table 5.7 does not include its operational cost without a battery. This is due to the infeasibility of the model when a battery is not included in the system. The restriction on imported energy leads to the system's inability to meet its demand at every moment without storage. Therefore, the operational cost of the model prior to the battery incorporation cannot be calculated. Additionally, the system's operational cost after the battery installation is significantly higher compared to the rest of the models, which can be attributed to the high maintenance cost that such a large battery requires.

| | **Operational cost (€)** | |
|---|---|---|
| **Model** | **Without battery** | **With battery** |
| Cost min: S1 | 2,221 | 2,088 |
| Cost min: S2 | 525 | - |
| Cost min: S3 | 369 | - |
| Cost min: S4 | 2,920 | 2,400 |
| Cost min: S5 | 2,884 | 2,120 |
| Cost min: S6 | - | 5,356 |
| $CO_2$ emissions min | 2,221 | 2,257 |
| SS max | 2,221 | 2,257 |
| SC max | 2,221 | 2,257.7 |

TABLE 5.7: Operational cost of the different scenarios and models over the analysis period.

Table 5.8 presents the findings of the financial analysis. It should be mentioned that for the calculation of the financial performance, the annual savings are calculated using linear extrapolation based on the eight-month analysis data. Furthermore, it is assumed that the annual savings remain constant throughout the lifetime of the system. However, these assumptions may not accurately represent realistic conditions because factors such as the degradation of the battery, fluctuations in PV energy generation and changes in demand can influence the overall performance over time.

| **Model** | **Payback Time (years)** | **ROI** | **NPV** |
|---|---|---|---|
| Cost min: S1 | 10.20 | 22.5% | 81.66 |
| Cost min: S2 | - | - | - |
| Cost min: S3 | - | - | - |
| Cost min: S4 | 8.31 | 50.4% | 1,793.89 |
| Cost min: S5 | 7.22 | 73.1% | 3,881.57 |
| Cost min: S6 | - | - | - |
| $CO_2$ emissions min | -456.75 | -102.7% | -24,598.36 |
| SS max | -456.74 | -102.7% | -24,598.36 |
| SC max | -446.87 | -102.8 % | -24,610.70 |

TABLE 5.8: Payback time, ROI and NPV for the resulting systems of the single-objective optimization models.

For the scenarios S1, S4 and S5 of the cost minimization models, all the evaluation methods agree that the battery investment is profitable. Only these three models result in long-term profitability, with a payback time of 10.2, 8.31 and 7.22 years, respectively. This finding suggests that the investment becomes profitable within a reasonable time frame. Moreover, the resulting ROIs of 22.5%, 50.4% and 73.1% indicate that the investment generates

returns 1.225, 1.504 and 1.731 times the initial investment and the positive NPVs assure that the investment will generate positive returns that exceed the initial cost of investment over its lifetime.

Additionally, it can be seen that for the $CO_2$ emissions minimization, as well as for the self-sufficiency and self-consumption maximization models, all the evaluation methods suggest that the investment is not profitable. The negative values of the payback time, ROI and NPV are due to the negative annual cash flows resulting from the investment. This outcome was anticipated, as these models do not account for the cost factors of the system, resulting consequently in larger battery sizes.

## 5.5 Lifelong Analysis

In this section, the results of the optimization model, which takes into consideration the projected data over the lifetime of the battery system, are presented. Since this research focuses on design optimization rather than operational optimization, the intention of this section is to illustrate overall trends rather than provide detailed information on the operational performance of the battery. Therefore, the figures presented in this section depict long-term patterns, illustrating trends over the battery's expected lifetime.

The lifelong analysis results in the findings of Table 5.9. For the scenarios of cost minimization, where electricity prices are fixed (S1), there is no financial incentive for feed-in energy (S4) and there is a constraint on exported energy (S5), the resulting battery sizes are slightly lower than the corresponding values of the 8-month analysis. This occurs mainly due to the reduction of generated PV energy and the simultaneous increase in demand, meaning that less energy is available to be stored in the battery. Additionally, the lower cost of buying electricity from the grid makes the investment in a storage solution less attractive. Despite the battery's capacity loss over time due to degradation, these factors reduce the optimal battery capacity of the system. The patterns of the battery's SoC, import and export energy, as well as battery charge and discharge for scenario S1, can be seen in Figure 5.44. As the resulting patterns between the aforementioned scenarios align closely, they are not displayed to avoid repetition.

| | **Battery Capacity (kWh)** | |
|---|---|---|
| **Model** | **8-month analysis** | **Lifelong analysis** |
| Cost min: S1 | 10.2 | 9.17 |
| Cost min: S2 | 0 | 0 |
| Cost min: S3 | 0 | 0 |
| Cost min: S4 | 32.4 | 26.87 |
| Cost min: S5 | 41.37 | 41.11 |
| Cost min: S6 | 594 | 4,387.4 |
| $CO_2$ emissions min | 120.2 | 267.5 |
| SS max | 120.2 | 242.5 |
| SC max | 120.2 | 242.5 |

TABLE 5.9: Comparison of the battery sizing optimization results of the 8-month and lifelong analysis.

From Figure 5.44, it becomes clear that the total available battery capacity decreases over time due to battery degradation. By the end of the analysis period, the available battery

capacity drops to 19% of its initial size. Additionally, while the amount of exported energy slightly declines, the imported energy slightly increases over time. This trend occurs due to the reduction of the generated PV energy in combination with the demand increase over the analysis period. For the case of the cost minimization scenario with constraints on exported energy (S5), the amount of exported energy remains constant over time, being equal to the average corresponding value of the baseline scenario (9.14 kWh). Furthermore, in the latter scenario, the amount of curtailed solar energy, during the battery's lifetime, is equal to 20.3 MWh.

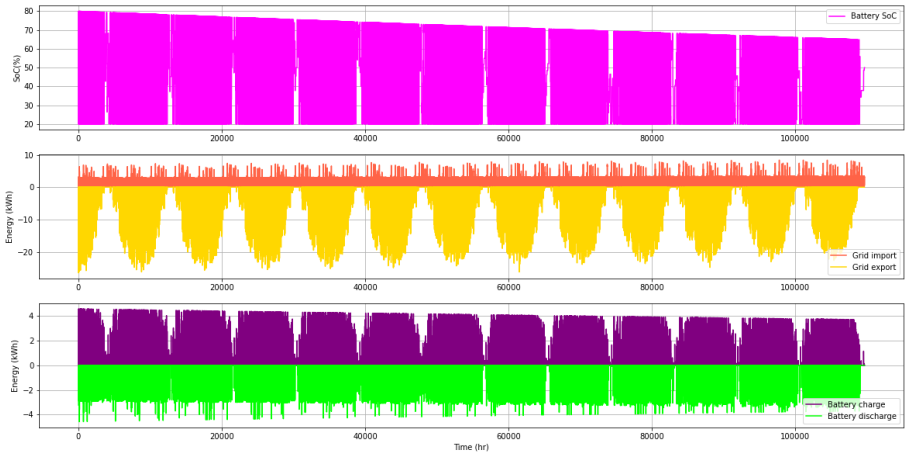


FIGURE 5.44: Results of scenario S1 for the lifelong analysis.

Regarding the scenarios of net metering (S2) and dynamic prices (S3), both the short-term and long-term analyses indicate that a battery is not beneficial for the system. On the other hand, the optimal battery size for the peak shaving scenario (S6) is significantly higher compared to the 8-month analysis. In this case, curtailment of energy does not take place. The considerable difference between the results of the two models is likely due to the restriction on imported energy. Since the demand covered by PV energy decreases over time, the system needs to import larger energy quantities. Additionally, considering capacity loss due to degradation, the model results in an increased optimal battery size to ensure that the demand is continuously covered. However, the result is unrealistically high and the daily SoC constraint cannot be implemented in this model, as it leads to infeasibility, meaning that the system would not be able to cover its needs.

Figure 5.45 illustrates the system's behaviour in the peak shaving scenario (S6). The battery is fully charged during summer and fully discharged during winter. Similarly to the aforementioned scenarios, the energy imports increase, while the energy exports decrease over time.

The objectives of $CO_2$ emissions minimization, self-sufficiency and self-consumption maximization result in optimal battery sizes of similar magnitudes. Specifically, the $CO_2$ emissions minimization model results in an optimal size of 267.5 kWh and total emissions of 32,004 kg $CO_2$ eq. over the 12.5-year battery lifetime. The self-sufficiency and self-consumption maximization models yield an optimal capacity of 242.5 kWh, while the corresponding rates are 0.66 and 0.65, respectively. In these models, the daily SoC constraint is included, meaning that the battery's SoC needs to be equal at the beginning of every day.

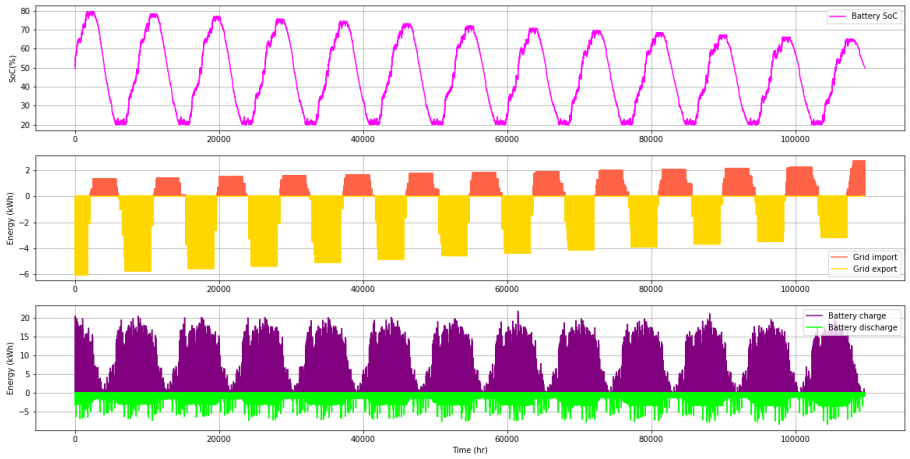


FIGURE 5.45: Results of scenario S6 for the lifelong analysis.

The optimal battery capacity for the $CO_2$ emissions minimization, self-sufficiency and self-consumption maximization models is more than double the size determined by the 8-month analysis. For the $CO_2$ minimization model, using a battery is still more advantageous, with respect to $CO_2$ savings, than importing electricity from the grid, even after the significant reduction in $CO_2$ emissions over time. Additionally, the need to account for battery degradation justifies the significant increase in battery size. The high resulting battery capacity of the self-sufficiency and self-consumption maximization models can be also attributed to the capacity loss due to degradation.

Figure 5.46 presents the operational patterns of the battery for the $CO_2$ emissions minimization model which closely aligns with the self-sufficiency and self-consumption maximization models. It can be seen that the daily SoC constraint has a significant influence on the battery operation, as the SoC fluctuates constantly around 50%. Additionally, energy export, which occurs exclusively during summer, decreases over time, while energy import slightly increases.

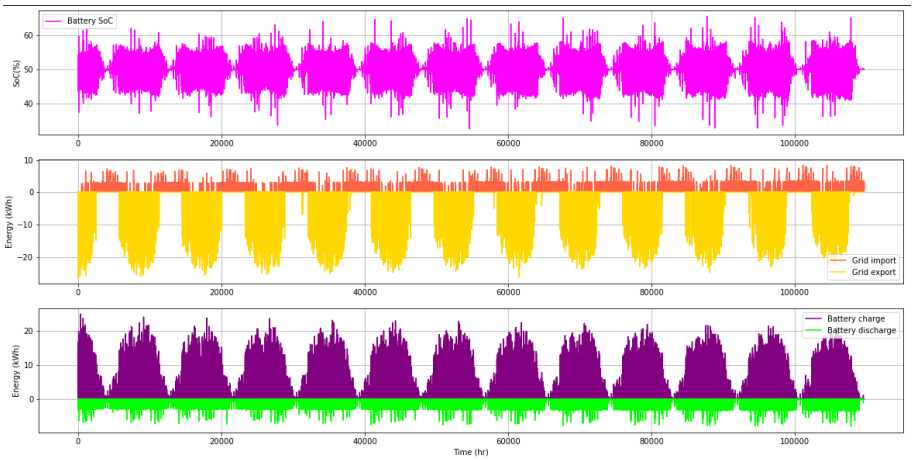


FIGURE 5.46: Results of the $CO_2$ emissions minimization scenario for the lifelong analysis.

### 5.5.1 Financial Analysis

Table 5.10 compares the operational costs of the different scenarios and models with and without a battery system. For the objectives that do not consider the economic implications of the model, namely $CO_2$ emissions minimization, self-sufficiency and self-consumption maximization, the operational cost with storage is higher than without storage. However, for the scenarios S1, S4 and S5, the battery proves to be advantageous for the system. Scenario S5 appears to have the highest savings among all the models. This can be attributed to the fact that without a battery, a large amount of energy needs to be curtailed (58 MWh), which incurs additional costs. Regarding the peak shaving scenario (S6), the system becomes infeasible without a battery, as the demand cannot be met due to the restriction on imported grid energy. Additionally, for the same scenario, the operational cost of the system after the incorporation of the battery is considerably high because of the high consequent maintenance cost. For models resulting in an optimal battery size of zero, the operational cost of the system without a battery appears to be significantly lower than the rest of the models, justifying the outcome of the analysis.

| | **Operational cost (€)** | |
|---|---|---|
| **Model** | **Without battery** | **With battery** |
| Cost min: S1 | 35,788 | 33,690 |
| Cost min: S2 | 26,040 | - |
| Cost min: S3 | 8,043 | - |
| Cost min: S4 | 42,985 | 36,173 |
| Cost min: S5 | 44,368 | 31,802 |
| Cost min: S6 | - | 560,382 |
| $CO_2$ emissions min | 35,788 | 51,831 |
| SS max | 35,788 | 48,701 |
| SC max | 35,788 | 48,702 |

TABLE 5.10: Operational cost for the different scenarios and models over the expected lifetime of the battery.

Table 5.11 shows the payback time, ROI and NPV of the battery investment for the multiple scenarios. While the methods of payback time and ROI agree that the investment is profitable for all the applicable scenarios with cost minimization objectives, the NPV method results in a negative value for the baseline scenario (S1). This discrepancy occurs due to the fact that the NPV method considers the time value of money throughout the entire lifetime of the battery system [75]. Therefore, for the baseline scenario (S1) where the annual savings are relatively low (up to 225€/year), the present value of the future cash flows is negative.

Regarding the models that do not account for the cost of the system, namely $CO_2$ minimization, self-sufficiency and self-consumption maximization models, all the evaluation methods indicate that the battery investment is not profitable. The values of the payback time, ROI and NPV are negative due to the negative annual cash flows resulting from the investment.

Therefore, only the scenarios, where there is no financial incentive for feed-in energy (S4) or there are constraints on exported energy (S5), result in profitability over the lifetime of the battery system. Specifically, the break-even point of the former is 9.86 years with an ROI of 26.8%, while of the latter is 8.18 years with an ROI of 52.8%, meaning that both

investments generate positive returns.

| **Model** | **Payback Time (years)** | **ROI** | **NPV** |
|---|---|---|---|
| Cost min: S1 | 10.93 | 14.4% | -37.24 |
| Cost min: S2 | - | - | - |
| Cost min: S3 | - | - | - |
| Cost min: S4 | 9.86 | 26.8% | 553.57 |
| Cost min: S5 | 8.18 | 52.8% | 2,687.61 |
| Cost min: S6 | - | - | - |
| $CO_2$ emissions min | -41.69 | -130% | -67,180.28 |
| SS max | -46.96 | -126.6% | -59,523.76 |
| SC max | -46.95 | -126.6 % | -59,524.51 |

TABLE 5.11: Payback time, ROI and NPV for the resulting systems of the single-objective optimization models of the lifelong analysis.

# Chapter 6

# Discussion

The findings of the battery sizing optimization model indicate that a battery is not always economically beneficial for the system. When electricity prices are low or regulations, such as net metering, allow the customers to use the grid as a battery, the system does not gain any financial advantage from incorporating a battery. Additionally, the analysis indicates that cost minimization scenarios that include restrictions on grid interaction tend generally to result in larger battery sizes compared to the rest of the cost minimization models. This occurs due to the consequent need of the system to decrease dependency on the grid and ensure continuous coverage of its needs. Since the grid regulations become constantly stricter, the demand for larger storage solutions is expected to rise.

In contrast, when the optimization objective aims at minimizing the system's environmental impact or increasing its self-sufficiency and self-consumption, incorporating a battery is always beneficial. However, these objectives result in unrealistically large battery sizes, as the system intends to store as much energy as possible for future use. Thus, it becomes clear that cost is a significant factor for battery sizing optimization. Without incorporating cost considerations into the model, the outcome is financially unfeasible, leading to expenses that outweigh the benefits of a storage solution during the battery's lifetime. Therefore, co-optimizing costs along with other objectives is crucial for achieving a more balanced outcome. This approach ensures that reducing the environmental impact of the system or its dependency on the grid does not compromise the system's financial viability.

Regarding the environmental impact of the resulting PV-battery systems, it is clear that larger battery sizes minimize emissions. By storing more energy, the system reduces its need to import grid electricity, which is associated with higher carbon intensity than storing PV energy in a battery. Therefore, incorporating a storage solution into the model can lead to a more sustainable manufacturing process, a fact that can be reflected in the "Digital Product Passport" of the manufactured objects.

Furthermore, for this assignment, multiple assumptions have been made that can influence the operational pattern and consequently, the optimal battery size of the system. Some of them refer to costs, battery efficiency and emissions, as well as potential regulatory changes, especially for the lifelong analysis. Additionally, for the analysis over the battery's expected lifetime, the projected data are based on forecasts, meaning that they may not accurately represent real-world scenarios. Nevertheless, since the purpose of this assignment is design optimization rather than operational optimization, meaning that the analysis is based on theoretical models, the projected data are sufficient.

It is important to note that the battery sizing optimization analysis takes, as input, data starting from the summer months, meaning that there is immediately available energy to be stored in the battery. This could possibly influence the resulting optimal battery capacity, particularly in the 8-month analysis. This is because certain models intend to store as much PV energy produced during the summer as possible for winter use. In the opposite case, where the data start from winter, less energy would be available for storage, possibly resulting in lower battery capacities.

Comparing the short and long-term analysis findings, while for certain models, the long-term analysis results in battery sizes of similar magnitude to those determined by the short-term analysis, in other models the optimal size differs significantly. Regarding the scenarios that aim at cost minimization, the resulting optimal battery size is similar or slightly lower in the long-term analysis, since there is less available energy to be stored and the cost of electricity is decreased. An exception is the scenario of peak shaving, where the limitation on imported energy leads to a significant increase in battery size. For the $CO_2$ minimization, self-sufficiency and self-consumption maximization models, the optimal battery size is larger in the long-term analysis due to the capacity loss from degradation over time.

Combining the findings of the 8-month and lifelong financial analysis, a battery generates positive returns only in two cost minimization scenarios, namely the scenarios where feed-in energy is not compensated (S4) and constraints on exported energy are applied (S5). In the rest of the scenarios, the battery investment is not profitable and this can be attributed to various reasons. Some objectives do not consider cost parameters, while others result in returns that are too low to be profitable. Additionally, regulations may force the system to select a large battery size, leading to expenses that outweigh the savings.

Moreover, it is likely that due to the continuous technological advancements and the increasing demand for lithium-ion batteries, battery cost to drop significantly in the future, meaning that battery investments will become more profitable. Besides this, in order to address the grid congestion problem, it is possible that batteries will be subsidized for use in energy systems with high penetration of renewable energy resources. This approach could significantly reduce the total cost of the system and consequently, affect the result of the optimization model.

# Chapter 7

# Conclusion

To conclude, the optimal battery size is influenced by multiple technical, financial, environmental and regulatory factors. For the purpose of this assignment, a MILP model was developed to consider these aspects. The result of the analysis indicates that when electricity prices are low or the system is under the net metering scheme, incorporating a storage solution is not beneficial for the system. Nevertheless, when grid limitations are applied to the system, the model results in larger battery capacities which may not always align with financial feasibility. Additionally, the models that exclude cost considerations result in impractically large battery sizes. Even though these objectives lead to lower environmental impact and reduced grid dependency, the resulting systems are not cost-effective. Thus, co-optimizing cost along with other objectives can result in a more balanced solution. Finally, comparing the results of the short and long-term analysis, while for certain models, the algorithm suggests battery sizes of comparable magnitude, in other models the optimal sizes differ significantly.

Future work should focus on analyzing how the optimal battery size varies after the addition of more machines into the system. As more machines are introduced, the consumption profile may change, potentially resulting in higher peak demand or smoother load profile, depending on the load of each individual machine. This variation could potentially lead to different battery requirements. Additionally, it is recommended to compare the results of the optimization model when different types of batteries are included. Since the different battery types have different lifetimes, investment and maintenance costs, the optimal battery size may change accordingly. Lastly, given that in some scenarios, a significant amount of energy is fed into the grid, it is suggested to examine the possibility of a smart grid implementation within the University of Twente. Instead of exporting the excess PV energy, that cannot be stored in the battery of Fraunhofer Innovation Platform for Advanced Manufacturing, this energy could be utilized by other buildings within the university infrastructure, increasing its economic resilience and grid independence.

# Bibliography


[1] European Environmental Agency. Industry, Jan 2024. URL https://www.eea.europa.eu/en/topics/in-depth/industry.

[2] David Spiers. Chapter iib-2 - Batteries in PV Systems. In Augustin McEvoy, Tom Markvart, and Luis Castañer, editors, *Practical Handbook of Photovoltaics (Second Edition)*, pages 721–776. Academic Press, Boston, second edition edition, 2012. ISBN 978-0-12-385934-1. doi: https://doi.org/10.1016/B978-0-12-385934-1.00022-2. URL https://www.sciencedirect.com/science/article/pii/B9780123859341000222.

[3] Gerwin Hoogsteen. Electricity Distribution Grids - Decentralized Energy Management Systems, 2023. URL https://canvas.utwente.nl/courses/12750/pages/lecture-3-electricity-distribution-grids?module_item_id=455259.

[4] J. L. Hurink. Decentralized Energy Management: A General Concept, 2023. URL https://canvas.utwente.nl/courses/12750/pages/lecture-2-decentralized-energy-management-a-general-concept?module_item_id=455261.

[5] Cristian Giovanni Colombo, Michela Longo, and Dario Zaninelli. *Batteries: Advantages and Importance in the Energy Transition*, pages 69–82. Springer International Publishing, 2024. ISBN 978-3-031-48359-2. doi: 10.1007/978-3-031-48359-2_5. URL https://doi.org/10.1007/978-3-031-48359-2_5.

[6] Zvonimir Šimić, Danijel Topić, Goran Knežević, and Denis Pelin. Battery energy storage technologies overview. *International journal of Electrical and Computer Engineering Systems*, 12:53–65, Apr 2021. doi: https://doi.org/10.32985/ijeces.12.1.6. URL https://ijeces.ferit.hr/index.php/ijeces/article/view/23.

[7] Mahdi Mehrtash, Florin Capitanescu, Per Kvols Heiselberg, Thomas Gibon, and Alexandre Bertrand. An enhanced optimal pv and battery sizing model for zero energy buildings considering environmental impacts. *IEEE Transactions on Industry Applications*, 56(6):6846–6856, 2020. doi: 10.1109/TIA.2020.3022742.

[8] Vjekoslav Salapic, Mirna Grvzanic, and Tomislav Capuder. Optimal sizing of battery storage units integrated into fast charging ev stations. *2018 IEEE International Energy Conference (ENERGYCON)*, pages 1–6, 2018. URL https://api.semanticscholar.org/CorpusID:49538776.

[9] U.S. Environmental Protection Agency. Sustainable Manufacturing, Jul 2015. URL https://www.epa.gov/sustainability/sustainable-manufacturing#:~:text=Sustainable%20manufacturing%20is%20the%20creation,employee%2C%20community%20and%20product%20safety.

[10] European Commission. Commission welcomes provisional agreement for more sustainable, repairable and circular products, 2024. URL https://ec.europa.eu/commission/presscorner/detail/en/ip_23_6257.

[11] Electricity Maps. Co2 Emissions of Electricity Consumption, 2024. URL https://app.electricitymaps.com/zone/NL.

[12] A.R. Dehghani-Sanij, E. Tharumalingam, M.B. Dusseault, and R. Fraser. Study of energy storage systems and environmental challenges of batteries. *Renewable and Sustainable Energy Reviews*, 104:192–208, 2019. ISSN 1364-0321. doi: https://doi.org/10.1016/j.rser.2019.01.023. URL https://www.sciencedirect.com/science/article/pii/S1364032119300334.

[13] Inkwood Research. Global Battery Market Forecast 2022-2030, Aug 2023. URL https://inkwoodresearch.com/reports/battery-market/.

[14] LOHUM. Battery Evolution: Lithium-ion vs Lead acid, Jan 2024. URL https://lohum.com/media/blog/evolution-of-batteries-lithium-ion-vs-lead-acid/.

[15] ShopSolar. Lithium Ion Solar Batteries, 2021. URL https://shopsolarkits.com/collections/lithium-ion-solar-batteries.

[16] Christiana Honsberg and Stuart Bowden. Lead acid batteries | PVEducation, 2019. URL https://www.pveducation.org/pvcdrom/batteries/lead-acid-batteries.

[17] Uwe Koehler. Chapter 2 - General Overview of Non-Lithium Battery Systems and their Safety Issues. In Jürgen Garche and Klaus Brandt, editors, *Electrochemical Power Sources: Fundamentals, Systems, and Applications*, pages 21–46. Elsevier, 2019. ISBN 978-0-444-63777-2. doi: https://doi.org/10.1016/B978-0-444-63777-2.00002-5. URL https://www.sciencedirect.com/science/article/pii/B9780444637772000025.

[18] Ambrose Obajik. Soleil lead acid batteries, Nov 2023. URL https://aptechafrica.com/soleil-lead-acid-batteries/.

[19] Batteries America. Bp-kut272bl : 4.8v 2500mah nimh battery, replaces ikusi bt24ik, 2305271, and iribarri, 2021. URL https://batteriesamerica.com/products/bp-kut272bl-replaces-ikusi-bt24ik-and-others.

[20] PVeducation. Other Battery Types. URL https://www.pveducation.org/pvcdrom/batteries/other-battery-types.

[21] THE EUROPEAN PARLIAMENT and THE COUNCIL OF THE EUROPEAN UNION. Directive 2006/66/ec of the european parliament and of the council, 2018. URL https://eur-lex.europa.eu/legal-content/EN/TXT/?uri=celex%3A32006L0066.

[22] Alcad. Solar NiCad Battery Range, 2024. URL https://www.alcad.com/solar-nicad-battery-range.

[23] IEA. Trends in batteries – Global EV Outlook 2023 – Analysis, 2023. URL https://www.iea.org/reports/global-ev-outlook-2023/trends-in-batteries.

[24] Boucar Diouf and Christophe Avis. The potential of li-ion batteries in ecowas solar home systems. *Journal of Energy Storage*, 22:295–301, 2019. ISSN 2352-152X. doi: https://doi.org/10.1016/j.est.2019.02.021. URL https://www.sciencedirect.com/science/article/pii/S2352152X18307369.

[25] Maria M. Symeonidou, Effrosyni Giama, and Agis M. Papadopoulos. Life cycle assessment for supporting dimensioning battery storage systems in micro-grids for residential applications. *Energies*, 14(19), 2021. ISSN 1996-1073. doi: 10.3390/en14196189. URL https://www.mdpi.com/1996-1073/14/19/6189.

[26] Nirmal-Kumar C. Nair and Niraj Garimella. Battery energy storage systems: Assessment for small-scale renewable energy integration. *Energy and Buildings*, 42(11):2124–2130, 2010. ISSN 0378-7788. doi: https://doi.org/10.1016/j.enbuild.2010.07.002. URL https://www.sciencedirect.com/science/article/pii/S0378778810002185.

[27] Marc Londo, Robin Matton, Omar Usmani, Marieke van Klaveren, Casper Tigchelaar, and Suzanne Brunsting. Alternatives for current net metering policy for solar pv in the netherlands: A comparison of impacts on business case and purchasing behaviour of private homeowners, and on governmental costs. *Renewable Energy*, 147:903–915, 2020. ISSN 0960-1481. doi: https://doi.org/10.1016/j.renene.2019.09.062. URL https://www.sciencedirect.com/science/article/pii/S0960148119313928.

[28] Ben Zientara. What is net metering and how does it work?, Jun 2023. URL https://www.solarreviews.com/blog/what-is-net-metering-and-how-does-it-work.

[29] Solarpower Europe. Top 10 EU Countries Solar Capacity per Capita, 2022. URL https://www.solarpowereurope.org/advocacy/solar-saves/fact-figures/top-10-eu-countries-solar-capacity.

[30] Chuka Nwanazia. The net-metering news: A closer look at the dutch decision, Feb 2024. URL https://solarmonkey.io/the-net-metering-news-a-closer-look/#:~:text=As%20discussions%20ensued%2C%20the%20government,%E2%82%AC700%20million%20annually%20thereafter.

[31] Marc Londo, Robin Matton, Omar Usmani, Marieke Klaveren, Casper Tigchelaar, and Suzanne Brunsting. Alternatives for current net metering policy for solar pv in the netherlands: A comparison of impacts on business case and purchasing behaviour of private homeowners, and on governmental costs. *Renewable Energy*, 147, 09 2019. doi: 10.1016/j.renene.2019.09.062.

[32] Enever.nl. Dynamische Energietarieven, Apr 2023. URL https://enever.nl/.

[33] Tjitte Mastenbroek. Energy monitor 2022: 50 URL https://www.acm.nl/en/publications/energy-monitor-2022-50-dutch-consumers-have-variable-rate\-energy-contracts.

[34] European Network of Transmission System Operators for Electricity. Transparency platform electricity generation, transportation and consumption for the european market, 2024. URL https://transparency.entsoe.eu/.

[35] S. Jayashree and K. Malarvizhi. Methodologies for optimal sizing of battery energy storage in microgrids : A comprehensive review. In *2020 International Conference on Computer Communication and Informatics (ICCCI)*, pages 1–5, 2020. doi: 10.1109/ICCCI48352.2020.9104131.

[36] Yuqing Yang, Stephen Bremner, Chris Menictas, and Merlinde Kay. Battery energy storage system size determination in renewable energy systems: A review. *Renewable and Sustainable Energy Reviews*, 91:109–125, 2018. ISSN 1364-0321. doi: https://doi.org/10.1016/j.rser.2018.03.047. URL https://www.sciencedirect.com/science/article/pii/S1364032118301436.

[37] M.A. Hannan, S.B. Wali, P.J. Ker, M.S. Abd Rahman, M. Mansor, V.K. Ramachandaramurthy, K.M. Muttaqi, T.M.I. Mahlia, and Z.Y. Dong. Battery energy-storage system: A review of technologies, optimization objectives, constraints, approaches, and outstanding issues. *Journal of Energy Storage*, 42:103023, 2021. ISSN 2352-152X. doi: https://doi.org/10.1016/j.est.2021.103023. URL https://www.sciencedirect.com/science/article/pii/S2352152X21007349.

[38] Kamal Anoune, Mohsine Bouya, Abdelali Astito, and Abdellatif Ben Abdellah. Sizing methods and optimization techniques for pv-wind based hybrid renewable energy system: A review. *Renewable and Sustainable Energy Reviews*, 93:652–673, 2018. ISSN 1364-0321. doi: https://doi.org/10.1016/j.rser.2018.05.032. URL https://www.sciencedirect.com/science/article/pii/S1364032118303757.

[39] Jonas Sievers and Thomas Blank. A systematic literature review on data-driven residential and industrial energy management systems. *Energies*, 16(4), 2023. ISSN 1996-1073. doi: 10.3390/en16041688. URL https://www.mdpi.com/1996-1073/16/4/1688.

[40] Bashar Chreim, Moez Esseghir, and Leila Merghem-Boulahia. Recent sizing, placement, and management techniques for individual and shared battery energy storage systems in residential areas: A review. *Energy Reports*, 11:250–260, 2024. ISSN 2352-4847. doi: https://doi.org/10.1016/j.egyr.2023.11.053. URL https://www.sciencedirect.com/science/article/pii/S2352484723015810.

[41] Di Wu and Xu Ma. Modeling and optimization methods for controlling and sizing grid-connected energy storage: A review. *Current Sustainable/Renewable Energy Reports*, 8(2):123–130, Mar 2021. doi: https://doi.org/10.1007/s40518-021-00181-9. URL https://link.springer.com/article/10.1007/s40518-021-00181-9#citeas.

[42] Giulia Mancò, Elisa Guelpa, Alessandro Colangelo, Alessandro Virtuani, Tommaso Morbiato, and Vittorio Verda. Innovative renewable technology integration for nearly zero-energy buildings within the re-cognition project. *Sustainability*, 13(4), 2021. ISSN 2071-1050. doi: 10.3390/su13041938. URL https://www.mdpi.com/2071-1050/13/4/1938.

[43] Nikolaos V. Sahinidis. Mixed-integer nonlinear programming 2018. *Optimization and Engineering*, 2019. doi: https://doi.org/10.1007/s11081-019-09438-1. URL https://link.springer.com/article/10.1007/s11081-019-09438-1.

[44] Antía Varela Souto. Optimization & Energy Management of a Microgrid Based on Frequency Communications by A . *TU Delft*, 2016. URL https://api.semanticscholar.org/CorpusID:59486685.

[45] Da Huo, Marcos Santos, Ilias Sarantakos, Markus Resch, Neal Wade, and David Greenwood. A reliability-aware chance-constrained battery sizing method for island microgrid. *Energy*, 251:123978, 2022. ISSN 0360-5442. doi: https://doi.org/10.1016/

j.energy.2022.123978. URL https://www.sciencedirect.com/science/article/pii/S0360544222008817.

[46] Fadi Agha Kassab, Berk Celik, Fabrice Locment, Manuela Sechilariu, Sheroze Liaquat, and Timothy M. Hansen. Optimal sizing and energy management of a microgrid: A joint milp approach for minimization of energy cost and carbon emission. *Renewable Energy*, 224:120186, 2024. ISSN 0960-1481. doi: https://doi.org/10.1016/j.renene.2024.120186. URL https://www.sciencedirect.com/science/article/pii/S0960148124002519.

[47] J.C. Hernández, F. Sanchez-Sutil, and F.J. Muñoz-Rodríguez. Design criteria for the optimal sizing of a hybrid energy storage system in pv household-prosumers to maximize self-consumption and self-sufficiency. *Energy*, 186:115827, 2019. ISSN 0360-5442. doi: https://doi.org/10.1016/j.energy.2019.07.157. URL https://www.sciencedirect.com/science/article/pii/S0360544219314999.

[48] MarketsandMarkets Research. Lithium-ion battery market size, share, industry report, revenue trends and growth drivers, 2023. URL https://www.marketsandmarkets.com/Market-Reports/lithium-ion-battery-market-49714593.html.

[49] Statista Research. Lithium-ion battery price worldwide from 2013 to 2023, 2023. URL https://www.statista.com/statistics/883118/global-lithium-ion-battery-pack-costs/.

[50] Renewable Energy Association (REA) Eaton. *Beyond the Tipping Point Flexibility gaps in future high-renewable energy systems in the U.K., Germany and Nordics.* Bloomberg New Energy Finance, 2018. URL https://www.ceer.eu/documents/104400/-/-/e4225227-ac33-c7c9-1454-ced8e18c38a8.

[51] Sandia National Laboratories. Mathematical Modeling — Pyomo 6.6.2, 2023. URL https://pyomo.readthedocs.io/en/stable/pyomo_overview/math_modeling.html.

[52] Praful V. Nandankar, Prashant P. Bedekar, and Prashantkumar V. Dhawas. Efficient dc-dc converter using variable switching frequency digital controller. In *2020 5th IEEE International Conference on Recent Advances and Innovations in Engineering (ICRAIE)*, pages 1–6, 2020. doi: 10.1109/ICRAIE51050.2020.9358294.

[53] Kevin Mallon, Francis Assadian, and Bo Fu. Analysis of on-board photovoltaics for a battery electric bus and their impact on battery lifespan. *Energies*, 10:943, 07 2017. doi: 10.3390/en10070943.

[54] Gurobi optimization. Dealing with big M constraints, Oct 2023. URL https://www.gurobi.com/documentation/current/refman/dealing_with_big_m_constra.html.

[55] Matthew Davison, Jesse Cranney, Terry Summers, and Christopher D. Townsend. Decentralised energy market for implementation into the intergrid concept - part 2: Integrated system. In *2018 7th International Conference on Renewable Energy Research and Applications (ICRERA)*, pages 287–293, 2018. doi: 10.1109/ICRERA.2018.8566719.

[56] Thunder Said Energy. Grid-scale battery costs: The economics, Nov 2023. URL https://thundersaidenergy.com/downloads/battery-storage-costs-the-economics/.

[57] NREL. Commercial battery storage, 2023. URL https://atb.nrel.gov/electricity/2023/commercial_battery_storage.

[58] Statista. Lithium-ion battery price worldwide from 2013 to 2023, 2023. URL https://www.statista.com/statistics/883118/global-lithium-ion-battery-pack-costs/.

[59] Kendall Mongird, Vilayanur Viswanathan, Jan Alam, Charlie Vartanian, Vincent Sprenkle, Pacific Northwest, and Richard Baxter. 2020 grid energy storage technology cost and performance assessment. *U.S. Department of Energy*, 2020. URL https://www.pnnl.gov/sites/default/files/media/file/Lithium-ion_Methodology.pdf.

[60] Eurostat. Electricity Price Statistics, 2024. URL https://ec.europa.eu/eurostat/statistics-explained/images/5/58/Electricity_prices_for_non-household_consumers_first_half_2023_V2.png.

[61] Zonne-energiegids.nl. Feed-in tarief (teruglevertarief), 2023. URL https://www.zonne-energiegids.nl/begrippenlijst/feed-in-tarief/.

[62] Alessandro Ciocia, Angela Amato, Paolo Di Leo, Stefania Fichera, Gabriele Malgaroli, Filippo Spertino, and Slavka Tzanova. Self-consumption and self-sufficiency in photovoltaic systems: Effect of grid limitation and storage installation. *Energies*, 14(6), 2021. ISSN 1996-1073. doi: 10.3390/en14061591. URL https://www.mdpi.com/1996-1073/14/6/1591.

[63] Christoph Kost. Study: Levelized Cost of Electricity- Renewable Energy Technologies, 2024. URL https://www.ise.fraunhofer.de/en/publications/studies/cost-of-electricity.html.

[64] Gridx. Peak Shaving, 2024. URL https://www.gridx.ai/knowledge/peak-shaving#:~:text=Peak%20shaving%2C%20also%20called%20load,demand%2C%20thereby%20lowering%20demand%20charges.

[65] Bart Nijenhuis. Integrating Scheduling and Online Control in an User-Centered EV Charging Hub. *Unpublished*, 2023.

[66] Gurobi optimization. Mixed Integer Programming (MIP) - A primer on the basics, Mar 2024. URL https://www.gurobi.com/resources/mixed-integer-programming-mip-a-primer-on-the-basics/.

[67] Statistics Netherlands. Nearly half the electricity produced in the netherlands is now renewable, Mar 2024. URL https://www.cbs.nl/en-gb/news/2024/10/nearly-half-the-electricity-produced-in-the-netherlands-is-now-renewable.

[68] The Advanced Rechargeable & Lithium Batteries Association. *PEFCR - Product Environmental Footprint Category Rules for High Specific Energy Rechargeable Batteries for Mobile Applications*. Recharge, 2018. URL https://www.sazp.sk/dokument/f/baterie-a-akumulatory-pdf.pdf.

[69] Jorge A Llamas-Orozco, Fanran Meng, Gavin S Walker, Amir, Heather L MacLean, I Daniel Posen, and Jon McKechnie. Estimating the environmental impacts of global lithium-ion battery supply chain: A temporal, geographical, and technological perspective. *PNAS nexus*, 2(11), Nov 2023. doi: https://doi.org/10.1093/pnasnexus/pgad361. URL https://www.ncbi.nlm.nih.gov/pmc/articles/PMC10683946/#:~:text=(A)%20Supply%20chain%20GHG%20emissions,56%20kgCO2eq%2FkWh.

[70] Schlömer S., T. Bruckner, L. Fulton, E. Hertwich, A. McKinnon, D. Perczyk, J. Roy, R. Schaeffer, R. Sims, P. Smith, and R. Wiser. *III ANNEX Technology-specific Cost and Performance Parameters Editor: Lead Authors: Contributing Authors: Technology-specific Cost and Performance Parameters Annex III*. Cambridge University Press, 2014. URL https://www.ipcc.ch/site/assets/uploads/2018/02/ipcc_wg3_ar5_annex-iii.pdf.

[71] Yang Zhang, Anders Lundblad, Pietro Elia Campana, and Jinyue Yan. Employing battery storage to increase photovoltaic self-sufficiency in a residential building of sweden. *Energy Procedia*, 88:455–461, 2016. ISSN 1876-6102. doi: https://doi.org/10.1016/j.egypro.2016.06.025. URL https://www.sciencedirect.com/science/article/pii/S1876610216300893. CUE 2015 - Applied Energy Symposium and Summit 2015: Low carbon cities and urban energy systems.

[72] Xin-She Yang. Chapter 14 - multi-objective optimization. In Xin-She Yang, editor, *Nature-Inspired Optimization Algorithms*, pages 197–211. Elsevier, Oxford, 2014. ISBN 978-0-12-416743-8. doi: https://doi.org/10.1016/B978-0-12-416743-8.00014-2. URL https://www.sciencedirect.com/science/article/pii/B9780124167438000142.

[73] Julia Kagan. Payback period explained, with the formula and how to calculate it, 2024. URL https://www.investopedia.com/terms/p/paybackperiod.asp.

[74] Jason Fernando. Return on investment (ROI): how to calculate it and what it means, 2024. URL https://www.investopedia.com/terms/r/returnoninvestment.asp.

[75] Jason Fernando. Net present value (NPV): what it means and steps to calculate it, 2024. URL https://www.investopedia.com/terms/n/npv.asp#:~:text=Net%20present%20value%20(NPV)%20is%20a%20financial%20metric%20that%20seeks,and%20then%20add%20them%20together.

[76] Ycharts. Netherlands Long Term Interest Rate Monthly Insights, 2024. URL https://ycharts.com/indicators/netherlands_long_term_interest_rates#:~:text=Netherlands%20Long%20Term%20Interest%20Rate%20is%20at%202.62%25%2C%20compared%20to,long%20term%20average%20of%203.24%25.

[77] Agata Mielcarek, Bartosz Ceran, and Jakub Jurasz. The impact of degradation of pv/battery-independent system components on technical and economic indicators and sizing process. *Energies*, 16(18):6642–6642, Sep 2023. doi: https://doi.org/10.3390/en16186642. URL https://www.mdpi.com/1996-1073/16/18/6642.

[78] International Energy Agency. *Electricity Market Report 2023*. IEA, 2023. URL https://iea.blob.core.windows.net/assets/255e9cba-da84-4681-8c1f-458ca1a3d9ca/ElectricityMarketReport2023.pdf.

[79] Aramis Perez, Rodrigo Moreno, Roberto Moreira, Marcos Orchard, and Goran Strbac. Effect of battery degradation on multi-service portfolios of energy storage. *IEEE Transactions on Sustainable Energy*, 7(4):1718–1729, Oct 2016. doi: https://doi.org/10.1109/tste.2016.2589943.

[80] Huangluolun Zhou. EU Energy Outlook to 2060: Power Prices and Revenues Predicted for Wind, Solar, Gas, Hydrogen, Dec 2023. URL https://energypost.eu/eu-energy-outlook-to-2060-power-prices-and-revenues-predicted-for-wind-solar-gas-hydro

[81] OECD. Renewable energy feed-in tariffs, 2019. URL https://stats.oecd.org/Index.aspx?DataSetCode=RE_FIT.

[82] Enerdata. The Netherlands unveils planned 2023-2030 solar PV net metering scheme, Mar 2023. URL https://www.enerdata.net/publications/daily-energy-news/netherlands-unveils-planned-2023-2030-solar-pv-net-metering-scheme.html.

[83] Emiliano Bellini. Netherlands to phase out net-metering scheme in 2027, May 2024. URL https://www.pv-magazine.com/2024/05/16/netherlands-to-phase-out-net-metering-scheme-in-2027/.

[84] Enerdata. CO2 Intensity of Electricity Generation, 2024. URL https://eneroutlook.enerdata.net/forecast-world-co2-intensity-of-electricity-generation.html.

[85] Abhishek Kumar Singh. Lecture 1- Solar Energy, PV Integration: Solar collectors and PV Systems, 2022. URL https://canvas.utwente.nl/courses/11941/files/3434386?module_item_id=379525.

[86] SolarEdge. Three phase inverter specifically designed to work with power optimizers. URL https://www.solaredge.com/sites/default/files/se-three-phase-inverter-with-setapp-configuration-datasheet.pdf.

[87] SolarEdge. SolarEdge Monitoring Server - API, 2022. URL https://knowledge-center.solaredge.com/sites/kc/files/se_monitoring_api.pdf.

[88] Gurobi Optimization. Python interface - Gurobi optimization, Aug 2022. URL https://www.gurobi.com/wp-content/plugins/hd_documentations/documentation/9.1/quickstart_windows.pdf.

# Appendix

| NPV | | | | | | | | | | | | | | | | |
|---|---|---|---|---|---|---|---|---|---|---|---|---|---|---|---|---|
| Interest rate (annual) | 2,62% | | | | | | | | | | | | | | | |
| Interest rate (half year) | 1,31% | | | | | | | | | | | | | | | |
| **Year** | **0** | **1** | **2** | **3** | **4** | **5** | **6** | **7** | **8** | **9** | **10** | **11** | **12** | **NPV (1-12 years)** | **12,5** | **NPV (12.5 years)** |
| PV factor | 1,0000 | 0,9745 | 0,9496 | 0,9253 | 0,9017 | 0,8787 | 0,8563 | 0,8344 | 0,8131 | 0,7923 | 0,7721 | 0,7524 | 0,7332 | | 0,8499 | |
| | | | | | | | | | | | | | | | | |
| **Cash flows** | | | | | | | | | | | | | | | | |
| Cost min: S1 | -2.040,00 | 194,89 | 189,91 | 185,06 | 180,34 | 175,74 | 171,25 | 166,88 | 162,62 | 158,46 | 154,42 | 150,48 | 146,63 | -3,32 | 84,98 | 81,66 |
| Cost min: S2 | - | - | - | - | - | - | - | - | - | - | - | - | - | - | - | - |
| Cost min: S3 | - | - | - | - | - | - | - | - | - | - | - | - | - | - | - | - |
| Cost min: S4 | -6.480,00 | 760,01 | 740,61 | 721,70 | 703,28 | 685,32 | 667,82 | 650,77 | 634,16 | 617,97 | 602,19 | 586,82 | 571,83 | 1.462,48 | 331,41 | 1.793,89 |
| Cost min: S5 | -8.274,00 | 1.116,57 | 1.088,07 | 1.060,29 | 1.033,22 | 1.006,84 | 981,13 | 956,08 | 931,67 | 907,89 | 884,71 | 862,12 | 840,11 | 3.394,68 | 486,89 | 3.881,57 |
| Cost min: S6 | - | - | - | - | - | - | - | - | - | - | - | - | - | - | - | - |
| CO2 min | -24.040,00 | -51,29 | -49,98 | -48,70 | -47,46 | -46,25 | -45,07 | -43,92 | -42,80 | -41,70 | -40,64 | -39,60 | -38,59 | -24.576,00 | -22,37 | -24.598,36 |
| SS max | -24.040,00 | -51,29 | -49,98 | -48,70 | -47,46 | -46,25 | -45,07 | -43,92 | -42,80 | -41,70 | -40,64 | -39,60 | -38,59 | -24.576,00 | -22,37 | -24.598,36 |
| SC max | -24.040,00 | -52,42 | -51,08 | -49,78 | -48,51 | -47,27 | -46,06 | -44,89 | -43,74 | -42,62 | -41,54 | -40,48 | -39,44 | -24.587,84 | -22,86 | -24.610,70 |

FIGURE 7.1: Detailed NPV calculations for the 8-month analysis.

| NPV | | | | | | | | | | | | | | | | |
|---|---|---|---|---|---|---|---|---|---|---|---|---|---|---|---|---|
| Interest rate (annual) | 2,62% | | | | | | | | | | | | | | | |
| Interest rate (half year) | 1,31% | | | | | | | | | | | | | | | |
| **Year** | **0** | **1** | **2** | **3** | **4** | **5** | **6** | **7** | **8** | **9** | **10** | **11** | **12** | **NPV (1-12 years)** | **12,5** | **NPV (12.5 years)** |
| PV factor | 1,0000 | 0,9745 | 0,9496 | 0,9253 | 0,9017 | 0,8787 | 0,8563 | 0,8344 | 0,8131 | 0,7923 | 0,7721 | 0,7524 | 0,7332 | | 0,8499 | |
| | | | | | | | | | | | | | | | | |
| **Cash flows** | | | | | | | | | | | | | | | | |
| Cost min: S1 | -1.834,00 | 219,98 | 206,74 | 196,73 | 143,09 | 115,90 | 104,48 | 114,58 | 135,96 | 142,38 | 129,86 | 119,13 | 111,11 | -94,04 | 56,80 | -37,24 |
| Cost min: S2 | - | - | - | - | - | - | - | - | - | - | - | - | - | - | - | - |
| Cost min: S3 | - | - | - | - | - | - | - | - | - | - | - | - | - | - | - | - |
| Cost min: S4 | -5.374,00 | 858,18 | 791,82 | 718,53 | 548,43 | 455,88 | 395,51 | 408,92 | 388,52 | 350,21 | 318,89 | 289,31 | 267,12 | 417,31 | 136,27 | 553,57 |
| Cost min: S5 | -8.224,00 | 1.521,89 | 1.411,90 | 1.269,75 | 1.006,07 | 873,16 | 757,94 | 770,85 | 729,81 | 648,80 | 605,12 | 542,29 | 506,91 | 2.420,49 | 267,13 | 2.687,61 |
| Cost min: S6 | - | - | - | - | - | - | - | - | - | - | - | - | - | - | - | - |
| CO2 min | -53.508,00 | -1.222,43 | -1.190,42 | -1.133,67 | -1.303,51 | -1.357,13 | -1.322,70 | -1.198,09 | -1.011,29 | -879,93 | -873,08 | -857,33 | -844,74 | -66.702,31 | -477,97 | -67.180,28 |
| SS max | -48.508,00 | -978,09 | -952,37 | -901,69 | -1.077,47 | -1.136,85 | -1.108,04 | -988,92 | -807,46 | -681,30 | -679,52 | -668,71 | -660,91 | -59.149,33 | -374,43 | -59.523,76 |
| SC max | -48.508,00 | -978,84 | -952,37 | -901,69 | -1.077,47 | -1.136,85 | -1.108,04 | -988,92 | -807,46 | -681,30 | -679,52 | -668,71 | -660,91 | -59.150,08 | -374,43 | -59.524,51 |

FIGURE 7.2: Detailed NPV calculations for the battery's lifelong analysis.